67338

Water Papers

September 2011

CLIMATE VARIABILITY AND CHANGE: A BASIN SCALE INDICATOR APPROACH TO UNDERSTANDING THE RISK TO WATER RESOURCES DEVELOPMENT AND MANAGEMENT

Kenneth Strzepek
Alyssa McCluskey
Brent Boehlert
Michael Jacobsen
Charles Fant IV

TABLE OF CONTENTS

Synopsis ..... **ix**

Acronyms and Abbreviations ..... **x**

Acknowledgments ..... **xi**

1. Introduction and Background **1**

1.1 Intended Use of Findings 1
1.2 Relevant Prior Work and Links to Other Studies 1
1.3 Key Indicators for Screening of Water Resource Projects 3
1.4 Overview of Report 4

2. Methodology: A Basin Scale Indicator Approach **6**

2.1 Analytical Framework 6
2.2 Data Inputs and Processing 16
2.3 Calculating Changes in Potential Evapotranspiration Under Climate Change 20
2.4 Modeling Changes in Global Runoff Under Climate Change 21
2.5 Calculating Changes in Hydrological Indicators Under Climate Change 26
2.6 Uncertainty 35

3. Illustrative Results: Uganda as an Example **40**

3.1 Maps of Hydrological Indicators across Basins 41
3.2 Box and Whisker Plots of Hydrological Indicators across GCMs 47
3.3 Final Comment on Using the Hydrological Indicators Data 49

Annexes **50**

Annex A. CRU and GRDC Data Sets: Description, Construction, Uncertainties, and Validation 51
Annex B. Overview of the CLIRUN-II Rainfall Runoff Model 64
Annex C. Comparison of CLIRUN-II Results Using GRDC versus In-Country Data: Selected Basin Study 70
Annex D. Guide to Navigation of the World Bank Climate Portal Hydrologic Indicators 87

Annex E. Basin Selection and Naming Convention 95
Annex F. Assessing the Impact of Climate Variability and Change in Botswana: The Role of Global Circulation Models and the CLIRUN-II Hydrologic Model 97
Annex G. Developing a Climate Change Adaptation Strategy in Michoacán: The Role of Global Circulation Models and the CLIRUN-II Hydrologic Model 110

References 121

TABLES

Table 1-1. Hydrological indicators for typical water projects 3

Table 2-1. Spatial resolution of IPCC AR4 GCMs 10

Table 2-2. Coverage area of a 1-degree latitude × 1-degree longitude 10

Table 2-3. Available combinations of IPCC GCMs and SRES scenarios B1, A1B, and A2 15

Table 2-4. Required inputs for CLIRUN-II 22

Table 2-5. Hydrological indicators and the most relevant water projects 28

Table 2-6. Exposure level thresholds for each indicator 29

Table 3-1. Dry, middle, and wet scenarios for Uganda basins in the 2030s and 2050s for the A1B SRES scenario 41

Table B-1. Calibration parameters in CLIRUN-II 69

Table C-1. Zambezi Basin calibration results 78

Table C-2. Vietnam Basin calibration results 78

Table C-3. Blue Nile and Ethiopia Basins calibration results 79

Table C-4. Vardar Basin calibration results 79

Table C-5. Vardar Basin calibration results at Gevegelija 79

Table C-6. Sao Francisco Basin calibration results 79

Table G-1. Future climate projections of the driest, wettest, and the median outcomes 115

Table G-2. No regrets and climate justified actions (adaptations) for crop systems 120

FIGURES

Figure 2-1. Diagram of the modeling process used in this study 6

Figure 2-2. The cone of uncertainty in scale and resolution of modeling 9

Figure 2-3. Section of Indian subcontinent showing 0.5 × 0.5 degree grid scale, 2.5 × 2.5 degree grid scale, and basin boundaries 12

Figure 2-4. Range of relative change from baseline for GCMs. Mean is shown in bold 13

Figure 2-5. Greenhouse gas emissions and estimated global surface warming for SRES scenarios, 2000 to 2100 15

Figure 2-6. Mean annual temperature (top map, in degrees Celsius) and precipitation (bottom map, in millimeters) in the 8,413 basins within World Bank client countries, 1961 to 1999 17

Figure 2-7. Map of the 8,413 global river basins within World Bank client countries 19

Figure 2-8. Locations of gauging stations used in the GRDC database 20

Figure 2-9. Schematic of water flows in CLIRUN-II 23

Figure 2-10. Calibration results (R^2) for 8,413 basins using CLIRUN-II 25

Figure 2-11. CLIRUN-II calibration results (R^2) for Africa and East Asia 25

Figure 2-12. Diagram of hydrological indicators 27

Figure 2-13. Storage yield curve for the Nile River at Aswan 30

Figure 2-14. Impact of climate change on a hypothetical storage yield curve 31

Figure 2-15. Example of a basin's mean monthly hydrograph 33

Figure 3-1. Change in mean annual runoff in Uganda's basins from the baseline to 2030 and 2050 under dry, middle, and wet scenarios 42

Figure 3-2. Change in basin yield in Uganda's basins from the baseline to 2030 and 2050 under dry, middle, and wet scenarios 43

Figure 3-3. Change in annual high flow (q10) in Uganda's basins from the baseline to 2030 and 2050 under dry, middle, and wet scenarios 44

Figure 3-4. Change in annual low flow (q90) in Uganda's basins from the baseline to 2030 and 2050 under dry, middle, and wet scenarios 45

Figure 3-5. Change in groundwater (baseflow) in Uganda's basins from the baseline to 2030 and 2050 under dry, middle, and wet scenarios 46

Figure 3-6. Change in reference crop water deficit in Uganda's basins from the baseline to 2030 and 2050 under dry, middle, and wet scenarios 47

Figure 3-7. Box and whisker plots of indicators for Uganda from the baseline to the 2030s (top) and 2050s (bottom), across climate scenarios 48

Figure A-1. Precipitation stations used for the CRU TS interpolation 52

Figure A-2. Temperature stations used for the CRU TS interpolation 53

Figure A-3. Precipitation coverage during different time periods. The shaded areas represent the half-degree coverage 53

Figure A-4.. Temperature coverage over various time periods. The shaded areas represent the half-degree coverage 54

Figure A-5. GRDC selected discharge gauging stations 58

Figure A-6. UNH-GRDC composite mean annual runoff for the globe 60

Figure A-7. WBM runoff correction coefficients 60

Figure A-8. UNH-GRDC basin boundaries (green) and the Hydro1k level 3 basins (brown) over Africa 62

Figure A-9. UNH-GRDC basin boundaries (green) and the Hydro1k level 3 (part of Southern Africa) 63

Figure A-10. UNH-GRDC basin boundaries (green) and the Hydro1k level 3 basins (brown) zoomed in to show the Unique Identifier labels (as an example) 63

Figure B-1. Schematic of water flows in CLIRUN-II 65

Figure C-1. Zambezi Basin map—all basins 71

Figure C-2. Blue Nile and Ethiopia Basins map—all basins 72

Figure C-3. Red River and Vietnam Basins map—all basins 74

Figure C-4. Vardar Basin map—all basins 75

Figure C-5. Vardar Basin map, showing the surrounding area 76

Figure C-6. Sao Francisco Basin map—upstream of the Juazeiro gauging station 77

Figure C-7. Annual comparison of CLIRUN-LOCAL, measured, CLIRUN-UNH, and UNH-GRDC runoff for the Watopa Pontoon Gauge Station 80

Figure C-8. Monthly comparison of CLIRUN-LOCAL, measured, CLIRUN-UNH, and UNH-GRDC runoff for the Watopa Pontoon Gauge Station. 81

Figure C-9. Precipitation and measured discharge for the Watopa Pontoon Gauge Station. 82

Figure C-10. Snapshot of monthly flows for the observed, full calibration, and month calibration for the Watopa Pontoon Gauge Station 83

Figure C-11. Monthly averages for the observed, full calibration, and month calibration for the Watopa Pontoon Gauge Station 83

Figure C-12. Sorted monthly flows for the observed, full calibration, and month calibration for the Watopa Pontoon Gauge Station 84

Figure C-13. Annual flows for the observed, full calibration, and month calibration for the Watopa Pontoon Gauge Station 84

Figure C-14. Sorted annual flows for the observed, full calibration, and month calibration for the Watopa Pontoon Gauge Station 85

Figure D-1. Locating basin or county or interest 88

Figure D-2. Getting access to data 89

Figure D-3. Viewing and downloading data 90

Figure D-4. Tabular display of indicator data, as percent change from baseline 90

Figure D-5. Example basin box plots for the 2030s and 2050s 91

Figure D-6. Example country box plot for the 2030s 91

Figure D-7. Interactive mapping tool interface 92

Figure D-8. Mapping tool pop-up window 93

Figure D-9. Detailed map results 94

Figure F-1. Map of the Republic of Botswana 98

Figure F-2. Interannual precipitation variability (mm) 99

Figure F-3. Intraannual and precipitation variability (mm) 99

Figure F-4. Basin Identification map of Botswana 101

Figure F-5. Box plot of average annual indicator statistics for south-central-eastern Botswana (Basin 5927) for 2030 to 2039 103

Figure F-6. Box plot of average annual indicator statistics for south-central-eastern Botswana (Basin 5927) for 2050 to 2059. 104

Figure F-7. Percentage change in the frequency of the 12-Month SPI (SPI12) due to predicted climate change in Botswana. GFDLCM21, A1b emissions scenario, 2046 to 2065. 106

Figure F-8. Percentage change in the frequency of the 12-Month SPI (SPI12) due to predicted climate change in Botswana, GFDLCM21, A1b emissions scenario, 2080 to 2100. 106

Figure F-9. Percentage change in the frequency of the PDSI for extreme drought levels, due to predicted climate change in Botswana, GCM inmcm30, A2 emissions scenario, 2046 to 2065. 107

Figure F-10. Percentage change in the frequency of the PDSI for extreme drought levels, due to predicted climate change in Botswana, GCM inmcm30, A2 emissions scenario, 2081 to 2100. 107

Figure G-1. Selected steps in risk identification, analysis, and evaluation 111

Figure G-2. The hydrologic regions and Subregions in the State of Michoacán 112

Figure G-3. Actual observed climate (left) and projections from the Earth Simulator 113

Figure G-4. Future hydrologic projections of the driest (A2), wettest (A1b), and the median (B1) outcomes 116

Figure G-5. Impact risk and vulnerability matrix of climate change for water, biodiversity, and health 117

Figure G-6. Adaptation to climate change for water, biodiversity, and health 119

THIS PAGE INTENTIONALLY LEFT BLANK

SYNOPSIS

The impact of climate change is likely to have considerable implications for water resource planning, as well as adding to the risks to water infrastructure systems and effecting return on investments. Attention is increasingly being paid to adaptation strategies at the regional and basin level; however, the current paucity of information regarding the potential risk to hydrological systems at this scale presents a substantial challenge for effective water resources planning and investment. This study is intended to help bridge the gap between high-level climate change predictions and the needs of decision-makers—including World Bank Task Team Leaders, government agencies, investors, and national economic development planners—whose programs and investments will be affected by basin- and regional-level impacts of climate change on water resources and related infrastructures.

This study evaluates the effects of climate change on six hydrological indicators across 8,413 basins in World Bank client countries. These indicators—mean annual runoff (MAR), basin yield, annual high flow, annual low flow, groundwater (baseflow), and reference crop water deficit—were chosen based on their relevance to the wide range of water resource development projects planned for the future. To generate a robust, high-resolution understanding of possible risk, this analysis examines relative changes in all variables from the historical baseline (1961 to 1999) to the 2030s and 2050s for the full range of 56 General Circulation Model (GCM) Special Report on Emissions Scenario (SRES) combinations evaluated in the Intergovernmental Panel on Climate Change (IPCC) Fourth Assessment Report (AR4).

To make this information easily accessible to Task Team Leaders and World Bank clients, the results from this study are available on the World Bank Climate Portal, a Web-based interface. On the Climate Portal, users can access graphic presentations illustrating the severity (that is, low, medium, high) of change that is projected for all of the studied variables in any country, basin, or country–basin intersection of interest. Users can also access tabular and graphic representations of all climatic and hydrological projections for analyzed areas.

Importantly, the results presented in this study are not intended for use at the project level; however, because the results provide an indication of risk or threat at the sub-basin level, they might appropriately provide input into decisions about the extent of analyses of climate change to be carried out at the site-specific project level.

The purpose of this document is to explain in-depth the methods used to develop these climate risk outputs, the reasons for the selected methodology, and the limitations of this research.

ACRONYMS AND ABBREVIATIONS

AAA	Analytical, Advisory Activity
AR4	Fourth Assessment Report (IPCC)
CMI	Climate Moisture Index
CMS	Cubic meters per second
CLIRUN	Climate runoff model
CRU	Climate Research Unit
CWR	Crop water requirement
ET	Evapotranspiration
FAO	UN Food and Agriculture Organization
GIS	Geographic Information System
GCM	General Circulation Model
GHCN	Global Historical Climatology Network
GRDC	Global Runoff Data Center
IPCC	Intergovernmental Panel on Climate Change
km	Kilometer
MAR	Mean annual runoff
MCM	Millions of cubic meters
mm	Millimeter
PDSI	Palmer Drought Severity Index
PET	Potential evapotranspiration
SIXPAR	Six parameter
SPI	Standardized Precipitation Index
SRES	Special Report on Emissions Scenarios
STN	Simulated Topological Network
TS	Time Series
UNH	University of New Hampshire
USGS	US Geological Survey
WatBal	Water Balance
WBM	Water Balance Model
WDI	Water Deficit Index

ACKNOWLEDGMENTS

The Water Partnership Program's funding for this study is gratefully acknowledged.

The report was prepared by Kenneth Strzepek, Alyssa McCluskey, Brent Boehlert, Michael Jacobsen, and Charles Fant IV. Janusz Strzepek provided modeling and data analysis, and Danya Rumore provided writing support and editing. Daniel Shemie and Miriam Fuchs assisted with research. The authors are grateful for useful comments provided by James Neumann. This report builds on earlier work completed by the World Bank Water Anchor.[1]

The concept for this project was approved at a Concept Note Review Meeting chaired by Jamal Saghir, and the report approved at a Decision Meeting chaired by Julia Bucknall. Invited peer review comments were received from Vahid Alavian, Ana Elisa Bucher, Michael Toman (all World Bank); Peter Droogers (Future Water); and Henk van Schaik (Co-operative Program on Water and Climate). Additional comments were received from Nagaraja Rao Harshadeep and Oivind Lier (both World Bank); H.C. Winsemius (Delft University); and Jaap Kwadijk (Deltares).

A large number of World Bank colleagues and other professionals have contributed their advice and suggestions to this report. While these individuals are too numerous to mention, the authors would like to acknowledge the contributions made early in the conceptual stage by John Matthews (Conservation International), Torkil Joenck Clausen (Danish Hydraulic Institute), Eugene Stakhiv (US Army Corp of Engineers), Henk van Schaik (Co-operative Programme on Water and Climate), and Al Duda (Global Environment Facility) as well as Vahid Alavian, Walter Vergara, Ahmed Kulsum, and Winston Yu and Ron Hoffer (all World Bank). Brian Blankespoor provided support with maps and databases, and Olusola Ikuforiji, Hywon Kim, Soo Jung Yoo, and Immaculate Bampadde all provided administrative assistance.

[1] Alavian, V. et al. 2009. *Water and Climate Change: Understanding the Risks and Making Climate Smart Investment Decisions*, Washington, DC: World Bank, November.

APPROVING MANAGER

Julia Bucknall, Sector Manager, TWIWA

CONTACT INFORMATION

This paper is available online at http://www.worldbank.org/water. The authors can be contacted through the Water Help Desk at whelpdesk@worldbank.org.

DISCLAIMER

1. INTRODUCTION AND BACKGROUND

It is now clear that, due to altering future temperature and precipitation patterns, climate change will significantly impact water supply and demand throughout the world. Varying spatially and temporally, these impacts are likely to have considerable implications for water resource planning as well as adding to the risks to water infrastructure systems and effecting return on investments in these systems (IPCC, 2007).

The variability of types of impacts has important implications for localized planning and water resources development; as a result, attention is increasingly being paid to adaptation strategies at the regional and basin level. However, the current paucity of information regarding the potential risk to hydrological systems at this scale presents a substantial challenge for effective water resources planning and investment.

1.1 Intended Use of Findings

The projections generated by this Analytical, Advisory Activity (AAA) study are intended to help bridge the gap between high-level climate change predictions (see IPCC, 2007) and the needs of decision-makers—including World Bank Task Team Leaders, government agencies, investors, and national economic development planners—whose programs and investments will be affected by basin- and regional-level impacts of climate change on water resources and related infrastructures. The results presented here are not intended for use at the project level; however, because the results provide an indication of risk or threat at the sub-basin level, they might appropriately provide inputs into decisions about the extent of analyses of climate change to be carried out at the site-specific project level. Thus, this AAA study is intended to serve three purposes:

- To assist decision-makers and stakeholders in assessing and planning for the climate risk to water resources and development in their regions.
- To assist World Bank Task Team Leaders and client country decision-makers in deciding on an appropriate level of effort for further studies at the project level.
- To stimulate additional, more detailed research at the regional and basin scales.

1.2 Relevant Prior Work and Links to Other Studies

This study is designed to build upon and extend prior work on global water resources risk under climate change, particularly the World Bank study by Alavian et al. (Alavian et al., 2009). Similarly to this study, Alavian et al. evaluated how climate change would affect hydrological indicators in World Bank client country basins; however, Alavian et al. only assessed basin-level changes in water resources under three climate scenarios—dry, medium, and wet—for each of the six World Bank regions. All World Bank regions (Latin America and Caribbean, Europe and Central Asia, Middle East and North Africa, Africa, South Asia, and East Asia and Pacific) are continental in scale. When the approach in Alavian et al. is used to assess water resources at the (sub-)basin or country level, it becomes clear that the climate

scenarios that result in dry, medium, and wet conditions at the continental scale might not correspond with the same climate scenarios for a particular country or basin within a given World Bank region. For example, the dry scenario for Africa might not be the dry scenario for Uganda or the Zambezi; the dry scenario might actually result in wetter conditions in these areas than do most other climate scenarios. Alavian et al. made evident, therefore, the levels of aggregation and the related scenario—that is, the wet, medium, or dry scenario—must be selected at the scale of interest to achieve the desired result.

Furthermore, the study by Alavian et al. clearly illustrated the importance of risk. By analyzing the full set of 56 climate scenarios for each basin, the current study explores the total extent of potential hydrologic outcomes possible within each of the world's basins. Indications of the likely outcomes as well as extremes are important for planning at the basin or country level and for making decisions on the appropriate level of effort for further analysis at the project level.

Several other studies have evaluated the effects of climate change on global water availability, but few have estimated the effects on a broad range of hydrological indicators and, to our knowledge, only Alavian et al. have studied changes in hydrological indicators across a broad suite of climate scenarios. Vörösmarty et al. (Vörösmarty et al., 2000) analyze the effect of climate change on global runoff at the 0.5 $\times$ 0.5 degree grid scale, using the Water Balance Model (WBM). This study, however, relied on only two General Circulation Models (GCMs) to generate projections. Employing a macro water model, Arnell (Arnell, 2004) considers the effects of 24 climate scenarios—four Special Report on Emissions Scenario (SRES) scenarios across six GCMs—on future runoff in 1,300 basins globally. However, Arnell focuses on runoff alone, rather than on multiple indicators of hydrological change. Milly et al.'s article (Milly et al., 2005) considers the outputs of 12 GCMs in their analysis of how climate change will affect runoff in 163 river basins, but also does not focus on diverse hydrological indicators. Using the WaterGAP model to compute monthly river discharge under climate change at both a grid and basin scale, Alcamo (Alcamo et al., 2007) evaluate the effects of climate change on worldwide water availability using a global runoff model; however, this analysis only used two GCMs under the A2 and B2 SRES scenarios (discussed in Section 2.1.3).

The results generated by this study have provided the basis for much work on water and climate change in the World Bank, including, but not limited to, work in the Sava Basin (Danube tributary), in Botswana, on the Uganda Water Resources Assistance Strategy, on the Zambezi River Basin, and on confronting a changing climate in Michoacán.[2]

[2] Kindler, J. et al. 2010. *Water and Climate Adaptation Plan for the Sava River Basin (Draft):. Europe and Central Asia*. Washington DC: World Bank. July.

World Bank. 2010. *Botswana Climate Variability and Change: Understanding the Risks*. November.

McCluskey, A. 2010. *Climate Change and Water Resources in Uganda: Review of Previous Studies and Climate Change Projections*. Technical Report submitted to World Bank.

World Bank. 2010. *The Zambezi River Basin: A Multi-Sector Investment Opportunities Analysis*. June.

World Bank. 2010b. *Confronting a Changing Climate in Michoacán*.

1.3 Key Indicators for Screening of Water Resource Projects

A host of physical and socioeconomic indicators are important for water resource project screening and planning. Physical indicators reflect conditions associated with geology, land characteristics, hydrology, hydrogeology, meteorology, water quality, and ecology; socioeconomic indicators provide insight into conditions related to institutions, demographics, economics, finance, legal systems, and culture (Helwig, 1985).This study focuses solely on hydrological indicators.

Table 1-1 provides an overview of typical water projects and the most relevant hydrological indicators for project screening. For example, when evaluating irrigation projects, mean annual runoff (MAR), reference crop water deficit, basin yield, baseflow, and monthly and annual low-flow events (described in Section 2.1.1) are the most relevant set of hydrological indicators. Each of these identified hydrological indicators is useful for providing insight into the risk of climate change on certain types of water projects; however, monthly low-flow events and daily, weekly, and monthly high-flow events were not analyzed due to the absence of a sufficiently detailed global data set.

Table 1-1. Hydrological Indicators for typical water projects

WATER PROJECT	MOST RELEVANT HYDROLOGICAL INDICATORS								
	Mean Annual Runoff	Reference Crop Water Deficit	Basin Yield	Baseflow	Daily/Weekly High-Flow Events	Monthly High-Flow Events	Annual High-Flow Events	Monthly Low-Flow Events	Annual Low-Flow Events
Irrigation and Drainage									
Irrigation	✓	✓	✓	✓				✓	✓
Drainage				✓	✓	✓	✓		
Water Supply and Sanitation									
Large-scale water supply (urban)	✓		✓	✓				✓	✓
Small-scale water supply (rural)	✓			✓				✓	✓
Wastewater treatment	✓			✓	✓	✓		✓	✓
Urban drainage	✓		✓		✓	✓			
Flood Protection									
Levies					✓	✓	✓		
Flood-control storage			✓		✓	✓	✓		
Watershed management	✓		✓	✓	✓	✓	✓	✓	✓

WATER PROJECT	MOST RELEVANT HYDROLOGICAL INDICATORS								
	Mean Annual Runoff	Reference Crop Water Deficit	Basin Yield	Baseflow	Daily/Weekly High-Flow Events	Monthly High-Flow Events	Annual High-Flow Events	Monthly Low-Flow Events	Annual Low-Flow Events
River Basin Management and Multipurpose Infrastructure									
Single-purpose agricultural reservoirs	✓	✓	✓						
Single-purpose hydropower reservoirs	✓		✓		✓	✓	✓		
Multipurpose reservoirs	✓	✓	✓		✓	✓	✓		

Key:

Evaluated in this study

Not evaluated in this study

Source: (Helwig, 1985)

1.4 Report Overview

As explained previously, Alavian et al. (Alavian, 2009) examined risks of climate change to the water sector at the basin (catchment) scale in an attempt to translate climate projections into projections of hydrologic indicators deemed useful for policy and planning of water investments. While Alavian et al.'s findings were helpful in developing a regional scale understanding of climate risk to water resources, the methodology employed did not produce results relevant at the basin level.

Building on the work of Alavian et al., this analysis provides projections for localized changes in climate, meteorological conditions, and hydrology under a range of possible future climate conditions for 8,413 river basins in World Bank client countries by region. To achieve these projections, this study examines the range of possible effects of climate change on temperature and precipitation, potential evapotranspiration (PET) and Climate Moisture Index (CMI), and runoff and six related hydrological indicators. To generate a robust high-resolution understanding of possible risk, this analysis examines relative changes in all variables from the historical baseline (1961 to 1999) to the 2030s and 2050s for the full range of 56 GCM SRES combinations evaluated in the Intergovernmental Panel on Climate Change (IPCC) Fourth Assessment Report (AR4). The data, methods, and tools used in this analysis are described in full in Section 2.

The intent of this research is to evaluate *changes* in risks to water resources at the basin level; therefore, this analysis provides relative changes in variable values rather than absolute magnitudes. The focus of

this analysis is on six hydrological indicators: MAR, basin yield, annual high flow (q10), annual low flow (q90), groundwater (baseflow), and reference crop water deficit. These indicators are described in detail in Sections 2.1 and 2.5.

To present a sense of the severity of climate change risk to each basin, exposure indices using a low, medium, and high scale were developed for the hydrologic indicators. In other words, for every basin, each indicator was categorized as facing a low, medium, or high level of threat from climate change. The exposure indices are explained in greater detail in Section 2.5.

To make this information easily accessible to Task Team Leaders and World Bank clients, the results from this study are available on the World Bank Climate Portal, a Web-based interface. On the Climate Portal, users can access graphic presentations illustrating the severity (that is, low, medium, high) of change that is projected for all of the studied variables in any country, basin, or country–basin intersection of interest. Users can also access tabular and graphic representations of all climatic and hydrological projections for analyzed areas; Section 3 presents illustrative results and a discussion of potential uses for this information.

Appendices A through C provide additional information on the historical baseline data sets and the hydrological model employed in this analysis. More information about the World Bank Climate Portal can be found in Appendix D, and the naming convention for the river basins is included as Appendix E. Appendices F and G present case studies that assess the impact of climate variability and change and adaptation strategies development in Botswana and Michoacán, Mexico.

The purpose of this document is to explain in-depth the methods used to develop these climate risk outputs, the reasons for the selected methodology, and the limitations of this study.

2. METHODOLOGY: A BASIN SCALE INDICATOR APPROACH

The approach applied in this analysis provides a robust yet tractable evaluation of the changes in risk to water resources due to climate change at the regional and basin scale for World Bank client countries. The intent of this study is to generate an understanding of the relative change in variable values, not absolute magnitudes of variable values. The results therefore provide an understanding of the range of potential consequences of climate change on water resources at the country and basin scale. These results are suitable for use as inputs to screening-level analyses of the impact of climate change on water-resource-dependent investments, such as irrigation and hydropower.

Expanding on prior work, this analysis incorporates a rigorous assessment of climate change outcomes for 8,413 river basins of the world, including monthly meteorological variables, and selected hydrological indicators under all 56 GCM-SRES climate change scenarios. The modeling process used to achieve this is presented in Figure 2-1.

This section provides an explanation of the analytical framework used in this study and describes the methods and data inputs employed. Uncertainties associated with the approach and data used are also addressed.

2.1 Analytical Framework

As portrayed in Figure 2-1, GCMs lie at the beginning of the analysis process. Projected changes in monthly temperature and precipitation for the 2030s (2030–2039) and the 2050s (2050–2059) were collected for each basin from all of the 56 available GCM-SRES combinations used in the IPCC AR4. Changes in these parameters were calculated from the historical baseline of 1961 to 1999. These 56 GCM scenarios, which incorporate three green house gasses emissions scenarios and 22 GCM frameworks (see Section 2.1.3), reflect the large variability in possible precipitation and temperature outcomes, as well as the likely variation in spatial distribution of these outcomes. Monthly GCM outputs were used in this study to capture seasonal variability in meteorological conditions over the year. The 2030s and 2050s were selected as the appropriate timeframe at which to evaluate the impacts of climate change on various hydrologic variables for two reasons: this is the relevant time-scale for current infrastructure planning, and uncertainties in projections increase dramatically beyond 2050.

Once projected changes in monthly temperature and precipitation for the 2030s and 2050s were gathered from all 56 GCM scenarios, these projections were then combined with historical data for the baseline period—1961 to1999—to produce absolute temperature and precipitation projections for each basin. These absolute temperature and precipitation projections were used to calculate projections for PET and CMI through use of the Modified Hargreaves model (Allen et al., 1998, Droogers and Allen, 2002). To generate runoff projections, inputs of PET, absolute temperature, and absolute precipitation projections were used in the climate runoff model (CLIRUN)-II, a two-layer, one-dimensional rainfall-runoff model. These processes and calculations are described below, and further details about CLIRUN-II are provided in Appendix B.

Figure 2-1. Diagram of the modeling process used in this study

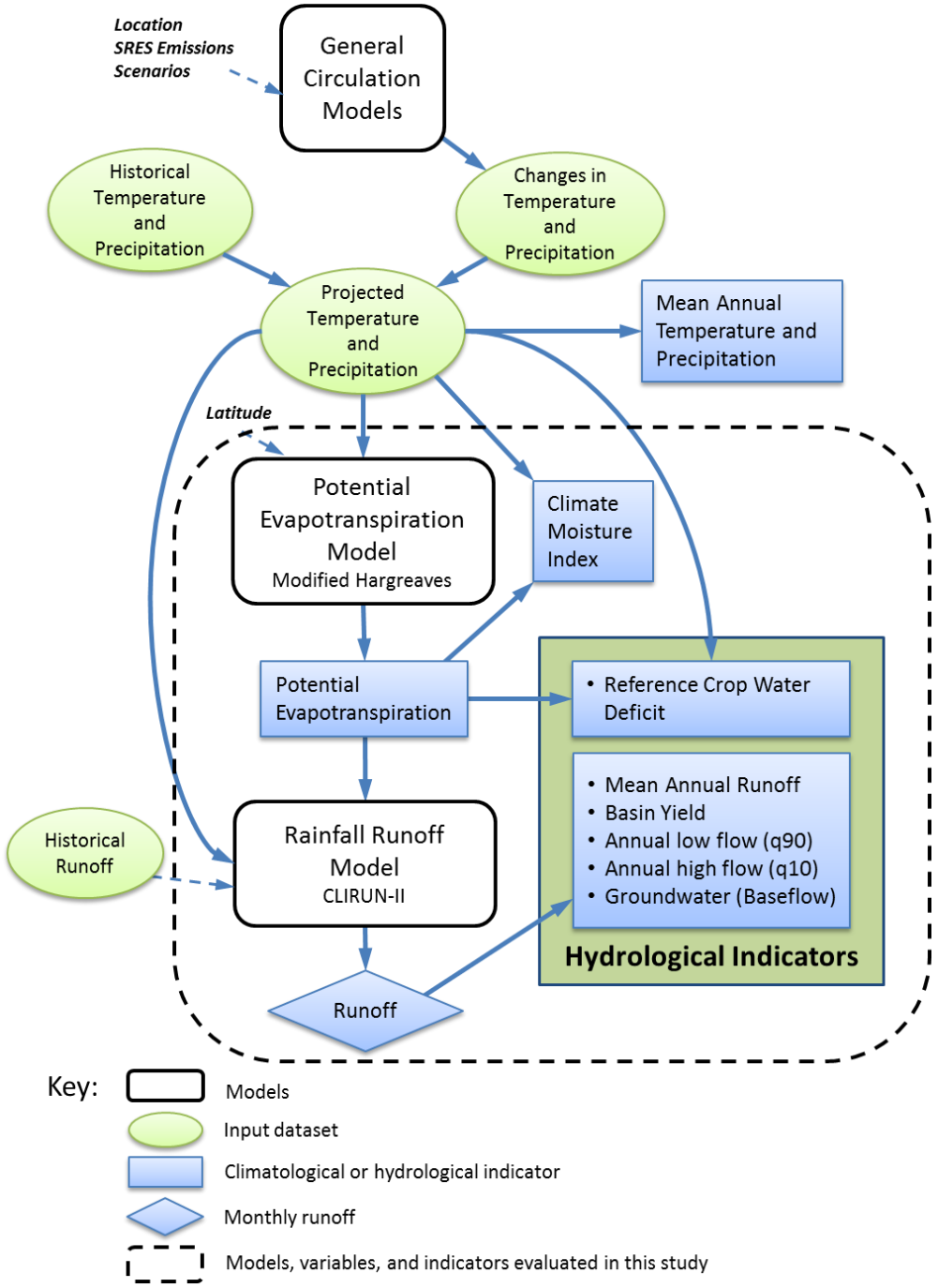

Source: Authors' representation of modeling framework

Runoff projections created by CLIRUN-II coupled with climate projections were then used to analyze the potential effect of climate change on the six hydrological indicators.

2.1.1 Hydrological Indicators

To assess the impact of climate change on water resources management and development, it was first necessary to select indicators that would provide key information about the performance of hydrological systems and water infrastructures in the near and distant future in areas that are under threat of climate change. Among others, Waggoner (Waggoner, 1990), Kirshen (Kirshen, 2005), and the United Nations World Water Assessment Program (UN/WWAP, (2003 and 2009) have proposed a set of such indicators that might be particularly helpful to policy makers and planners making decisions related to water resources investment and planning.

Drawing on insights derived from this literature, indicators were chosen for this analysis with the intent of providing an understanding of the possible impacts of climate change on water resources for those involved with World Bank water resource development projects. The indicators chosen include the following: two GCM outputs, temperature and precipitation; two calculated meteorological variables, PET and CMI; and six hydrologic variables, MAR, basin yield, annual high flow (q10), annual low flow (q90), groundwater (baseflow), and reference crop water deficit. While temperature, precipitation, PET, and CMI are useful indicators of climatic and hydrological conditions, the focus of this analysis is on the six hydrological indicators:

- **MAR:** the average annual runoff across years in a given period, for example, the 2030s.
- **Basin yield:** the maximum sustainable reservoir releases within a basin.
- **Annual high flow (q10):** the annual runoff that is exceeded by 10 percent of years in a given period, also referred to as the 10 percent exceedence flow. In a 10-year period, the q10 flow would be the second highest flow of the 10 available, which is exceeded only by the highest flow in that decade. Change in q10 is used as an indicator of flood risk.
- **Annual low flow (q90):** the converse of annual high flow, this is the 90 percent exceedence flow, or the annual runoff that is exceeded by 90 percent of years in a designated period. For a 10-year period, this would correspond to the second lowest recorded flow. Change in annual low flow is used as an indicator of drought risk.
- **Groundwater (baseflow):** the sustained flow in a river basin resulting from groundwater runoff. This indicator is used as a proxy for groundwater availability.
- **Reference crop water deficit:** the crop water demand that exceeds available precipitation. Because it was not possible for this study to measure biophysical crop water demand, PET was used to represent the water demands of a typical perennial grassland.

See Section 2.5 for more information on these indicators and the methods through which they were analyzed.

2.1.2 Resolution and Scale

Following the selections of appropriate indicators, a suitable scale and resolution for this analysis had to be established. In deciding on an appropriate scale and resolution, it is important to recognize that there is a trade-off between precision and accuracy, which Figure 2-2 visually represents. The diagram demonstrates that as resolution increases, so does uncertainty, which is due to the more detailed

information necessary to achieve this higher resolution. Similarly, a larger scale allows for a higher level of accuracy, but does not provide the precision needed for some analyses. In sum, there is price in accuracy for more precise information. Therefore, where precision is necessary, the additional uncertainty must be recognized and taken into account when assessing impacts. For this reason, the goal of an assessment—that is, what the analysis is trying to achieve and whom it is trying to inform—should ultimately drive the decision about relevant scale and resolution.

Figure 2-2. The cone of uncertainty in scale and resolution of modeling

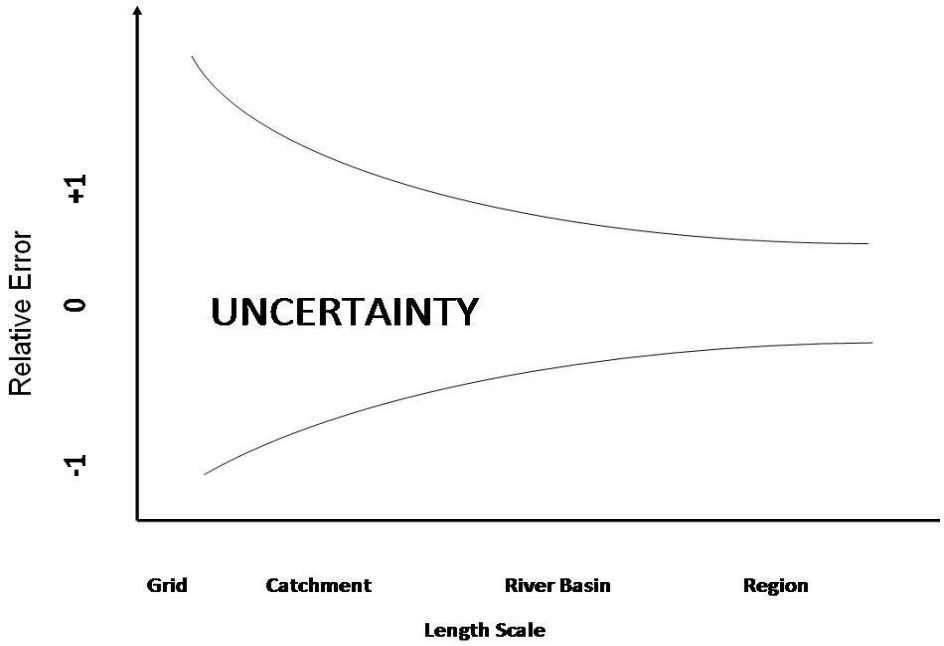

Source: Authors' representation of uncertainty in scale and resolution of modeling

Given the desire to inform water resources planning and development at the regional and local level, the basin was easily identified as the appropriate scale for this analysis. The basins defined in this study vary significantly in size, ranging from approximately 2,500 km^2, which is similar to a grid cell of 0.5 × 0.5 degrees, to more than 62,500 km^2, which is similar to a grid cell of 2.5 × 2.5 degrees.

As with most water planning and management analyses—which often require a 0.5 × 0.5 degree grid resolution (approximately 50 × 50 km) or finer for project level analyses—a basin scale assessment requires a relatively fine resolution. Problematically, GCMs provide climate change projections at a low spatial resolution (typically in the range of a 2.5 × 2.5 degree grid). Therefore, it was necessary to match the lower resolution GCM outputs with the higher resolution basin scale. For reference, Table 2-1 provides spatial resolutions for the 22 IPCC AR4 GCMs, and Table 2-2 shows typical areas of a 1 degree latitude × 1 degree longitude area across a range of latitudes.

Table 2-1. Spatial resolution of IPCC AR4 GCMs

GENERAL CIRCULATION MODELS	LAT	LONG	AREA AT 40° LATITUDE (KM^2)
Bjerknes Centre for Climate Research, Bergen Climate Model 2.0	2.81	2.81	75,115
Center for Climate Modeling and Analysis, Coupled GCM 3.1	3.75	3.75	133,538
Center for Climate Modeling and Analysis, Coupled GCM 3.1.t63	2.81	2.81	75,115
Centre National de Recherches Météorologiques, Coupled Model 3	2.81	2.81	75,115
Commonwealth Scientific and Industrial Research Organization, Mk 3.0	1.88	1.88	33,384
Commonwealth Scientific and Industrial Research Organization, Mk 3.5	1.88	1.88	33,384
Geophysical Fluid Dynamics Laboratory, Climate Model 2.0	2	2.5	47,480
Geophysical Fluid Dynamics Laboratory, Climate Model 2.1	2	2.5	47,480
Goddard Institute for Space Studies, Atmospheric Ocean Model	3	4	113,952
Goddard Institute for Space Studies, ModelEH	3.91	5	185,792
Goddard Institute for Space Studies, ModelER	3.91	5	185,792
Institute of Atmospheric Physics, Climate Model System FGOALS G 1.0	3	2.81	80,123
Institute for Numerical Mathematics, Climate Model 3.0	4	5	189,920
Institut Pierre Simon Laplace, Climate Model 4	2.5	3.75	89,025
Model for Interdisciplinary Research on Climate 3.2, High Resolution	1.13	1.13	12,018
Model for Interdisciplinary Research on Climate 3.2, Medium Resolution	2.81	2.81	75,115
Max Planck Institute for Meteorology, European Center Hamburg Model 5	1.88	1.88	33,384
Meteorological Research Institute, Coupled General Circulation Model 2.3.2a	2.81	2.81	75,115
National Center for Atmospheric Research, Community Climate System Model 3.0	1.41	1.41	18,779
National Center for Atmospheric Research, Parallel Climate Model	2.81	2.81	75,115
UK Met Office, Hadley Center Climate Model 3	2.47	3.75	87,806
UK Met Office, Hadley Center Global Environmental Model 1	1.24	1.88	22,103
Average	**2.6**	**3.0**	**80,211**

Source: IPCC AR4 background material

Table 2-2. Coverage area of a 1-degree latitude × 1-degree longitude

LATITUDE	1˚ LONG (KM)	1˚ LAT (KM)	AREA (KM^2)
0	111	111	12,393
40	85	111	9,496
60	56	111	6,181

There are a number of downscaling methods available for mapping the large-scale signals from GCMs (that is, at the scale of hundreds of kilometers) to a finer resolution (that is, at the scale of tens of kilometers). These include statistical downscaling, or the use of empirical relationships; dynamical

downscaling, or the use of regional climate models rather than global models; and spatial techniques, such as linear interpolation, krigging, spline fitting, and intelligent interpolation.[3]

Selecting a downscaling method requires careful consideration. In addition to reproducing the fundamental uncertainties associated with GCMs, many downscaling techniques introduce added uncertainties and biases. Fundamentally, through increasing the detail of information, downscaling increases the uncertainties associated with this information, as the GCM outputs are manipulated below the scale at which the physics of the GCMs themselves are mathematically described. Some downscaling schemes, due to their algorithms, violate the balances of water and energy over the GCM scale. Additionally, dynamical and statistical downscaling techniques require extensive quantification of the sensitivities on the assumptions underpinning both the GCMs and the downscaling algorithms; this can result in the need for exhaustive numerical experimentation. Hence, time and costs rarely allow the use of more than a couple GCMs in dynamical and statistical downscaling exercises. Given these challenges, running multiple GCMs at a coarser resolution might provide more insight into the range of possible future outcomes than does a higher resolution run of a few GCMs.

Essentially, there is no single best method for downscaling; rather, the most appropriate and effective method for a given analysis must strike a careful balance between resolution and confidence in the projections. For the reasons stated previously, dynamical and statistical downscaling techniques were not desirable for this analysis. Hence, a spatial technique was employed.

The projections for the 56 GCM-SRES combinations were run at their native spatial grid scale (see Table 2-1). The projected changes in temperature and precipitation for the 2030s and 2050s for each GCM-SRES were then directly mapped onto a 0.5 × 0.5 degree grid. This grid was combined with a corresponding same-size grid of historical monthly precipitation and temperature data to generate absolute temperature and precipitation projections for each 0.5 × 0.5 degree cell. This approach captures the range of potential climate change impacts at a higher resolution without downscaling the GCMs themselves, thereby achieving a balance between precision and accuracy. This process is described in greater depth in Section 2.2.

To allow for a basin-level analysis and to reduce some of the uncertainty associated with interpolating GCM outputs to a higher resolution, the 0.5 × 0.5 degree gridded temperature and precipitation data were then reaggregated to the basin scale. Basins range significantly in size, from the smallest catchments of less than one square kilometer to drainage areas for rivers such as the Nile or Amazon that are well over the typical grid scale of a GCM (that is, 2.5 × 2.5 degrees). To allow for reasonable accuracy, basin sizes were selected to be no smaller than the solution of available climatic data (0.5 × 0.5 degree); a total of 8,413 basins in World Bank regions were analyzed.

Basin scale aggregation was achieved using GIS software to overlay basin boundaries with the 0.5 × 0.5 degree grids, and then aggregating cells based upon their weighted area in each basin. Using a section of India, Figure 2-3 shows the three scales relevant to this study: the 0.5 × 0.5 degree grid, the 2.5 × 2.5 degree grid, and the basins.

[3] Commonly considered a variation of downscaling, spatial techniques do not involve a downscaling algorithm. The majority of downscaling being done use a spatial technique type of method.

Figure 2-3. Section of Indian subcontinent showing 0.5 × 0.5 degree grid scale, 2.5 × 2.5 degree grid scale, and basin boundaries

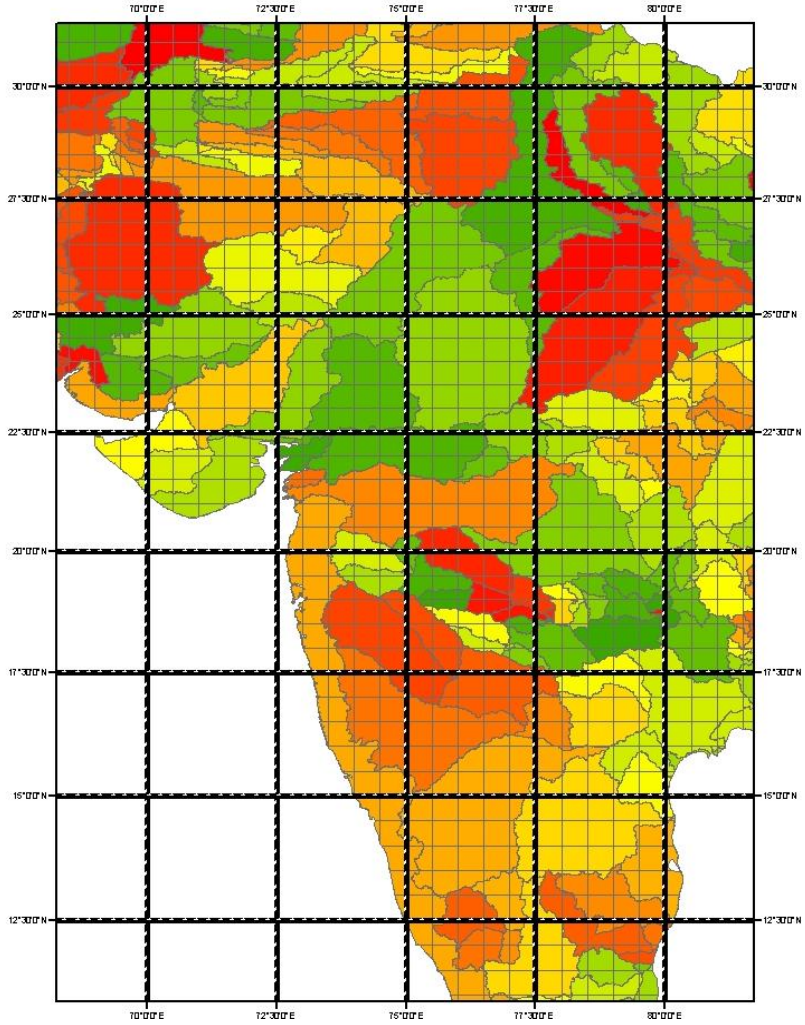

Source: Model representation. Basin boundaries are USGS Hydro 1K level 4

2.1.3 Climate Scenarios

As mentioned previously, relying on outputs from a single or handful of GCMs is problematic for a variety of reasons. There are errors in every model and natural variability in any particular run, creating significant uncertainty. An estimate of the uncertainty due to natural variability can be produced through running a single model multiple times with different initial conditions. However, this does not address the uncertainties associated with the fundamental assumptions, model physics, and parameterization built into the model itself.

Employing a group of GCMs rather than one individual GCM can help account for model biases and errors. Yet the use of multimodel ensembles raises its own questions, predominantly: how to capture the full range of results from model runs.

Using the mean of multiple models with the assumption that the mean is a good representation of all runs can lead to wrong conclusions, and therefore strong caution is advised when using this approach. Of particular concern, relying on a mean might mask extreme values. For example: a multimodel ensemble mean of near zero could signify that all models predict near-zero change; however, it could also be the result of two polar opposite outputs canceling each other out. This is demonstrated in Figure 2-4. In water management and planning, risk is typically associated with extremes, so failing to capture these extremes could be highly problematic.

Figure 2-4. Range of relative change from baseline for GCMs. Mean is shown in bold

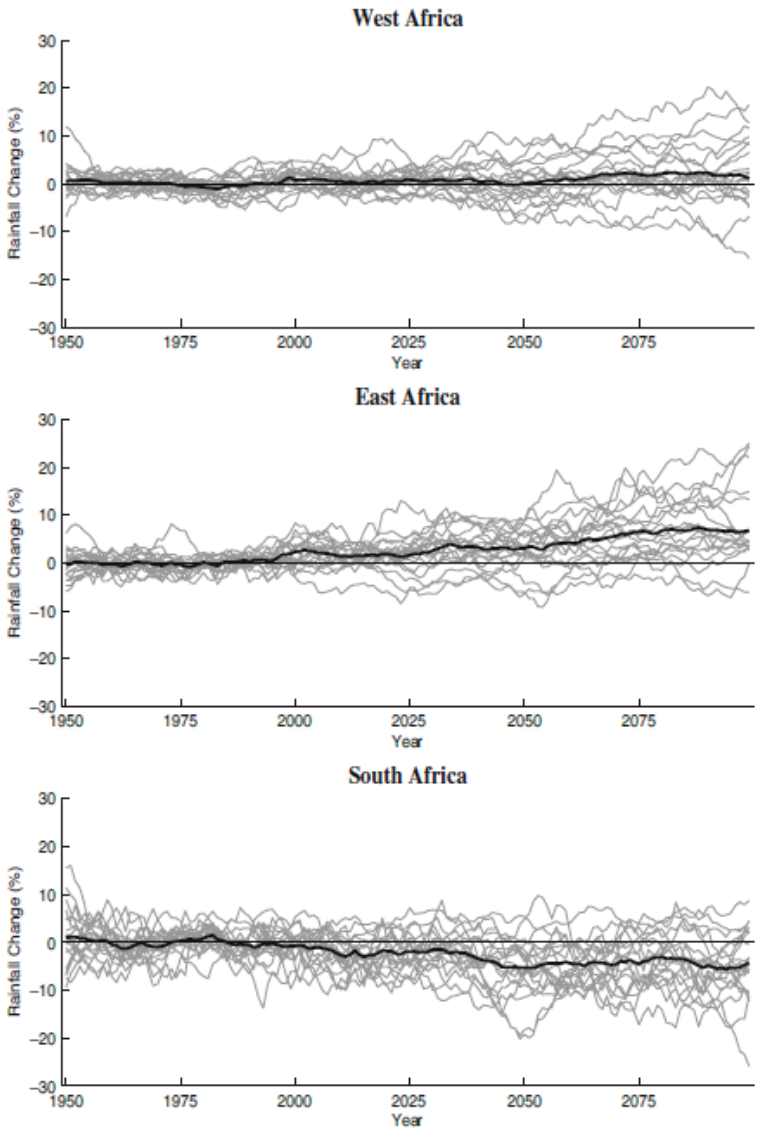

Source: (Giannini et al. 2008)

An additional challenge associated with multimodel ensembles is that the variation in model outcomes might potentially be construed as noise. Fortunately, evidence indicates a certain amount of consistency

in some of the more significant outputs generated by multimodel ensembles, suggesting that—while one should not rely on a single model alone—each model run can potentially produce important information that should not be ignored. Often, the direction of change is consistent among the climate models, and the range of possible outcomes that they produce should be considered explicitly in assessments of potential future impacts.

While filtering out any GCM scenarios that are implausible—or extremely unlikely—for the region of concern could improve the use of multiple models, it is difficult to unequivocally ascertain which scenarios should be excluded, and there are currently no definitive criteria for making this determination. Techniques that would determine which scenarios are most applicable to each region based upon probabilistic analysis are currently being developed; however, these are not yet available for practical use.

Given these challenges and constraints, it was decided that this analysis would employ climate projections from the full range of available models for the B1, A1B, and A2 SRES scenarios (17, 22, and 17 GCMs, respectively, for a total of 56 GCM-SRES combinations). These scenarios were chosen because they are generally in the middle range of the marker SRES scenarios identified by the IPCC, and are the most commonly used emissions scenarios for impact and adaptation assessments. Figure 2-5 presents a range of SRES scenarios and their emissions outputs.[4]

The three SRES scenarios used in this study follow:

- **B1: low-end emissions scenario**. This scenario represents a world where population peaks in the middle of the 21st century, economic structures rapidly move toward a service and information economy, and resource-efficient technologies are introduced with commensurate reductions in material intensity.
- **A1B: moderate emissions scenario.** Part of the broader A1 family of scenarios, A1B population peaks mid-century, economic growth occurs rapidly, efficient technologies are introduced, and a mix of fossil and nonfossil fuels are adopted.
- **A2: high-end emissions scenario.** Under A2, global population continually increases and economic growth is regional and slower than in other scenarios.

The 22 GCMs that were run for each of the three selected SRES scenarios are displayed in Table 2-3.

Each of these 56 GCM-SRES combinations was used to generate projections of temperature and precipitation for the 2030s and 2050s for all 8,413 basins. The process used to translate these temperature and precipitation projections into changes in hydrological indicators in each basin is explained further below.

[4] There are a total of 40 SRES scenarios, organized into four scenario families (A1, A2, B1, and B2). Marker scenarios represent a given scenario family, although they are not considered to be any more likely to occur than the other scenarios. These marker scenarios include A1B, A2, B1, and B2, and two additional scenarios for the groups A1F1 and A1T. For further details, see (IPCC, 2009).

Figure 2-5. Greenhouse gas (GHG) emissions and estimated global surface warming for SRES scenarios, 2000 to 2100

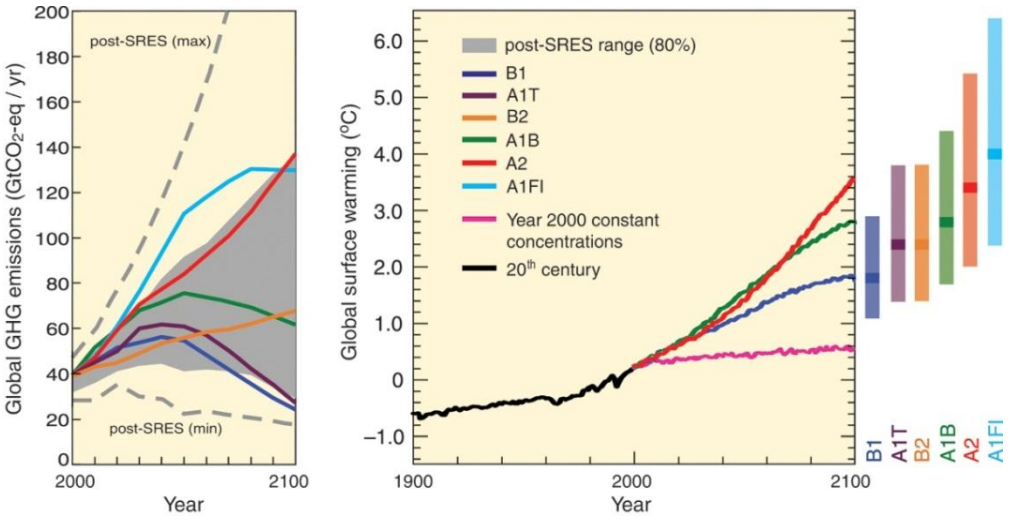

Source: IPCC AR4

Table 2-3. Available combinations of IPCC GCMs and SRES scenarios B1, A1B, and A2

GENERAL CIRCULATION MODELS	COUNTRY OF ORIGIN	SRES SCENARIO		
		B1	A1B	A2
Bjerknes Centre for Climate Research, Bergen Climate Model 2.0	Norway	✓	✓	✓
Center for Climate Modeling and Analysis, Coupled GCM 3.1	Canada	✓	✓	✓
Center for Climate Modeling and Analysis, Coupled GCM 3.1.t63	Canada	✓	✓	
Centre National de Recherches Météorologiques, Coupled Model 3	France	✓	✓	✓
Commonwealth Scientific and Industrial Research Organization, Mk 3.0	Australia	✓	✓	✓
Commonwealth Scientific and Industrial Research Organization, Mk 3.5	Australia	✓	✓	✓
Geophysical Fluid Dynamics Laboratory, Climate Model 2.0	US		✓	✓
Geophysical Fluid Dynamics Laboratory, Climate Model 2.1	US	✓	✓	✓
Goddard Institute for Space Studies, Atmospheric Ocean Model	US	✓	✓	
Goddard Institute for Space Studies, ModelEH	US		✓	
Goddard Institute for Space Studies, ModelER	US	✓	✓	✓
Institute of Atmospheric Physics, Climate Model System FGOALS G 1.0	China	✓	✓	
Institute for Numerical Mathematics, Climate Model 3.0	Russia	✓	✓	✓
Institut Pierre Simon Laplace, Climate Model 4	France	✓	✓	✓
Model for Interdisciplinary Research on Climate 3.2, High Resolution	Japan	✓	✓	
Model for Interdisciplinary Research on Climate 3.2, Medium Resolution	Japan	✓	✓	✓
Max Planck Institute for Meteorology, European Center Hamburg Model 5	Germany	✓	✓	✓
Meteorological Research Institute, Coupled General Circulation Model 2.3.2a	Japan	✓	✓	✓
National Center for Atmospheric Research, Community Climate System Model 3.0	US	✓	✓	✓
National Center for Atmospheric Research, Parallel Climate Model	US		✓	✓
UK Met Office, Hadley Center Climate Model 3	UK		✓	✓
UK Met Office, Hadley Center Global Environmental Model 1	UK		✓	✓

Source: IPCC AR4

2.1.4 Hydrological Model Selection

As mentioned previously, CLIRUN-II was the hydrologic model used in this study. While several global hydrologic models could have been used for this analysis, the results likely would not have differed significantly, as each of these models use similar governing equations.

For this analysis, CLIRUN-II was calibrated and validated using a separate set of historical runoff, temperature, and precipitation data. The CLIRUN-II model and the process used to calibrate and validate it are discussed in Section 2.4

2.2 Data Inputs and Processing

PET projections were calculated through use of the Modified Hargreaves method (Allen et al. 1998, Droogers and Allen 2002) using four core inputs: baseline temperature, precipitation from historical data sets, and projected temperature and precipitation generated by the 56 GCM-SRES combinations. In conjunction with the other inputs, PET projections were then used to generate CMI and the reference crop water deficit.

The core inputs and PET were inserted into CLIRUN-II to generate projections of future runoff, which was then used to calculate projected impacts on the six hydrological indicators. Here, we describe these baseline and projected data sets, along with the steps to process them into a form compatible with the PET and runoff models.

2.2.1 Baseline Temperature and Precipitation Data

To calculate future temperature and precipitation projections, which are critical inputs for CLIRUN-II, it was necessary to gather baseline precipitation and temperature data for 1961to 1999, the historical period used as a baseline in this study. This baseline climate data was taken from the University of East Anglia's Climate Research Unit (CRU) Time Series (TS) 2.1 data set. Typically used by the World Meteorological Organization as the standard reference baseline for climate change impact studies, the CRU TS 2.1 data set provides a monthly time series of precipitation and temperature for 1901 to 2002 on a 0.5×0.5 degree grid. The mean temperature and precipitation for the world's 8,413 basins between 1961 and 1999, according to the CRU data set, are show in Figure 2-6. Additional information on construction, validation, and uncertainties of the CRU data set are provided in Appendix A.

Figure 2-6. Mean annual temperature (top map, in degrees Celsius) and precipitation (bottom map, in millimeters) in the 8,413 basins within World Bank client countries, 1961 to 1999

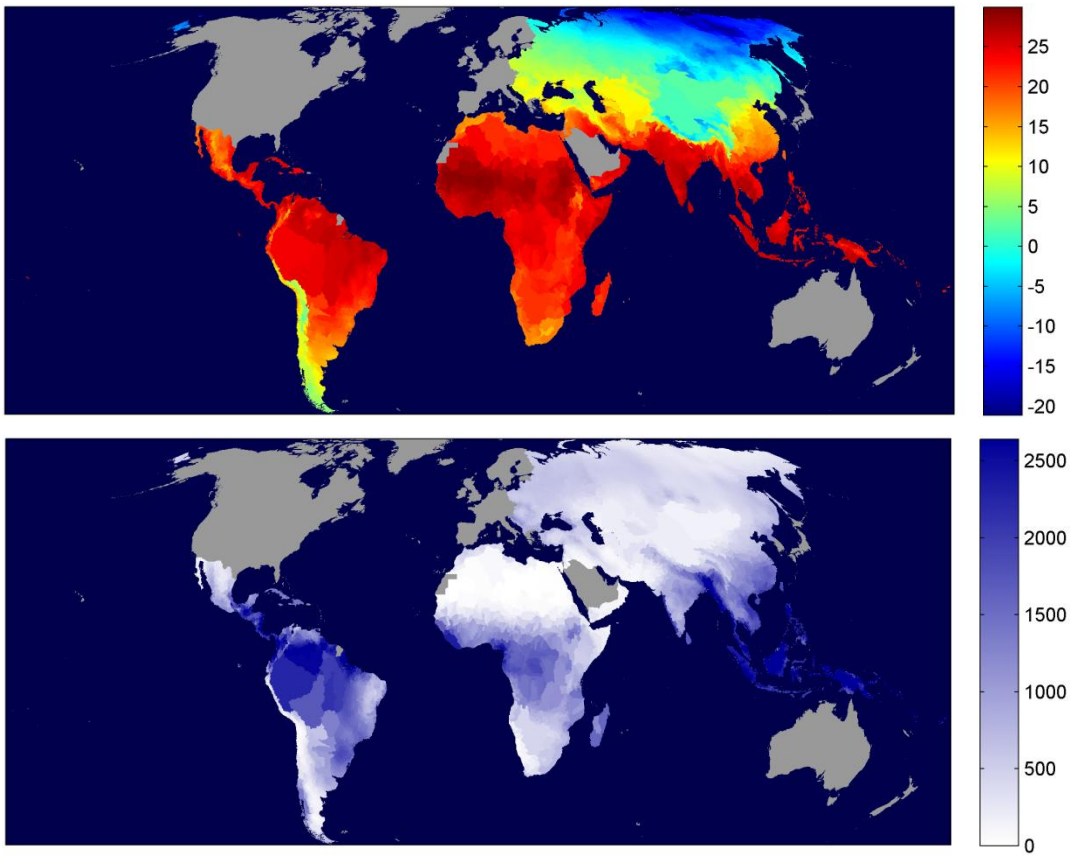

Source: CRU TS 2.1 data set

2.2.2 Projections of Temperature and Precipitation under Climate Change

As described previously, climate change projections for the timeframes of interest (that is, the 2030s and 2050s) were derived from each of the 56 GCM-SRES scenarios.

Archived outputs from the IPCC include modeled monthly baseline (1961 to 1999) and projected precipitation and temperature for each GCM-SRES combination. Importantly, a modeled baseline was used rather than the actual historical baseline to control for upward or downward biases in GCMs, thereby allowing for the most accurate representation of relative change.

To effectively compare projected changes in temperature and precipitation across different GCMs with different modeled baselines, it is necessary to first translate the modeled baselines and projections provided by the IPCC into changes relative to the baseline. To do this, these modeled baseline and projected outputs were first averaged by month, so that within each grid cell, variable, and GCM-SRES combination, there were 12 mean monthly outputs for the 39-year baseline and 12 projected monthly projections for temperature and precipitation for each future decade of interest. The modeled baseline and projected temperature and precipitation outputs were then translated from the GCMs' native

resolution into the 0.5 × 0.5 degree resolution (see Section 2.1.2 for details on this process). Changes in precipitation and temperature were generated using the delta method, whereby the mean monthly decadal values were converted to changes relative to the baseline by subtracting the modeled baseline from the projected values to produce delta temperature and precipitation:

$$\Delta P = P_{\text{projected}} - P_{\text{baseline}}$$

$$\Delta T = T_{\text{projected}} - T_{\text{baseline}}$$

Where *P* represents precipitation and *T* represents temperature.[5]

Finally, these relative changes were coupled with the CRU historical data set to generate absolute monthly projections of temperature and precipitation at the 0.5 × 0.5 degree resolution under each GCM-SRES combination.[6]

2.2.3 Converting Gridded Data to the Basin Scale

To generate basin-level runoff, CLIRUN-II requires absolute temperature and precipitation projections for each basin. Therefore, it was necessary to process the absolute precipitation and temperature projections from the 0.5 × 0.5 degree resolution to the basin scale.

To do this, GIS was used to overlay basin boundaries with the 0.5 × 0.5 degree grid of absolute temperatures and precipitations. Cells were then aggregated within basin boundaries based upon their weighted area in that basin. This overlay of scales is demonstrated in Figure 2-3. The result is a matrix of 8,413 basin values for each of the 56 GCM-SRES combinations for baseline runoff and both baseline and projected precipitation and temperature. Figure 2-7 presents the 8,413 river basins.

[5] The so called delta method has been widely applied in water planning studies. Typically, the delta method applies monthly changes in temperature and precipitation from a GCM to an observed set of station or gridded temperature and precipitation data that are inputs to a hydrologic model (Hamlet et al., 2010).

[6] Note that if the change in precipitation calculated for a particular grid cell, GCM, and month is negative and greater in absolute value than the observed historical value, then the projected precipitation value would be negative. For example, if modeled precipitation for a grid cell, month, and GCM for the 2030s is 50 mm and GCM-modeled baseline precipitation is 100 mm, the delta precipitation would be –50 mm. If observed, or actual, precipitation is 40 mm in the baseline, then the resulting projected precipitation would be –10 mm [that is, 40 mm + (–50 mm)]. In these instances, projected precipitation is set to 1 mm.

Figure 2-7. Map of the 8,413 global river basins within World Bank client countries

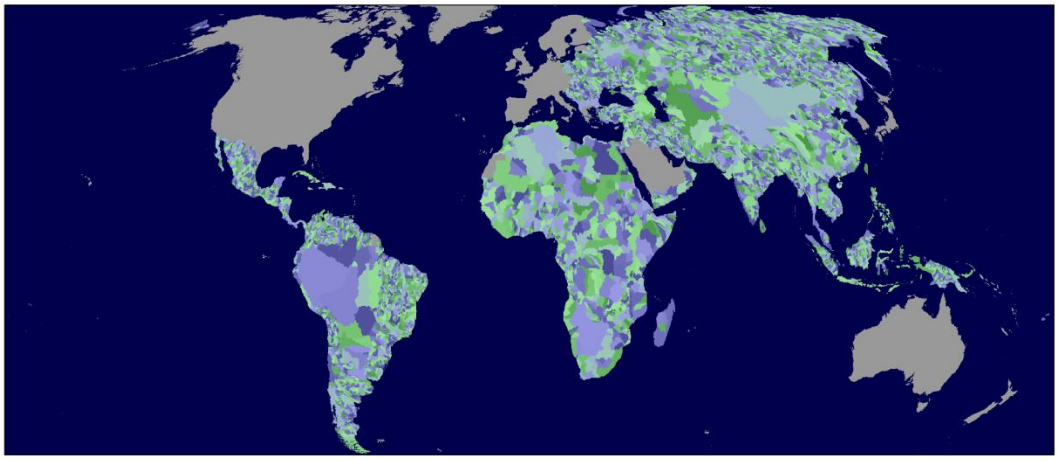

Source: Model representation. Catchments from USGS Hydro 1 K level 3 (Africa) and 4 (rest of the world)

2.2.4 Baseline Basin Runoff

In addition to requiring absolute precipitation and temperature inputs, CLIRUN-II also requires baseline natural runoff inputs for calibration. Rainfall runoff models simulate the relationship between precipitation (rain and snow) and natural, unmanaged runoff. As such, these models require natural runoff data to calibrate the simulated runoff outputs. Historical average monthly runoff was gathered from the University of New Hampshire (UNH) Global Runoff Data Center (Fekete et al., 2000, GRDC, 2007). This data set—the UNH-GRDC Composite Runoff Fields V 1.0—is derived from observed discharge information through use a climate-driven water balanced model (gauge locations are shown in Figure 2-8). Through using combined runoff fields, the UNH-GRDC approach preserves the accuracy of the discharge measurements as well as the spatial and temporal distribution of simulated runoff, thereby providing the best estimate of terrestrial runoff over large domains. It employs a gridded river network at the 0.5 $\times$ 0.5 degree spatial resolution to represent riverine pathways and to link continental landmasses to oceans through river channels. The UNH-GRDC data set provides 12 monthly mean values and a MAR for more than 50,000 global 0.5 $\times$ 0.5 degree grids, covering much of the global land area outside of the permanently ice-covered areas such as Antarctica and much of Greenland.

Figure 2-8. Locations of gauging stations used in the GRDC database

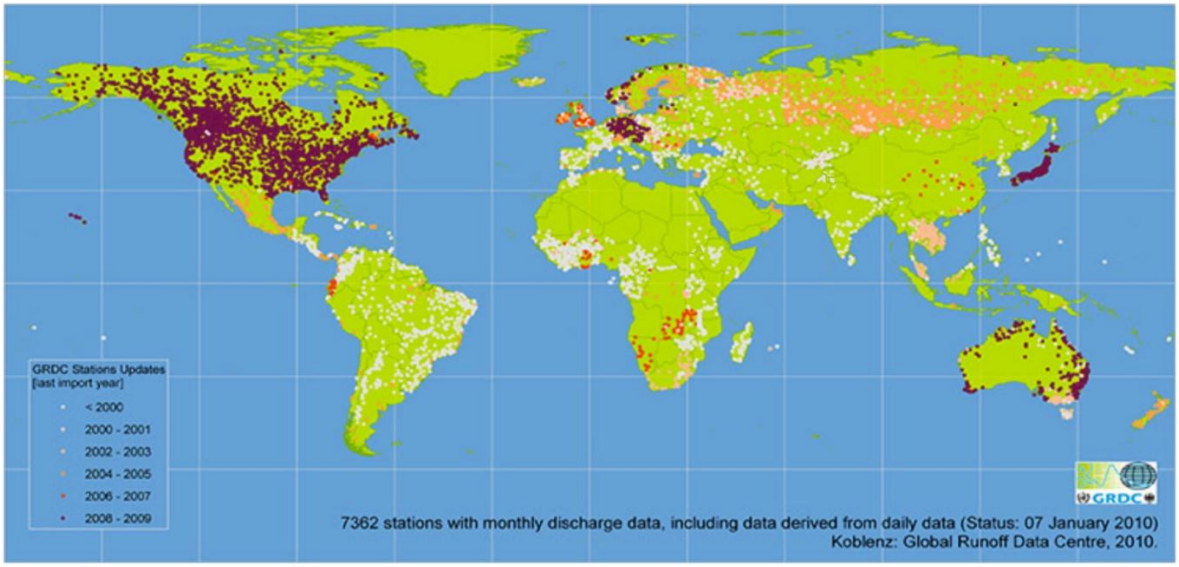

Source: (GRDC, 2007)

Similar to absolute temperature and precipitation projections, baseline runoff data had to be processed from the 0.5 × 0.5 scale to the basin scale; this was achieved through using GIS to overlay basin boundaries with the 0.5 × 0.5 degree grid of historical baseline runoff values. Cells were then aggregated within basin boundaries based upon their weighted area in that basin. The final outcome was 8,413 basin scale historical baseline runoff values. Additional information on construction, validation, and uncertainties of the UNH-GRDC data set are provided in Appendix A.

2.3 Calculating Changes in PET under Climate Change

Once projections of absolute temperature and precipitation under climate change and baseline runoff had been gathered for each basin, basin-level estimates of PET and CMI were made for each of 56 GCM-SRES combinations. PET is a necessary input into CLIRUN-II and is also used to calculate CMI and reference crop water deficit, two of the outputs of this analysis. CMI is a measure of aridity; projected changes in CMI are included in the data portal to provide an understanding of the general changes in hydroclimatic conditions at the basin level due to climate change.

2.3.1 Calculating Changes in PET

Average annual evapotranspiration (ET) is a measure of the amount of water lost to the atmosphere from the surface of soils and plants through the combined processes of evaporation and transpiration (that is, water consumed by vegetation) during the typical year. By contrast, average annual PET is a calculated parameter that represents the amount of water lost through evaporation and transpiration (that is, water consumed by vegetation) during a typical year under the condition that sufficient water is available at all times. PET depends upon several variables, including temperature, humidity, solar radiation, and wind velocity. If adequate water is available, ET should be equal to PET.

As mentioned previously, PET is a necessary input into CLIRUN-II, as well as a factor used to calculate CMI and reference crop water deficit. In this study, the Modified Hargreaves method (Allen et al., 1998, Droogers and Allen, 2002) was used to calculate PET. Baseline basin-level PET was calculated based on historical precipitation and temperature data taken from the CRU data set, along with the latitude of the basin centroid which is used to estimate solar radiation. Projected absolute temperature and precipitation were used to calculate projected PET for each basin under all 56 GCM-SRES combinations. Because this analysis is concerned with changes due to climate change, the change between baseline and projected PET was then assessed.

2.3.2 Calculating changes in the climate moisture index

Once baseline and projected PET were calculated, these values were used to generate baseline and projected CMI for each basin under all 56 GCM scenarios.

CMI, an indicator of aridity, is a function of both annual precipitation and average annual PET. If PET exceeds precipitation, the climate is considered dry. To the contrary, if precipitation is greater than PET, the climate is considered moist. Using P to represent precipitation, the equation for CMI is $CMI = (P/PET) - 1$ when $PET > P$; and $CMI = 1 - (PET/P)$ when $P > PET$. A CMI of -1 is very arid and a CMI of $+1$ is very humid. As such, CMI is a useful indicator of overall hydroclimatic conditions.

Baseline basin-level CMI was calculated using calculated baseline PET and the CRU historical baseline data for precipitation. Projected basin-level CMI was calculated using projected PET and projected absolute precipitation for all 56 GCM-SRES scenarios. Baseline CMI and projected CMI were then used to assess the projected change in CMI for each basin under all 56 GCM scenarios.

2.4 Modeling Changes in Global Runoff under Climate Change

To model changes in runoff, this study employed CLIRUN-II: a two-layer, one-dimensional infiltration and runoff estimation tool that uses historic runoff as a means to estimate soil characteristics.[7] This section provides an overview of CLIRUN-II and its inputs, outputs, and calibration process; a more detailed description of the model, the calibration and validation process, and uncertainties can be found in Appendix B.

2.4.1 Background

CLIRUN-II (Strzepek and Fant, 2010) is the latest model in a family of hydrologic models developed specifically for the analysis of the impact of climate change on runoff. Kaczmarek (Kaczmarek, 1993) presented the theoretical development for CLIRUN, a single-layer, lumped, watershed rainfall runoff model, which he applied to the Yellow River in China (Kaczmarek, 1998). Yates (Yates, 1996) expanded on the basic CLIRUN model by adding a snow-balance model and providing a suite of possible PET models; he then packaged the expanded CLIRUN model in a Water Balance (WatBal) model. WatBal has

[7] Note that runoff estimates are available from the GCMs directly for some models. Within GCMs, runoff is modeled by the land surface component at a scale that varies from GCM to GCM. Validation of modeled runoff takes place at a continental or large-scale river basin level. Thus, at the scale of the catchments for this analysis, GCM runoffs can be unreliable.

been used on a wide variety of spatial scales from small and large watersheds to globally on a 0.5 × 0.5 degree grid (Strzepek et al., 1999, Huber-Lee et al., 2005, Strzepek et al., 2005).

While CLIRUN and WatBal were able to successfully model mean monthly and annual runoff, which is important for water supply studies, they did not accurately model the runoff distribution tails, which are representative of floods and droughts. Incorporating most of the features of WatBal and CLIRUN, CLIRUN-II, which operates at a monthly time-step, was developed specifically to address the issue of modeling extreme events at the monthly and annual level.[8] CLIRUN-II has adopted a two-layer approach following the framework of the six-parameter (SIXPAR) hydrologic model (Gupta and Sorooshian, 1983, 1985) and employs unique conditional parameter estimation procedures.

2.4.2 Model Inputs

CLIRUN-II requires inputs of monthly precipitation and temperature, mean range in daily temperature for monthly PET, and observed monthly runoff. The baseline climate variables and observed runoff are used for calibration, and both the baseline and projected climate variables are subsequently used for simulation, that is, generation of modeled runoff outputs. As described previously, the baseline and projected inputs for CLIRUN-II were synchronized at a 0.5 × 0.5 degree resolution, and then spatially aggregated using river basin boundaries in GIS. PET was estimated based on precipitation, temperature, temperature range, and latitude using the Modified Hargreaves approach, described in Section 2.3. The required input data along with the source and units are listed in Table 2-4.

Table 2-4. Required inputs for CLIRUN-II

INPUT PARAMETER	BASELINE/ PROJECTED	UNIT	SOURCE
Precipitation	Baseline	mm/month	CRU TS 2.1
	Projected		CRU TS 2.1 and GCMs
Temperature	Baseline	˚C	CRU TS 2.1
	Projected	˚C	CRU TS 2.1 and GCMs
Temperature Range	Baseline	˚C	CRU TS 2.1
Observed Runoff	Baseline	mm/month	UNH-GRDC

Source: CLIRUN-II model documentation

2.4.3 Model Structure

CLIRUN-II models runoff as a lumped watershed with climate inputs and soil characteristics averaged over the watershed, simulating runoff at a gauged location at the mouth of the basin. The model reports surface runoff, subsurface runoff, baseflow, and total runoff, where total runoff is the sum of surface runoff, subsurface runoff, and baseflow. In this study, four of the hydrological indicators (MAR, q10, q90,

[8] Given the availability of runoff data at the global scale, this study projects changes in the magnitude of annual low and high flow events at the basin scale only. Although CLIRUN-II is capable of evaluating changes at the monthly level, this would require a longer time series than is available through the GRDC.

and basin yield) rely on the total runoff output, and the groundwater indicator relies on the baseflow output.

A schematic of the model is included in Figure 2-9. The figure shows the mass balance of water in the CLIRUN-II system. Water enters via precipitation and leaves via ET and runoff. The difference between inflow and outflow is reflected as change in storage in the soil or groundwater. Soil moisture is modeled as a two-layer system: a soil layer (upper layer) and a groundwater layer (lower layer). These two components correspond to a quick and a slow runoff response to effective precipitation (that is, precipitation plus snowmelt). Quick runoff is the portion of the effective precipitation that directly enters the stream system as surface runoff. Direct runoff is a function of the soil surface and is modeled differently for frozen soil and nonfrozen soil, which is determined by temperature. The remaining effective precipitation infiltrates into the soil layer and generates slow runoff. A nonlinear set of equations determines how much water leaves the soil as subsurface runoff, how much is percolated to the groundwater, and how much goes into soil storage. The subsurface runoff has a linear relation of soil water storage, and percolation has a nonlinear relationship of both soil and groundwater storage. Groundwater receives percolation from the soil layer and baseflow is generated as a linear function of groundwater storage.

Figure 2-9. Schematic of water flows in CLIRUN-II

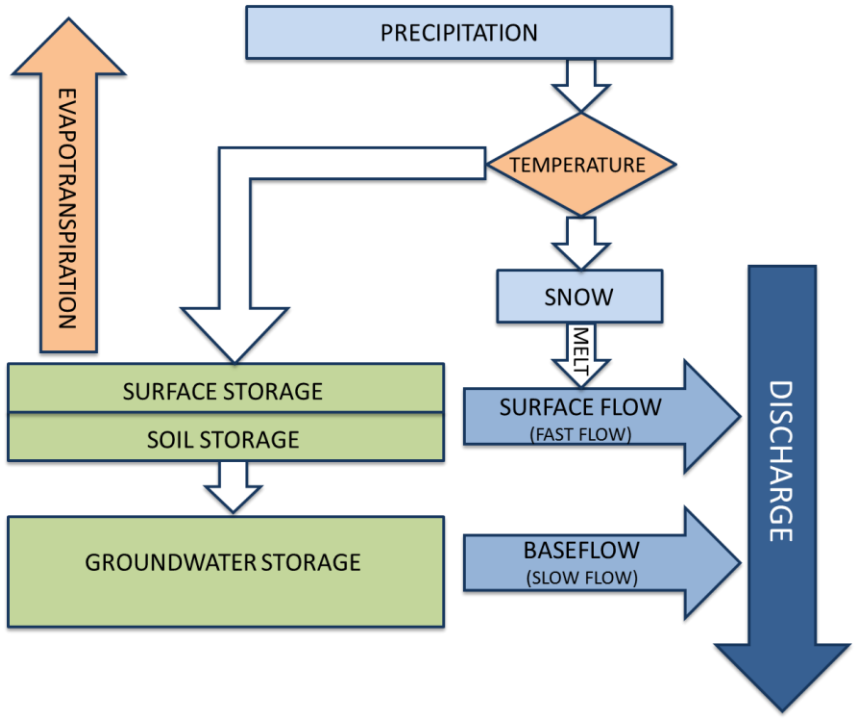

Source: Authors' representation of water flows in CLIRUN-II

2.4.4 Calibration

The CLIRUN-II model was calibrated with data from the UNH-GRDC data set described in Section 2.2.4; through calibration, the squared deviation between the 12 monthly GRDC runoff values and the 12

monthly averaged CLIRUN-II model outputs from the 10-year simulation period are minimized. The 10-year simulation period was chosen to best represent the decade used to generate the 12 months of GRDC runoff data. Although a longer simulation period could have been used to calibrate CLIRUN-II, the additional years would have been less coincident with the GRDC data to which the model was being calibrated. The following parameters are adjusted during the calibration process:

- soil depth,
- snowmelt temperature,
- snow formation temperature.
- surface runoff coefficient,
- percolation coefficient,
- subsurface runoff coefficient, and
- canopy intercept.

During the calibration process, the parameters are adjusted so that the modeled runoff values for 120 months (that is, 10 years of monthly data) most closely match the mean modeled monthly runoff with the GRDC data.

Once calibration was completed, the resulting modeled runoff was checked for any unacceptable variations from the UNH-GRDC runoff data, as well as for any unrealistic maximum or minimum runoff projections.

Figure 2-10 shows the R^2 for the CLIRUN-II calibration for all basins modeled. Most of the basins had a calibration R^2 of above 0.8, indicating the model is doing a good job of reflecting the major sources of variation in basin scale runoff. However, there were a number of basins (northern and far eastern Africa, Central Asia, and southern South America) that had poor calibration (see Figure 2-11). From the maps, it appears that the poor calibrations tend to correspond with dry areas; accordingly, good calibrations tend to correspond with wetter areas.

The difference in calibration can largely be attributed to errors in the data provided by the UNH-GRDC data set used for calibration: areas of poor calibration correlate to the areas where there are few to no gauge stations and, hence, a paucity of data (see Figure 2-8). A comparison of the performance of CLIRUN-II with GRDC inputs versus in-country data is provided in Appendix C.

Figure 2-10. Calibration results (R^2) for 8,413 basins using CLIRUN-II

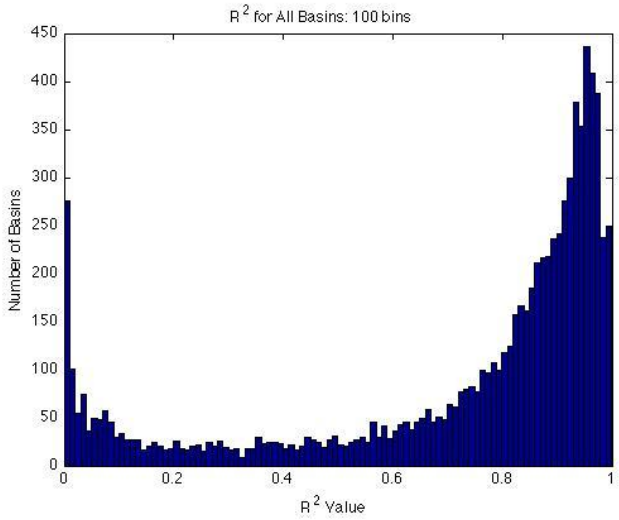

Source: Model results based on authors' calculations

Figure 2-11. CLIRUN-II calibration results (R^2) for Africa and East Asia

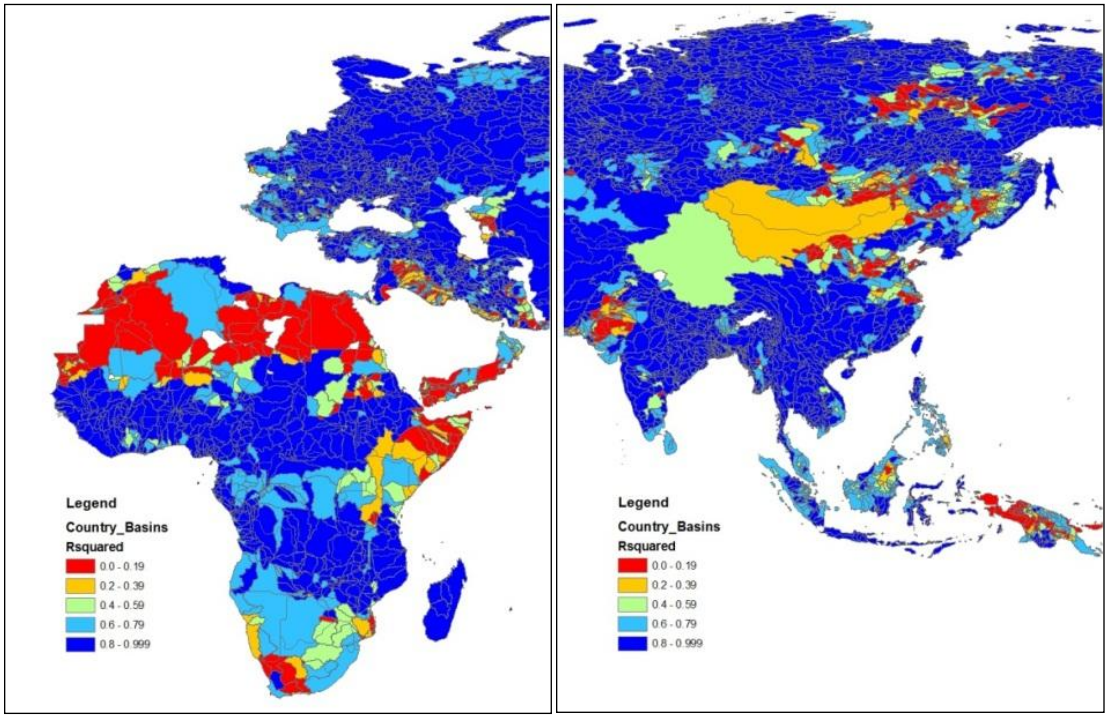

Source: Model results based on authors' calculations

2.4.5 Outputs

After calibration, CLIRUN-II is used to generate modeled monthly baseline and projected runoff in each of the 8,413 basins based on temperature and precipitation inputs from CRU and the GCMs. Importantly,

the baseline runoff being used to compare with runoff under climate change is not historically observed runoff; it is the modeled runoff generated through use of the CRU climate data set. UNH-GRDC runoff data is only used to calibrate the CLIRUN-II model for each basin.

Once absolute modeled baseline runoff and projected runoff had been generated by CLIRUN-II for each basin under all GCM-SRES scenarios, these runoff values were used to calculate changes in the six hydrological indicators.[9]

2.5 Calculating Changes in Hydrological Indicators under Climate Change

While there are 10 indicators reported in this study (see Section 2.1), the focus of the analysis is on six hydrologic indicators: MAR, basin yield, annual high flow, annual low flow, groundwater (baseflow), and reference crop water deficit. Using calculated baseline and projected PET and the modeled baseline and projected runoff generated by CLIRUN-II, basin-level changes in these variables were analyzed for all 56 GCM-SRES combinations. Figure 2-12 provides a diagrammatic representation of these indicators and their interactions with the hydrological cycle.

[9] Each of the separate runoff values—surface runoff, subsurface runoff, baseflow, and total runoff—is directly output as a runoff depth per unit time (mm/month). However, some indicator calculations require runoff in volume per unit time, such as cubic meters per second (cms) or million cubic meters (MCM) per month. To convert runoff depth per unit time to volume per unit time, the depth per unit time value is multiplied by the area of each basin.

Figure 2-12. Diagram of hydrological indicators

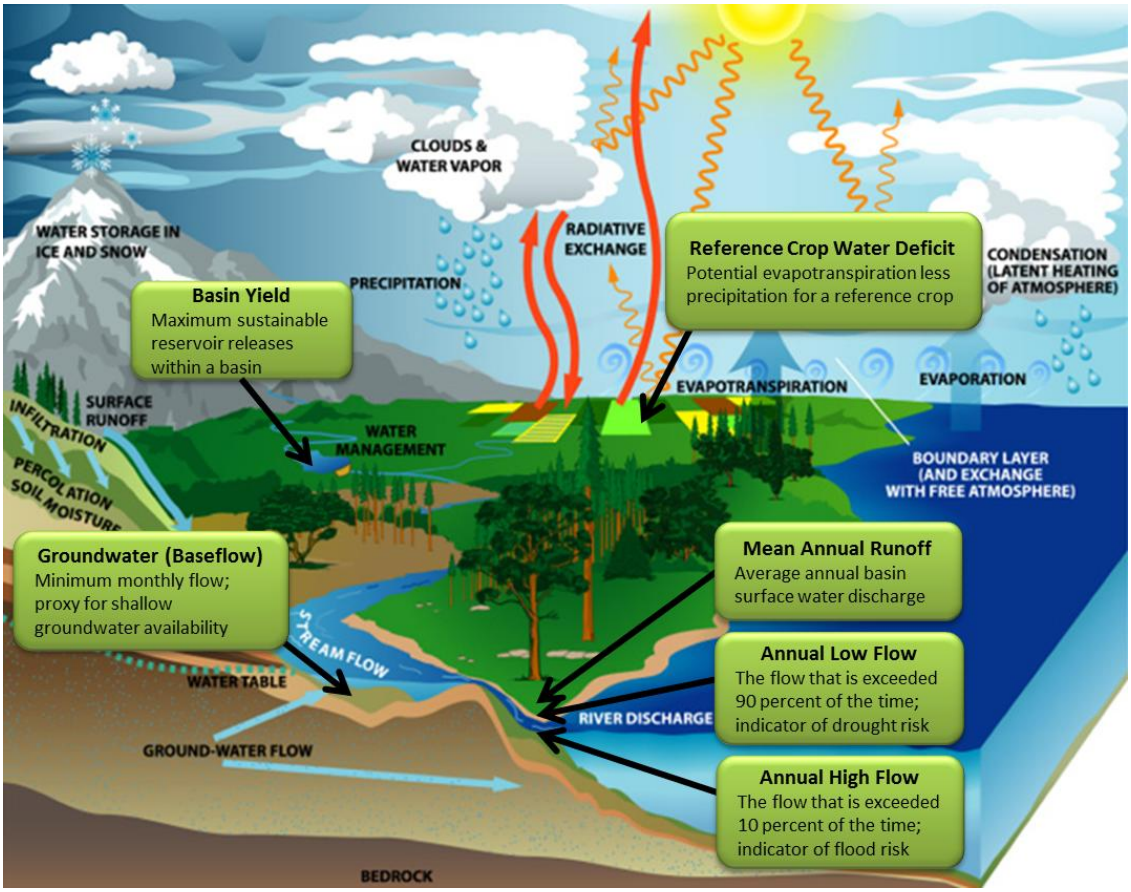

Background image source: NASA

Ultimately, the purpose of this assessment is to assist decision-makers and stakeholders in planning for climate risk to water resources and related infrastructure, and to inform decisions on appropriate levels of effort for further project-level studies. Table 2-5 presents the hydrological indicators that are most relevant to five different types of water projects: irrigation and drainage, large water supply and wastewater treatment (urban), small water supply and wastewater treatment (rural), flood protection, and river basin management and multipurpose infrastructure (supply water for multiple purposes).

Table 2-5. Hydrological indicators and the most relevant water projects

HYDROLOGICAL INDICATOR	MOST RELEVANT WATER PROJECTS
MAR	• *Irrigation and drainage.* Relevant for systems that are dependent upon direct withdrawals from rivers.
Annual low flow (q90)	• *Large-scale water supply and wastewater treatment (urban).* These systems rely heavily on reliability of water supply, so reductions in the lowest annual flows might pose large risks. • *Small-scale water supply and wastewater treatment (rural).* Relevant for rural systems that depend upon minimum availability of stream flow for supplies.
Annual high flow (q10)	• *Flood protection.* If this indicator increases, then the likelihood of high flows and long-term floods will increase.
Groundwater (baseflow)	• *Small-scale water supply and wastewater treatment (rural).* Rural systems often rely on groundwater for water supplies.
Basin yield	• *Irrigation and drainage.* Important for irrigation systems that rely on reservoir releases. • *Large-scale water supply and wastewater treatment (urban).* Relevant for urban systems that rely on releases from reservoirs. • *River basin management and multipurpose infrastructure.* Basin yield is relevant to both single- and multipurpose reservoirs and other water resources infrastructure.
Reference crop water deficit	• *Irrigation and drainage.* Indicates potential changes in irrigation water deliveries needed for the project.

Source: Authors' assessment

To provide an easily understandable and usable summary of impacts on the six hydrologic indicators, an exposure index was developed for each indicator. This exposure index classifies each indicator as subject to a low, medium, or high exposure to climate change and future variability based upon the findings of this analysis. A low exposure level indicates that there is little or no concern about the variable's exposure to current or future climate variability and change, a medium exposure level signifies that there is some concern, and a high exposure level denotes that there is significant risk. Medium and high exposure levels indicate that further analysis is necessary.

Low, medium, and high exposure levels were classified for each hydrological indicator based on the authors' expert judgment, which draws upon 20 years of experience in climate change impact and adaptation analyses and work with a wide range of international water resource experts. Exposure levels and the values that they signify are explained below in Table 2-6.

Table 2-6. Exposure level thresholds for each indicator

EXPOSURE LEVEL	CHANGE THRESHOLD
Reference crop water deficit and q10	
Low	< +5%
Medium	+5% to +15%
High	> +15%
Groundwater and q90	
Low	> –5%
Medium	–5% to –15%
High	< –15%
MAR and basin yield	
High decrease	< –15%
Medium decrease	–5% to –15%
Low decrease	–5% to 0%
Low increase	0% to +5%
Medium increase	+5% to +15%
High increase	> +15%

Source: Authors's assessment

The significance of the hydrological indicators and the methods through which they were analyzed are described in the next sections.

2.5.1 MAR

MAR, the average annual runoff over a period of interest, is an overall measure of the available surface water in a region. For this reason, MAR is a primary indicator used for water resource planning and development.

As discussed in Section 2.4, monthly runoff values were produced by CLIRUN-II for both the 2030s and 2050s. To calculate MAR for each decade, these values were summed across months and then averaged across the 10 years in each decadal period. Projected MAR values for all 56 GCM-SRES combinations were then compared with modeled baseline MAR values to determine the percent change in MAR for both the 2030s and 2050s under all climate scenarios in all basins, which were then used to classify each basin as facing low, medium, or high risk.

It is important to note that MAR does not provide any indication of the seasonality of flows. For instance, an area can have an overall high MAR, but severely low flows during the growing season, therefore making it an arid region. Similarly, the seasonality of runoff can change from year to year even if mean annual runoff is unchanged. Given that MAR does not supply information about the seasonality of flows, it alone is not a sufficient indicator of the overall impact of climate change on hydrological systems. However, it does provide critical information about hydroclimatic changes that can be expected in basins.

2.5.2 Basin Yield

Basin yield is a measure of the amount of water reliably available to a basin in an average year. Due to natural variability between seasons and years, much of the water resource that is available in a basin during a given year (that is, annual runoff) is lost if not stored. Reservoirs, by storing water from when it becomes available until it is needed, greatly increase the percentage of annual runoff that is reliably available for use. Therefore, basin yield is directly related to the amount of reservoir storage available.

As an indicator, basin yield provides information about the mean runoff, minimum runoff, and the runoff variability. Basin yield is also indicative of a basin's ability to absorb the impact of potential runoff variability resulting from climate change. As such, it is a very useful measure in analyzing the climate risk to water resources at the basin level.

Water resource planners have developed the storage yield curve as a way to estimate basin yield as a function of reservoir storage in a basin. The storage yield curve is a time series of estimated annual or monthly basin-level flows that provides information regarding how much storage is needed to provide certain amounts of annual reliable yield, and the level of reliable yield that can be achieved for a given amount of storage.

Figure 2-13 provides an example of a storage yield curve for the Nile River at Aswan. The maximum yield on the curve corresponds with the average annual runoff in the basin, while the lowest yield on the curve corresponds with the minimum flow in the time series. In a basin without any storage (that is, zero on the *x*-axis), it is assumed that the basin yield will be the lowest recorded annual flow. On the other hand, in a basin with excess storage, it is assumed that the basin yield will be the MAR.

Figure 2-13. Storage yield curve for the Nile River at Aswan

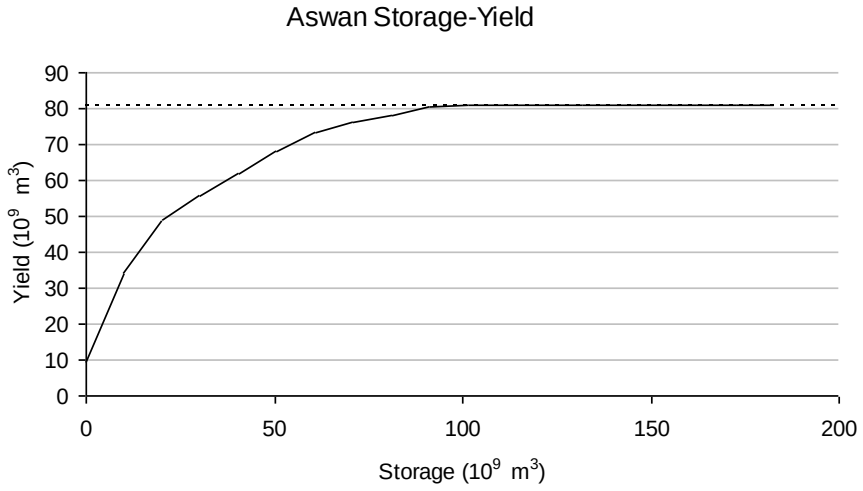

Source: Authors' calculations based on available data on Aswan and the river Nile

The shape of the storage yield curve is a function of the variability of a basin's runoff, both within and among years. A steep curve reflects low variability; a flatter curve is indicative of higher variability. In other

words, a basin with highly variable runoff requires more storage than does a less variable basin to achieve the same basin yield. Climate change has the potential to alter not only the average annual runoff in a basin but also the annual runoff variability, thereby potentially affecting the shape of a basin's storage yield curve. Figure 2-14 shows how a change in annual runoff might translate into a decrease in the maximum basin yield for a basin, as well as the increase in storage required to maintain a constant basin yield.

Using baseline and projected annual runoff and low-flow values, baseline and projected storage yield curves were created for every basin for all 56 GCM-SRES combinations. Absent information on the reservoir storage available in each basin, this analysis assumes that existing storage provides 60 percent of baseline MAR, which defines Y_{Base} in Figure 2-14, and therefore also K_{Base}.[10] Next, the new basin yield under climate change (Y_{CC} in the figure) was calculated using the new storage yield curve. The baseline and climate change basin yield values were then compared to determine the percent change in each basin's yield under climate change. These projected changes were used to categorize each basin as facing low, medium, or high risk due to change in basin yield under each of the 56 GCM-SRES combinations.

Figure 2-14. Impact of climate change on a hypothetical storage yield curve

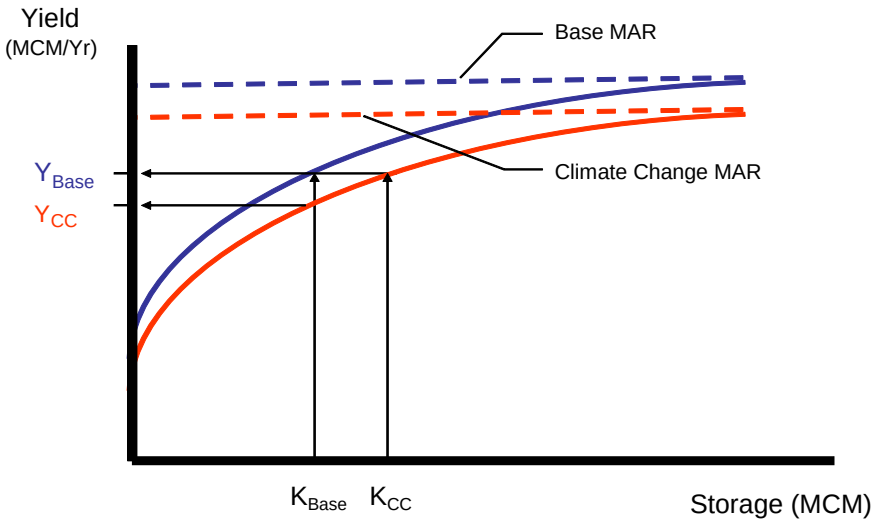

Source: Illustration by authors

[10] Sixty percent of baseline MAR was selected as an estimate of basin yield based on the environmental flows needed to maintain ecosystem conditions. In the world's river basins, between 20 and 50 percent of MAR is required to maintain riparian ecosystems in fair condition; these requirements are 40 percent in basins that have relatively stable flows (for example, Amazon and Congo), and closer to 30 percent in basins with more variable flows (Smakhtin, 2008). We assume that an average of 40 percent of MAR is needed to support ecosystems in each basin annually, leaving 60 percent of MAR for storage yield, which we assume is fully used each year.

2.5.3 Annual Low Flow (q90)

Annual runoff and basin yield provide valuable information about the average conditions in a given basin. However, key hydrologic impacts on society and economic development are often the result of extreme events—for example, floods and droughts—rather than average conditions. Therefore, indicators that represent these extreme events are necessary for an analysis of climate change's risk to water resource management and development.

Following Alavian et al. (Alavian et al., 2009), this analysis uses q90 (annual low flow) as an indicator of drought. The q90 flow value refers to the flow that is exceeded 90 percent of the time, which means that there is a 10 percent chance in a given time period of a flow lower than this value. A decrease in the q90 value signifies an increase in the likelihood of a given low flow and therefore is an indication of increased drought risk.

For each of the basins, projected q90 runoff values for each of the 56 GCM-SRES combinations were compared to modeled baseline q90 runoff values to assess relative change. The relative changes were then used to categorize each basin as facing a low, medium, or high level of risk from changes in drought due to climate change.

It is important to note that q90 flows can represent quite different flows depending on a basin's hydrological regime. For example, in a dry basin, the q90 flow might be considerably lower than in a wet basin. Additionally, some basins are more prone to droughts than others and will be more sensitive to increased drought as a result of decreases in q90. While these complexities were not explicitly addressed in this analysis, it is important to keep them in mind when analyzing the possible impacts of climate change in drought risk for any particular basin.

2.5.4 Annual High Flow (q10)

In this analysis, annual high flow (q10) was used as an indicator of flood risk. In contrast to annual low flow (q90), q10 represents the flow value that is exceeded 10 percent of the time, which means that there is a 90 percent chance in each time period of a flow lower than this. As q10 increases, so does the likelihood of high flows; therefore, an increase in q10 corresponds with an increase in flood risk.

Annual high flow is an indicator of long-term and large-scale flooding events that can be identified based on monthly and annual runoff data. This indicator does not provide information on the frequency, duration, or magnitude of short-term floods that are based on weekly events, or of flash floods that are based on daily events.

Projected q10 runoff values for each of the 56 GCM-SRES scenarios were compared to the modeled baseline q10 runoff values for all basins to evaluate the relative change. The relative changes in q10 from historical values were used to provide an indication of the projected change in flooding. These values, in turn, were used to categorize each basin as facing a low, medium, or high risk from change in flooding due to climate change.

Similarly to q90, q10 can represent significantly different flows depending on a basin's hydrological regime, for example, in a dry basin, the q10 flow might be considerably lower than in a wet basin. Some basins might be more prone to flooding than others, making them more sensitive to even moderate increases in q10 flows. As with q90, these complexities were not explicitly addressed in this study, but should be considered in assessing the increase in risk due to climate change for any particular basin.

2.5.5 Groundwater (Baseflow)

Groundwater plays an integral role in reservoir storage, streamflow, and runoff. Additionally, many regions of the world are directly reliant on groundwater-fed wells for water supply and small-scale irrigation. For these reasons, it is important to provide an indicator of the possible impact of climate change on local groundwater resources.

Although groundwater is often considered separate from surface water, the two water sources are integrally connected (see USGS, 1998). An aquifer can be described as having an appetite for water. As groundwater supply decreases, the aquifer's appetite increases, causing every water supply that shares a boundary with the aquifer to lose water. This interaction between groundwater and surface water is difficult to observe and to measure, making it difficult to accurately estimate. Since modeling the global groundwater system is beyond the scope of this analysis, baseflow—a screening level proxy indicator (Freeze and Cherry, 1979)—was used to provide an indication of the groundwater available in each basin

For each basin and GCM-SRES scenario, the 39-year time series of projected runoff flows was analyzed and a mean monthly hydrograph was developed (see Figure 2-15). The 12 monthly values were sorted for each year and a minimum annual flow was determined. For example, in Figure 2-15, the minimum annual flow for September was at approximately 7 CMS.

Figure 2-15. Example of a basin's mean monthly hydrograph

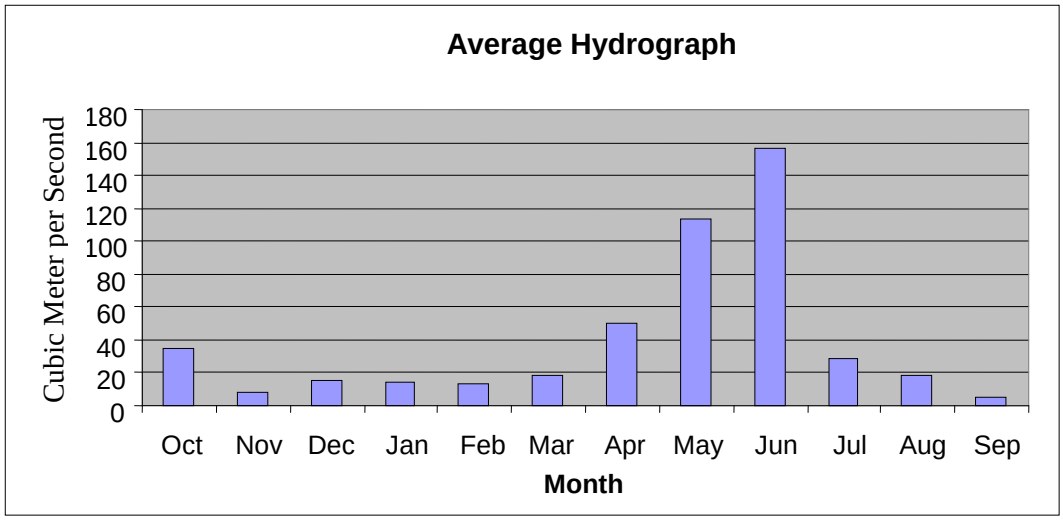

Source: Example illustration by authors

The contribution of groundwater to annual runoff was assumed to be 12 times the lowest monthly flow for each year.[11] It is assumed that the groundwater contribution to runoff can be modeled as a linear reservoir. That is

$$Baseflow(t) = \alpha \times GS(t)$$

where α = groundwater – surface water interaction coefficient, and $GS(t)$ = groundwater storage in month t.

This approach allows for an understanding of the future direction of groundwater availability and whether it should be of concern in a given region.

Once annual baseflow projections had been developed for every basin under each GCM-SRES combination, these were compared to modeled baseline baseflow to analyze relative change. Projected relative change was used to categorize each basin as facing low, medium, or high risk due to change in groundwater availability.

2.5.6 Reference Crop Water Deficit

Both rain-fed and irrigated agriculture are key aspects of economic development in many countries. Because agricultural systems could be considerably impacted by climate change, an indicator of the impact of climate change on water availability for crops was needed.

Detailed crop modeling and analysis of agricultural water use at the global basin scale was far beyond the scope of this work. However, simplified methods can provide an understanding of reference crop water deficit at a broader scale. The Water Deficit Index (WDI) is one such method employed for climate change analyses at the regional and local levels (Woli et al., 2008), and was used in this analysis.

$$WDI = \Sigma\,(CWR - Precip)_t \quad \text{if } CWR_t - Precip_t > 0, \text{ else } 0$$

where $CWR = K_c(t) \times PET(t)$, and K_c = crop factor.

K_c, the crop factor, translates PET into actual crop water demand; the WDI assumes a reference perennial grass crop factor, K_c, which has a value of one. The PET data used in the equation was consistent with what is used in the CLIRUN-II model (see Section 2.4). The calculation of the CWR was performed at the 0.5 × 0.5 degree gridded scale, and then aggregated to the basin level.

For each basin, baseline WDI was compared with projected WDI for each GCM scenario to determine relative change. Given that WDI was used to represent reference crop water deficit, changes in WDI were used to categorize each basin as facing low, medium, or high risk from changes in reference crop water deficit.

[11] This approach relies on the constant discharge method for baseflow separation.

While reference crop water deficit—as represented by WDI—does not describe the actual agricultural water demand experienced in any basin, it does offer a broad perspective on agricultural performance. Therefore, changes in this indicator provide useful information about the potential impacts of climate change on both rainfed and irrigated agriculture for planners and policy-makers.

2.6 Uncertainty

In climate change impact analyses, there are significant uncertainties stemming from a range of sources. Sources of uncertainty include, but are not limited to:

- Limitation of assumptions, model physics, and parameterization of the global circulation models
- Unpredictability of future development pathways and the resulting scenarios for emissions of greenhouse gases, land use changes, and other factors influencing climate change
- Fundamental uncertainties in climate change's impact on the hydrologic cycle and water resources and the modeling hereof
- Limitations of the selected hydrologic model
- Data limitations with regard to baseline climate inputs and baseline runoff inputs.

The initial three sources are typical—and to a large extent unavoidable. This chapter will concentrate on the two last bullet points, which are more specific to this study.

However, it is important to note that for decision makers, it is the total uncertainty in predicting future climate and its impacts that matter. Some of this has been captured by the proposed methodology above (for example the variability in results from alternative combinations of GCMs and emission scenarios). Another part can be addressed by using decision tools that place appropriate emphasis on uncertainty and promote suitably flexible investment and planning decisions.

2.6.1 Uncertainty Due to Global Circulation Models and Emission Scenarios

Sources of uncertainty directly related to climate change projections include the inherent variability of the climate system, unpredictability of future emissions, and the limitations of the fundamental assumptions, model physics, and parameterization built into models themselves (Bates et al. 2008). The overall level of uncertainty associated with climate projections increases with the length of the time horizon, and projections of precipitation tend to be less certain than temperature projections.

2.6.2 Fundamental Uncertainty in Forecasting Climate Change Impacts on Hydrology

Where hydrological models, such as CLIRUN-II, are used to project impacts on water resources, uncertainties arise from a variety of additional sources, including the scale mismatch between climate projections and hydrological systems and related issues caused by downscaling techniques (discussed in Section 2.1), as well as fundamental uncertainties in climate change's impact on the hydrologic cycle and water resources.

Beyond these typical—and largely unavoidable—sources of uncertainty, uncertainty in this analysis was also caused by the limitations of the CLIRUN-II model and poor data sets.

2.6.3 Uncertainty in Rainfall Runoff Models

The inputs used for global climate change studies generally represent our best guess of physical, geographic, and hydrologic properties. Due to the nature of climate research, these inputs tend to be estimated values averaged over large areas (for example, GCMs have an average resolution of 2.6 × 3.0 degrees). As a result, rainfall runoff models used for global climate change studies typically tend to be relatively simple, and often require a minimal amount of input to reduce both the uncertainty associated with inputs and the possibility of compounding errors. As a result, there are several reasons for uncertainty directly related to these rainfall runoff models, including the following:

- **Rainfall runoff models make simplifying assumptions.** For example, CLIRUN-II is a simple rainfall runoff model in which there are two soil layers that allow water to move with restrictions into, between, and out of the bottom of the soil profile. CLIRUN-II assumes that each of the two soil layers has uniform properties at a given time. However, in reality, soil properties vary to some extent through each of the soil layers. CLIRUN-II also assumes uniform soil and weather properties within each basin, while in reality these parameters often vary; for example, the northeast section of the basin could be different from the southwest section. To produce one soil and weather value representing the entire basin, CLIRUN-II takes the average of these properties across the basin. These simplifications, while necessary in global runoff studies, impact the accuracy of CLIRUN-II and other rainfall runoff models, and therefore are a cause of uncertainty in this analysis.

- **Calibration results might not well represent the physical parameters**. In global climate change studies, a calibration scheme is required in rainfall runoff models to account for all of the unknown basin characteristics (soil layer thickness, ground cover properties, and so on). The calibration process estimates physical basin properties based on the observed runoff used in the analysis, and it is possible that the calibration scheme's estimations do not always well represent reality. For example, the ground cover properties could be exaggerated to account for inaccurately observed runoff data, or one basin property could be exaggerated to account for another exaggerated basin property (for example, layer thickness could account for ground cover properties). Calibration would presumably be more reliable if some or all of these physical basin properties were physically measured, but this alternative would be very expensive and time consuming. These issues associated with rainfall runoff model calibration result in some level of uncertainty in runoff outputs.
- **Observed runoff is rarely naturalized flow (climate induced flow).** Hydrologists generally make the distinction between "naturalized" and "gauged" runoff. Naturalized runoff is the runoff caused by the weather (precipitation, temperature, and so on) and the earth's surface (topology, soils, ground cover, and so on), without consideration of anthropological impacts. Gauged runoff, on the other hand, accounts for anthropological impact such as dams, reservoirs, and ground cover changes. CLIRUN-II was built to model naturalized runoff, meaning that the equations built into the model do not include the effects of civilization. Although the UNH-GRDC runoff data is based on a naturalized flow model, in cases where the UNH-GRDC results were corrected using observed streamflow, the annual runoff data could represent gauged runoff instead of naturalized runoff. Where UNH-GRDC

runoff data is based on gauged flows, CLIRUN-II is actually calibrated to human-influenced flow rather than naturalized flow, therefore introducing a level of uncertainty in results.

- **Extreme runoff events may be under-represented.** If the runoff and historical climate data sets under-represent extreme events, rainfall runoff models will under-represent extreme runoff events as well. Because both the UNH-GRDC data set and the CRU TS 2.1 data set have the tendency to include too few extreme events (runoff and weather, respectively), there is a good chance that extreme runoff events are under-represented in the CLIRUN-II results.
- **Limitations to scope of CLIRUN-II.** In this analysis, there are a number of topics that were not taken into account when running CLIRUN-II. For example, water system management aspects (for example, reservoirs, routing, and extractions for different demands) were not included in the analysis. While simplistic groundwater was included, detailed groundwater modeling was not. Also, while CLIRUN-II does have a snowmelt component, it does not include glacier modeling and therefore does not account for this aspect of hydrological systems. These limitations reduce the certainty of the outputs.

The authors believe that runoff is well represented by the CLIRUN-II model at the scale of analysis undertaken, and that the previously mentioned simplifications do not impact the overall validity of results, with the important caveat that, as explained in Section 1 and addressed later, that data should not be used at the project level.

Additional detail on the uncertainties in the CLIRUN-II model and the data inputs used in this study are explored in Appendices A, B, and C.

2.6.4 Uncertainty in the Geographic Extent of River Basins

This study relies on the Hydro1k data set from the US Geological Survey (USGS) for geographic delineation of basin boundaries. To estimate these boundaries, the USGS used 1 $\times$ 1 km resolution digital elevation models to evaluate the spatial extent of river drainages based on topography. Although the authors believe that Hydro1k is the best source available on the spatial extent of the world's river basins, to the extent that there are inaccuracies in the underlying digital elevation models, or there are differences between the local understanding of basin boundaries and the boundaries calculated by the USGS, the basin boundaries in this study might be inaccurate. At the scale of analysis undertaken, these inaccuracies might cause small shifts in the geographic distribution of modeled runoff, but are unlikely to have a significant impact on the indicator results.

2.6.5 Uncertainty Due to CRU Baseline Climate Inputs

The CRU TS 2.1 data set, which was used to provide climatic baseline inputs for this analysis, incorporates weather data from gauging stations all over the globe. However, station data is not always available for every time and place, an issue that tends to be more common in developing countries where station coverage is often poor. When and where weather records are not available, the CRU team uses an interpolation method to fill in missing data. Depending on the characteristics of a particular region, this interpolation might be a more or less accurate depiction of real historical weather. Interpolation accuracy

is of particular concern in areas with significant variations in elevation. The questionable accuracy of the original station data, in itself, is a source of notable uncertainty.

Additionally, in the CRU interpolation method, the 1961 to 1999 seasonal mean is used to fill in missing data. Hence, the CRU data set is biased toward seasonal means. While the assumption that the seasonal mean is appropriate for filling in missing data is scientifically sound, this is problematic for water resource and natural disaster planning, where information on extreme (that is, less likely) events is generally more important than what happens on average (that is, the seasonal mean).

This potential bias affects the accuracy of CLIRUN-II results, and adds particular uncertainty to the use of these results to predict changes in extreme events such as flooding and drought (see Sections 2.5.3 and 2.5.4). Given this bias in baseline inputs, the risk of extreme events is likely to be underrepresented in this study's results. Accuracy of the CRU data set is described in further detail in Appendix A.

2.6.6 Uncertainty Due to UNH-GRDC Baseline Runoff Inputs

As the UNH-GRDC data was used to calibrate the CLIRUN-II model, its accuracy is a primary determinant of the overall accuracy of the calibration results and, therefore, the accuracy of the CLIRUN-II runoff outputs. Potential sources of uncertainty in the UNH-GRDC data set include the following:

- **Scope and data availability issues with UNH-GRDC.** There are four main issues with the UNH-GRDC calibration runoff data that add to uncertainty in the analysis: (1) there are large areas (especially in dry regions) that do not have gauge data, (2) the time period of available gauge data varies by station, therefore the resulting monthly discharge regimes are not fully consistent, (3) the historical climate data used in the Water Balance Model (WBM) of the UNH-GRDC data set is not the same that was used in the CLIRUN-II model analysis, and (4) the data set is only provided for 12 average monthly values, not for a full time series.
- **Input data inaccurate in some areas.** The UNH-GRDC team generated gridded runoff data for the globe based on a composite of available station data and modeled runoff using the WBM. Therefore, the accuracy of the UNH-GRDC runoff data is contingent upon the accuracy of both the WBM and its data sources. For basic soil information, the WBM relies on the UN Food and Agriculture Organization (FAO) Soil Map of the World, which contains estimates of soil properties all over the globe. These estimates are based on soil samples collected and interpolated for each region. There is significant room for errors in the soil samples, the methods used to interpolate them, and the way in which this information was used by the WBM. Additionally, any errors in the WMB's 0.5×0.5 degree gridded representation of river networks could cause runoff to be associated with the wrong river network, leading to miscalculations of annual runoff at the basin level.
- **Annual rather than monthly error adjustment.** The annual rather than monthly error adjustment of UNH-GRDC data set is another source of potential uncertainty. In a given basin, all of the modeled runoff in each grid cell is summed to produce a total runoff at the mouth of the basin. The modeled runoff total was then 'corrected', i.e., adjusted, to match actual gauged runoff. This adjustment was done annually instead of seasonally, and adjustment coefficients typically ranged from approximately 0.01 to 100. By making the correction annually, the UNH-GRDC team maintains the seasonality from the weather data (from CRU TS 2.1) instead of using the seasonality from the gauged runoff. In many

cases, the seasonality from the weather data does not match gauged runoff seasonality; this affects CLIRUN-II results, which are calibrated to the UNH-GRDC results, and therefore is a source of uncertainty in this study.

- **Observed runoff data missing over large areas.** In areas where observed runoff was not available, the UNH-GRDC data set only represents WBM results, due to the fact that observed streamflow was not available to constrain the modeled results. Therefore, in these cases, any errors in WBM outputs would not have been "corrected". This basically means that in situations where the gauged runoff was not available, CLIRUN-II is calibrated to the WBM-modeled runoff alone. The fact that the adjustment coefficients described previously range from approximately 0.01 to 100 implies that the WBM miscalculated runoff in some areas by a factor of 100 (either 100 times greater or 100 times smaller). Hence, in the places where gauged runoff was not available, there is a significant room for error in UNH-GRDC data, which leads to possible uncertainty in the CLIRUN-II results.

Possible errors in the UNH-GRDC data set and their potential effect on the CLIRUN-II results are covered in greater depth in Appendix A. Note that the UNH-GRDC gridded data is the best currently available source of naturalized global runoff data. Despite the uncertainties mentioned previously, the authors believe that this data set provides a reasonable representation of global runoff at the scale of analysis undertaken.

2.6.7 Results are Not Intended for Use at the Project or Design Level

Because of the uncertainties, the indicator results can be used on a screening or planning level, but these results are not intended to be used at a project or design level. Users are advised to conduct more detailed studies before any major decisions are made based on interpretations of the results presented here.

3. ILLUSTRATIVE RESULTS: UGANDA AS AN EXAMPLE

To provide an illustration of how the results of this study, available on the World Bank Climate Portal, might be used and interpreted, this section uses projections for the river basins of Uganda as an example.[12] Results for Uganda's basins are presented in two formats: as maps showing differences in severity of impacts across basins for the six hydrological indicators, and as box and whisker diagrams showing the range of projected impacts across the 56 GCM-SRES combinations for the full set of 10 indicators. The spatial results presented on the maps provide a perspective on how the six hydrological indicators are anticipated to vary across basins and time, as well across the climate scenarios; as such, they provide a snapshot of the risks to water resources systems projected by the climate models. The box and whisker diagrams, which show the statistical distribution of the results across climate scenarios, provide a complementary perspective on the variability of the projected changes in hydrological indicators under climate change. Given that highly uncertain future outcomes will call for different solutions than more certain outcomes, this information is a critical piece in forward-looking water resources planning.

A note of caution: in using the results presented here and on the World Bank Climate Portal, it is important to keep in mind that these results are based on projections of current climate models, and therefore are limited by the state of the science and are subject to uncertainty, as discussed in Section 2.6 and throughout this document. As indicated in Box 3-1, these limitations should to be considered when using and interpreting the results from this analysis.

Box 3-1. Using results on the World Bank Climate Portal

The indicator results are not intended to be used at the project level. Although the results can be used on a basin and annual level, users are advised to conduct more detailed studies before any major decisions are made based on interpretations of the results presented here.

[12] As mentioned in the introduction, the results of this analysis are available on the World Bank Climate Portal, a Web-based interface that makes this information easily accessible to World Bank clients, planners, and policy-makers. Climate Portal users can access graphic presentations of the severity (that is, low, medium, high) of change that is projected for all studied indicators across basins and regions of interest for the 2030s and 2050s, as well as tabular representations of this information and GIS files for each basin. The information available on the Climate Portal and its navigation is further discussed in Appendix D.

3.1 Maps of Hydrological Indicators across Basins

Using Uganda's river basins as an example, this section provides an illustration of how projected changes in the six hydrological indicators might be used. For each hydrological indicator, a set of maps reflecting the severity of changes for each basin are provided for dry, middle, and wet climate scenarios; these scenarios are based upon minimum, median, and maximum aggregate runoff for each basin across the 22 GCMs run for the A1B SRES scenario, which is the moderate emissions scenario used in this analysis. The dry, middle, and wet GCMs in the 2030s and 2050s for Uganda are presented in Table 3-1. This representation of results allows for comparison of projected impacts across basins, temporal scale, and climate scenarios.

Table 3-1. Dry, middle, and wet scenarios for Uganda basins in the 2030s and 2050s for the A1B SRES scenario

DECADE	DRY SCENARIO	MIDDLE SCENARIO	WET SCENARIO
2030s	giss_model_er	gfdl_cm2_1	cccma_cgm3_1
2050s	giss_model_er	inmcm3_0	cccma_cgcm3_1_t63

Source: Authors' assessment

Note that the illustrations in the figures presented in this chapter provide an example of changes in indicators at the country scale, and as such, show only the portions of Uganda's basins within the country boundaries.

3.1.1 MAR

The projected percent change of MAR for Uganda's basins is portrayed in Figure 3-1 for both the 2030s and 2050s under the dry, middle, and wet scenarios. As the maps show, within each climate scenario, the results indicate relatively consistent impacts spatially and temporally; that is, exposure levels across the basins and decades are similar. However, among climate scenarios, the results suggest highly variable impacts, ranging from significant increases to significant decreases in MAR.

In light of these results, it might be concluded that water resource decision-making in Uganda needs to take into account the fact that there is a large amount of uncertainty about future MAR. Accordingly, water resource planning should build in the flexibility to deal with either significant increases or decreases in runoff.

Figure 3-1. Change in mean annual runoff in Uganda's basins from the baseline to 2030 and 2050 under dry, middle, and wet scenarios

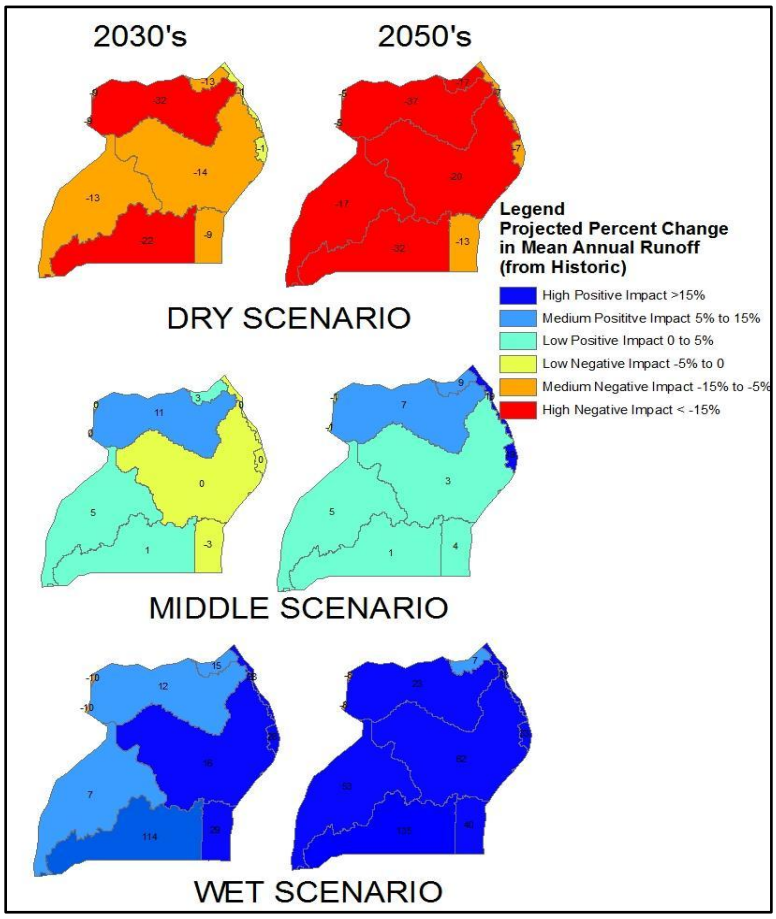

Source: Based on Authors' calculations

3.1.2 Basin Yield

The projected percent change of basin yield for Uganda's basins is portrayed in Figure 3-2 for both the 2030s and 2050s under the dry, middle, and wet scenarios. The results depicted in the maps indicate that, in general, the central part of the country will experience low negative impact under most climate scenarios. The impact on basin yield in the northern and southern regions of Uganda is much less certain. This suggests that, while the central part of the nation might not need to significantly alter their available storage, the northern and southern regions should conduct more detailed analyses to evaluate their ability to handle runoff variability.

Figure 3-2. Change in basin yield in Uganda's basins from the baseline to 2030 and 2050 under dry, middle, and wet scenarios

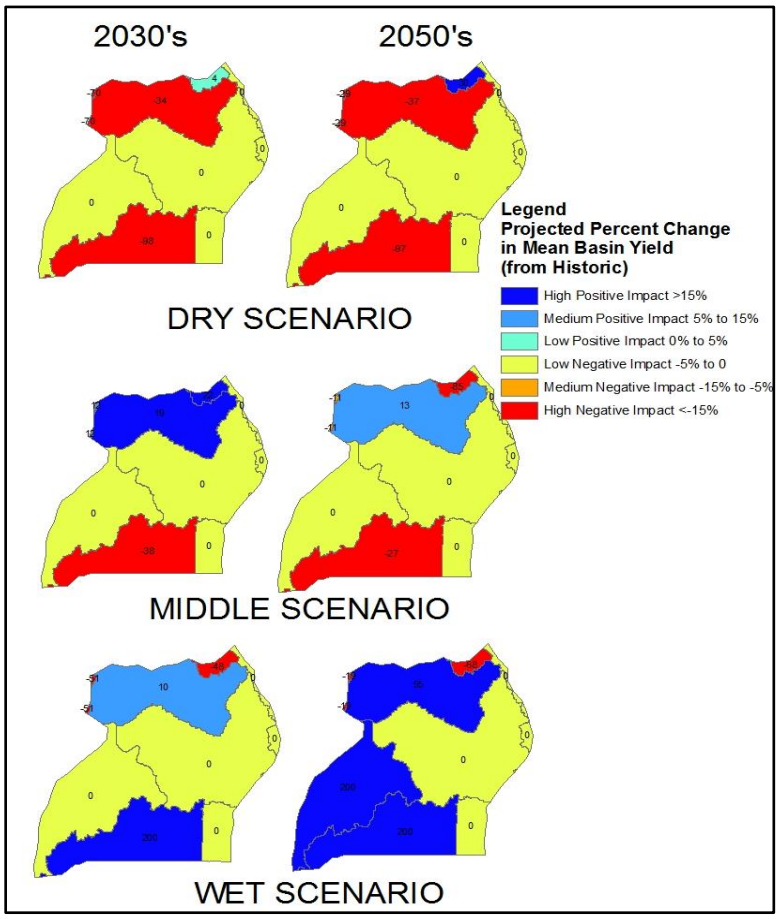

Source: Based on authors' calculations

3.1.3 Annual High Flow (q10)

The projected percent change in annual high flow (q10) for Uganda's basins is portrayed in Figure 3-3 for both the 2030s and 2050s under the dry, middle, and wet scenarios. Q10, as explained previously, can be used to represent flood risk; hence, changes in q10 provide some indication of future changes in likelihood of flooding.

The projection results indicate that, as would be assumed, the risk of flooding increases significantly as the climate projections become wetter. While the results suggest that flood risk is unlikely to change significantly in the northwest regions before 2030, by 2050, all of Uganda is projected to experience a highly increased risk of flooding events under the wet scenario. These results suggest a high level of variability but an overall indication of potentially significant impacts, and so indicate that more in-depth analysis of flooding risk is merited.

Figure 3-3. Change in annual high flow (q10) in Uganda's basins from the baseline to 2030 and 2050 under dry, middle, and wet scenarios

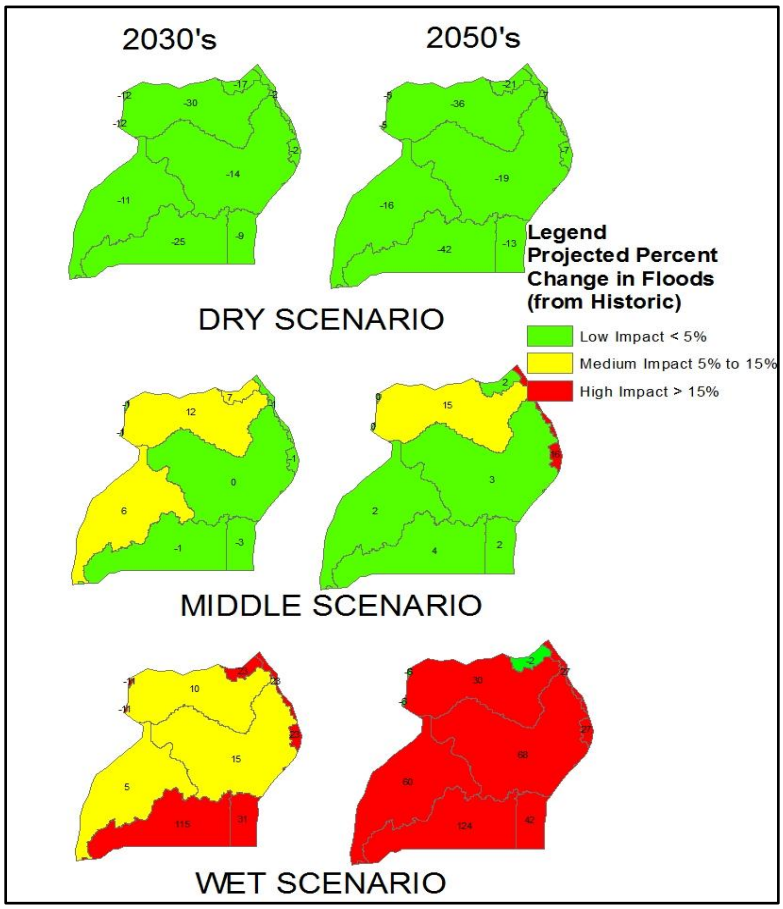

Source: Based on authors' calculations

3.1.4 Annual Low Flow (q90)

The projected percent change in annual low flow (q90) for Uganda's basins is portrayed in Figure 3-4 for both the 2030s and 2050s under the dry, middle, and wet scenarios. As discussed previously, q90 provides an indication of drought risk, and therefore might offer an idea of the potential impact of future drought under climate change scenarios.

As the maps show, the results suggest little change in low flow under middle and wet scenarios. However, this should not be assumed to mean that the increased risk from drought is low. Even though the dry scenario is the only scenario projecting high impacts, it represents an equally valid potential future consequence of climate change. Decisions and planning efforts that could be impacted by monthly droughts must take into consideration the potential of significantly increased drought risk in the future, particularly in the 2050s and beyond.

Figure 3-4. Change in annual low flow (q90) in Uganda's basins from the baseline to 2030 and 2050 under dry, middle, and wet scenarios

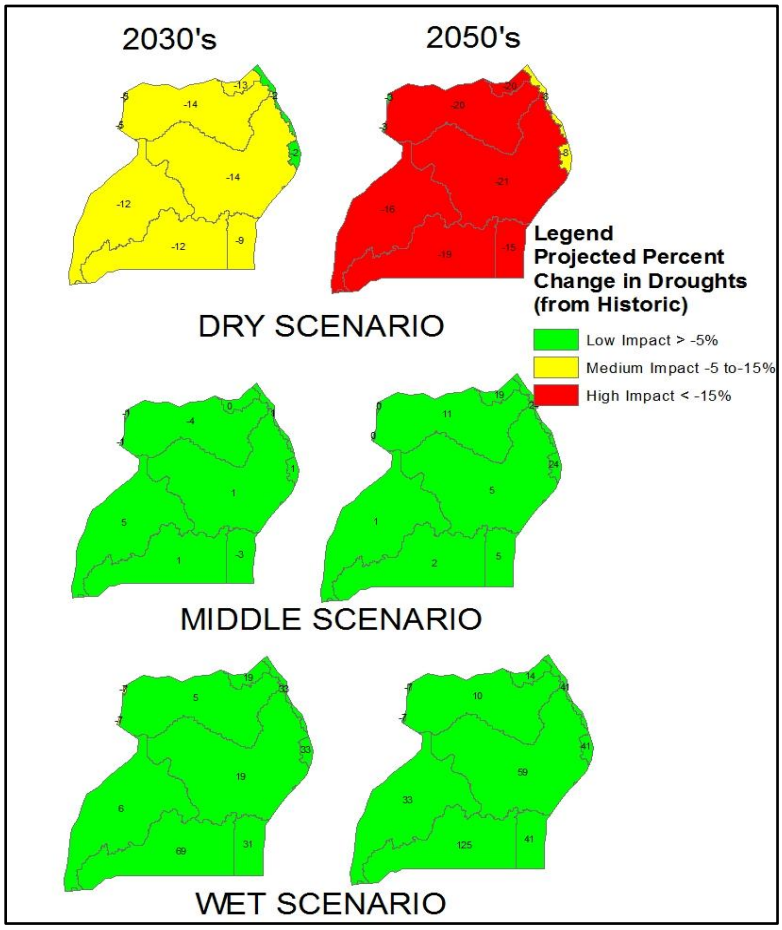

Source: Based on authors' calculations

3.1.5 Groundwater (Baseflow)

The projected percent change in groundwater (baseflow) for Uganda's basins is portrayed in Figure 3-5 for both the 2030s and 2050s under the dry, middle, and wet scenarios.

The results show relatively consistent effects across basins under each scenario; however, there is considerable variability between the dry scenario and the wet and middle scenarios, with the potential of severe impacts under dry conditions. Because groundwater availability particularly affects groundwater-using rural populations and small-scale irrigation, these results indicate a need for particular attention to communities and systems that depend on groundwater for their livelihoods and well-being.

Figure 3-5. Change in groundwater (baseflow) in Uganda's basins from the baseline to 2030 and 2050 under dry, middle, and wet scenarios

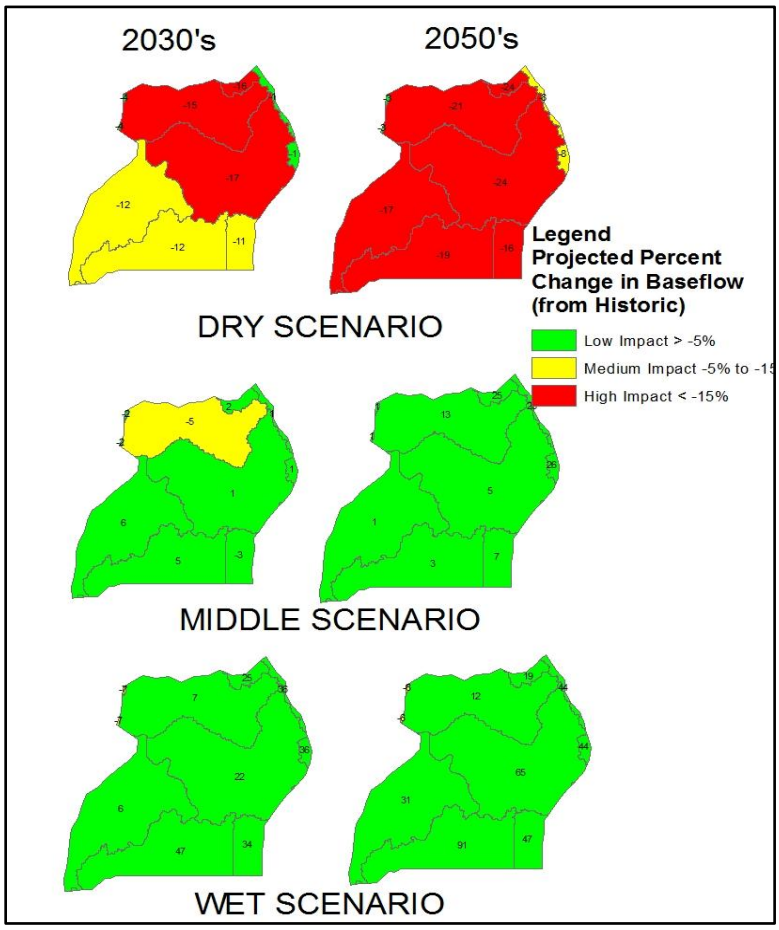

Source: Based on authors' calculations

3.1.6 Reference Crop Water Deficit

The projected percent change in reference crop water deficit for Uganda's basins is portrayed in Figure 3-6 for both the 2030s and 2050s under the dry, middle, and wet scenarios.

The results show considerable variability in projected changes in reference crop water deficit. In areas that are projected to potentially experience significant increases, additional inquiry into the ability to increase irrigation supply is merited. This is particularly important in the southwest portion of Uganda, which is most likely to experience a noticeable increase in reference crop water deficit. Given the potential for increased demand throughout Uganda, these results should be considered when evaluating future agriculture and irrigation development plans throughout the country.

Figure 3-6. Change in reference crop water deficit in Uganda's basins from the baseline to 2030 and 2050 under dry, middle, and wet scenarios

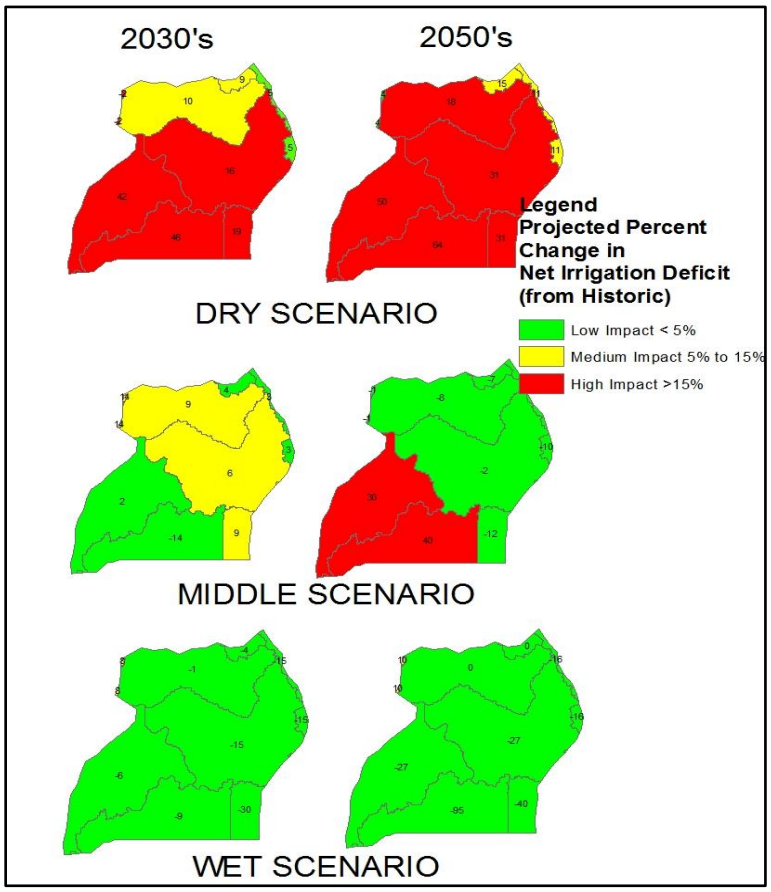

Source: Based on authors' calculations

3.2 Box and Whisker Plots of Hydrological Indicators across GCMs

The maps discussed previously in this chapter provide a meaningful overview of results, and are particularly useful for temporal comparisons within and spatial comparisons among basins. By contrast, box and whisker plots illustrate the variation that occurs within results due to uncertainties in GCM model structure and emission scenarios. For this reason, box and whisker plots are a useful representation of the variation in indicator results across climate scenarios, and give a better indication of the full distribution of GCM results.

Figure 3-7 shows two sets of box and whisker plots showing the variation in results for all indicators in the 2030s and the 2050s are provided for the aggregated basins in Uganda. Projections for each indicator (listed across the *x*-axis) are provided for each SRES scenario (also listed across the *x*-axis). The variation represented by the box and whiskers for each indicator-SRES combination reflects the range of projection results associated with each GCM run for each SRES scenario.

Figure 3-7. Box and whisker plots of indicators for Uganda from the baseline to the 2030s (top) and 2050s (bottom), across climate scenarios

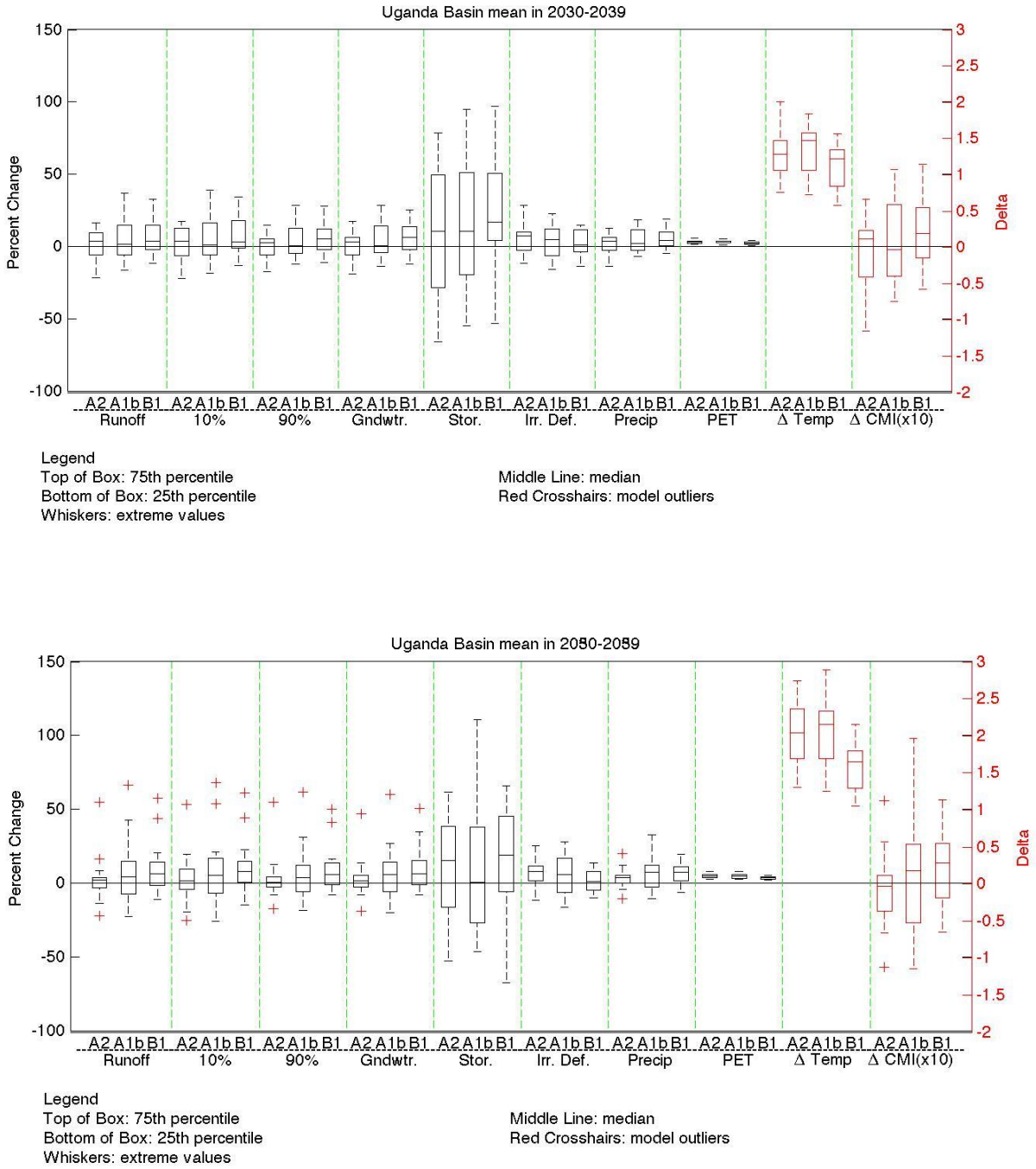

Source: Based on authors' calculations

In the box and whisker plots of Figure 3-7, results for MAR, q10 (denoted by 10 percent), q90 (denoted by 90 percent), baseflow (denoted by gndwtr.), basin yield (denoted by stor.), and reference crop water deficit (denoted by irr def), PET, and precipitation (denoted by precip) are shown as percent changes. Results for temperature (denoted by temp) and CMI are shown as absolute changes; in order to allow CMI to be displayed on the same scale as temperature, absolute changes in CMI are multiplied by 10. These box and whisker plots are formatted the same way as plots on the World Bank Climate Portal.

For each indicator's box and whisker plot, the middle line represents the mean projected parameter, and the top and bottom of the open rectangle (the box) represent the 25th and 75th percentiles of the projections, respectively. The dashed lines extending above and below the boxes (the whiskers) show the range of extreme values of the projected results, and the cross-hairs show the model outliers. Outliers are retained in the plots because they provide some indication of the worst case scenarios for indicators.

Box and whisker plots of indicators were created for each of the 8,413 basins. More information about the box plots available on the World Bank Climate Portal is provided in Appendix D.

Based on the projections of the parameters presented here, we can conclude that water resource planning and management need to be designed in a manner that takes into account large uncertainty about both the magnitude and, to some extent, the direction of future change. For this reason, water resource decisions need to allow for increased flexibility, which could open up an entirely new paradigm for dealing with infrastructure investments and water management frameworks.

3.3 Final Comment on Using the Hydrological Indicators Data

Anyone who uses the data produced through this analysis should be aware of the limitations and uncertainties of the results. While highly valuable for planning, these results should not be used on a project scale, for reasons discussed previously. Additionally, users should be aware that the extreme event estimations from this analysis are less certain than results for other indicators. However, despite these limitations, the results from this analysis provide a highly helpful indication of basin scale impacts that, in conjunction with an understanding of large-scale impacts (that is, country and regional mean impacts), should be considered by World Bank Team Leaders and decision-makers when making water resource planning, management, and investment decisions.

ANNEXES

ANNEX A: CRU AND GRDC DATA SETS: DESCRIPTION, CONSTRUCTION, UNCERTAINTIES, AND VALIDATION[13]

A.1 CRU Description[14]

The Climate Research Unit (CRU) of the University of East Anglia has developed an open source, global land surface time series and historical record of nine weather parameters at a resolution of 0.5 by 0.5 degree. The data set has undergone many revisions, the first of which spans from 1901 to 1995 and is titled CRU TS 1.0. The version used in this analysis is the most recent revision and is titled CRU TS 2.1 and spans from 1901 to 2002 (1,224 monthly values for each variable and each 0.5 degree cell). Mean temperature, minimum temperature, maximum temperature, diurnal temperature range, precipitation, wet day frequency, frost day frequency, vapor pressure, and cloud cover are all included in the data set. The variables used in this analysis are precipitation, mean temperature, and diurnal temperature range.

A.1.1 Data Used for Construction

The CRU TS data sets were constructed using a network of meteorological observing stations. According to the CRU TS 2.1 documentation, the station data is preferred to satellite data for two reasons: "satellite information only becomes available after 1970, and satellite measures conditions through the depth of the atmosphere rather than at the surface (for example, Susskind et al. 1997)" (Mitchell and Jones, 2005). However, building a global database from station data is not trivial. Previous attempts to build a suitable station database include: the Global Historical Climatology Network (GHCN) (Vose et al., 1992; Peterson and Vose, 1997), the Jones temperature database (Jones, 1994, Jones and Moberg, 2003), and the Hulme precipitation database (Eischeid et al., 1991, Hulme et al., 1998). These three databases serve as the primary source for the CRU TS 2.1 precipitation and temperature time series. Additional data sets were used when available to fill in some of the spatial and temporal holes. Each collection of weather variables was absorbed into the database. The data were absorbed in sequence in order to give priority to the sources that are considered to be more reliable[15]. The station locations used to develop this database are shown for precipitation (Figure A-1) and temperature (Figure A-2). The station coverage for various periods of time are shown for precipitation (Figure A-3) and temperature (Figure A-4). The total number of stations is shown as N_1 in Figures A-1 and A-2, and N in Figures A-3 and A-4 (New et al., 2000). There is a significant decrease in the number of stations used in 1995 from the number of stations used in 1981 (evident in Figures A-3 and A-4). This phenomenon is counterintuitive because one assumes that there should be more available stations in more recent years. This assumption is most likely

[13] Excerpted from (Strzepek and Fant IV, 2010).
[14] The following is primarily a summary from two sources: (Mitchell and Jones, 2005 and http://www.cru.uea.ac.uk/~timm/grid/CRU_TS_2_1.html. For a more detailed discussion please refer to these sources.

[15] The following information is extracted from Table 1 in Mitchell and Jones, 2005. The data were included in the following order: 1) tmp from 1701-2002 (Jones and Moberg, 2003); 2) pre from 1697-2001 from personal communication with Mike Hulme;3) tmp, dtr and pre from 1702-2001 from Peterson and Vose, 1997; 4) tmp, dtr, vap, cld, spc from 1701-1999 from New et al, 2000; 5) tmp, vap, cld from 1971-1996 from Hahn and Warren, 1999; 6) tmp, pre, vap, spc, wet from 1990-2002 from personal communication with William Angel and 7) tmp, tr, pre, vap, spc from 1994-2002 from UK MET office, personal communication.

accurate, especially in developed countries. The CRU team documents and explains the decrease in station coverage (which starts in the early 90s) as follows:

> The recent reduction in station numbers is primarily in areas with good or reasonable station coverage. However, the spatial coverage of stations reporting diurnal temperature ranges shows a more serious reduction in the 1990s. This, in due course, should be alleviated by the inclusion of mean monthly maximum and minimum temperature in the post-1995 monthly CLIMAT reports and by updated data sets for the former USSR and China, once they are included in the CRU data set. (New et al., 2000)

So the current data set (CRU TS 2.1) was most likely constructed using more stations (resulting in better spatial accuracy), but time series maps were not shown in the recent reports (for example, Mitchell and Jones 2005). Figures A-1 through A-4 were taken from New et al., which was published before the CRU TS 2.1 data set was available. For the CRU TS 2.1 data set, more stations were used from 1990 to 1995 than shown in Figures A-3 and A-4. But the other station maps shown in these two Figures (1901, 1921,…, 1981) are accurate for the CRU TS 2.1 data set.

Figure A-1. Precipitation stations used for the CRU TS interpolation

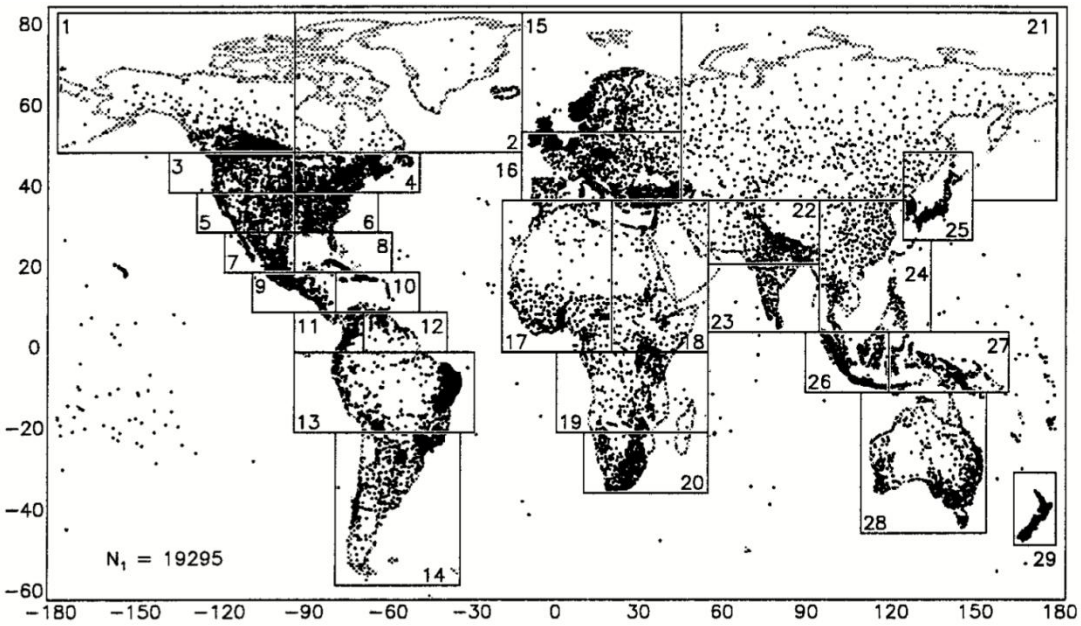

Source: (New et al. 2000)

Figure A-2. Temperature stations used for the CRU TS interpolation

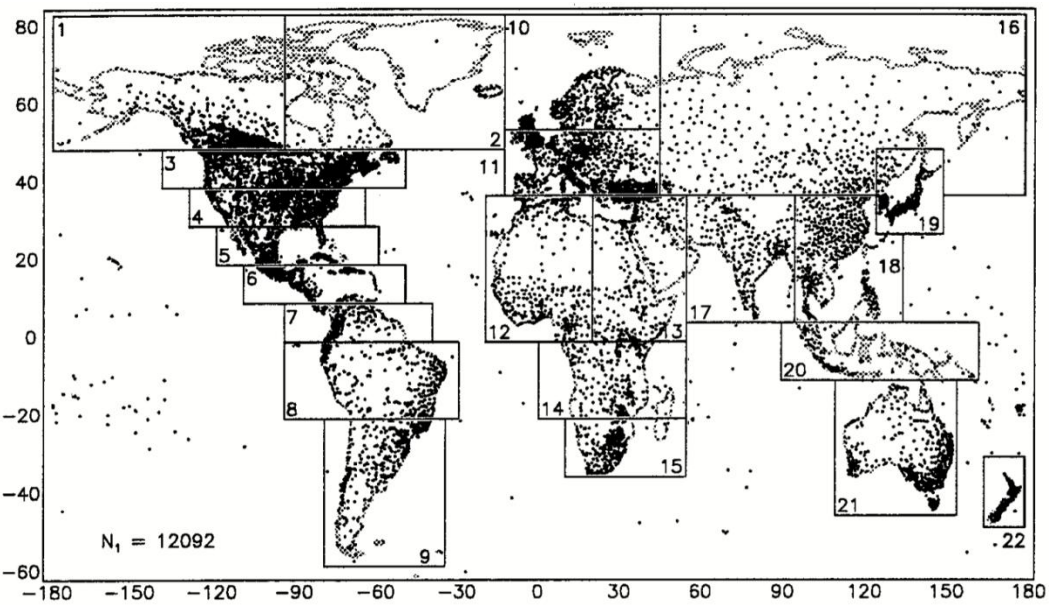

Source: (New et al. 2000)

Figure A-3. Precipitation coverage during different time periods. The shaded areas represent the half-degree coverage

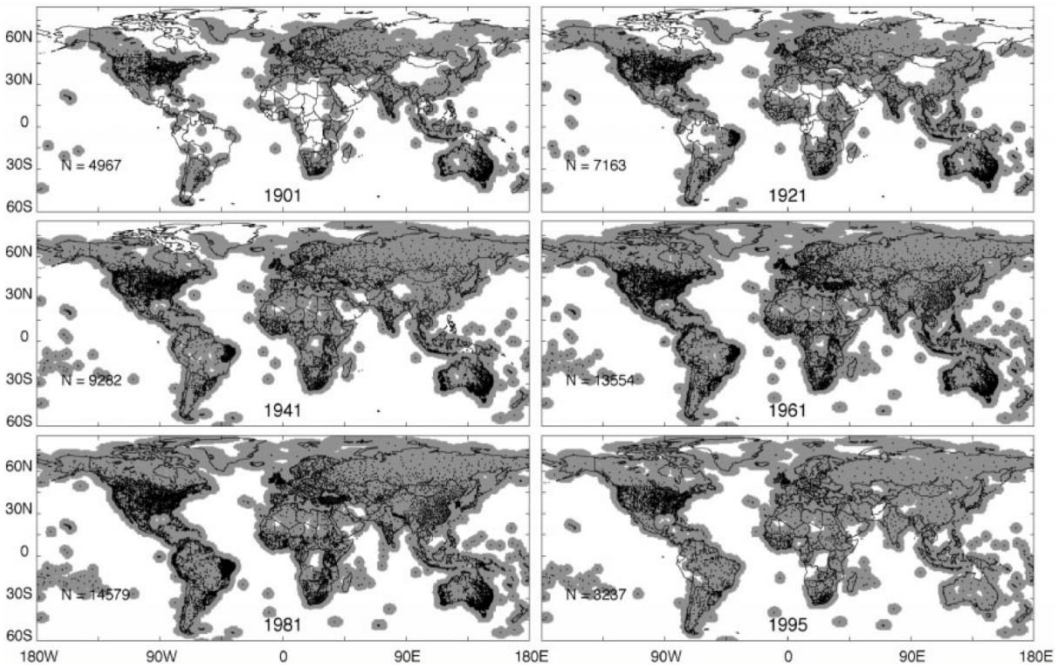

Source: (New et al. 2000)

Figure A-4.. Temperature coverage over various time periods. The shaded areas represent the half-degree coverage

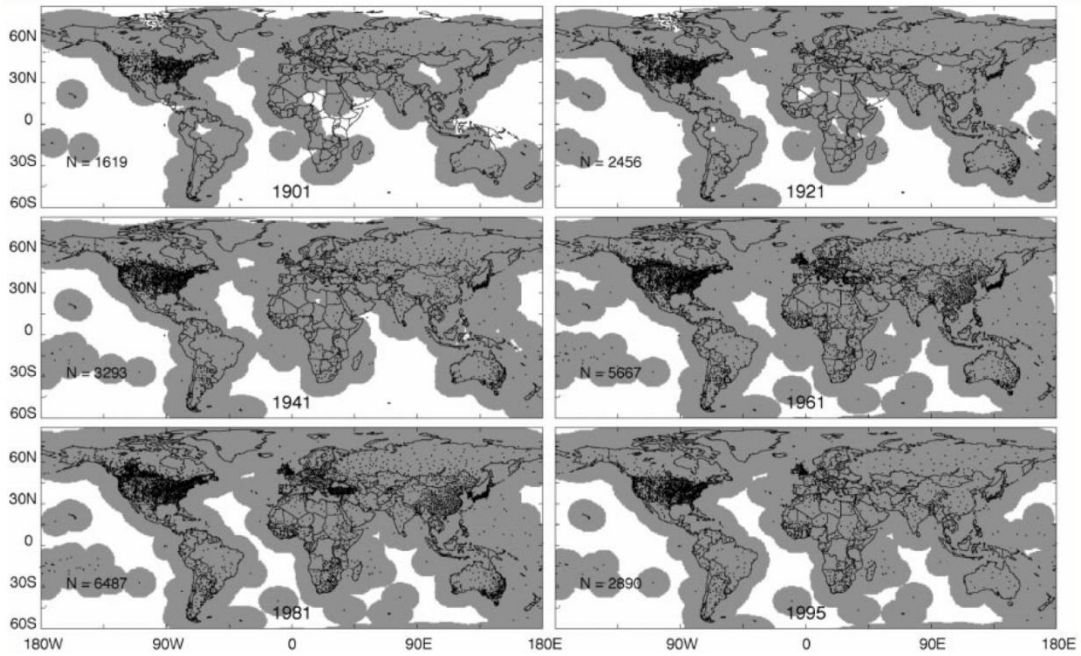

Source: (New et al. 2000)

A.1.2 Construction Method

To expand the weather station data into a land surface, global, time-series database, three major tasks remained: verify the quality of the observed data (homogeneity with climate variations and related observed weather), complete the stations with missing temporal data, and aggregate or expand the station data to half-degree grids.

In order to accomplish the first task, the team at the CRU used an iterative method, where the first pass was used to identify all potential inhomogeneities, and the subsequent passes were used to remove any data that was considered untrustworthy. The goal of the iterative process included the following steps (Mitchell and Jones, 2005):

1. New station records must be checked to ensure that they present a homogeneous record in which variations are caused only by variations in climate.
2. Information from additional sources must be checked against the existing database, to guard against unnecessary duplication.
3. Where new information is available for an existing station, it must be ensured that the different sources provide consistent records.
4. The number of stations useful for constructing grids must be maximized.

The iterative method used is a modified version of the GHCN method of homogenization. The GHCN method is well documented and was developed for global data sets similar to CRU TS 2.0 (Peterson and Easterling, 1994, Easterling and Peterson, 1995). In this method, a subsection of the candidate and a

neighboring reference time series are correlated using a residual sum of squares statistic to check for abrupt or gradual discontinuities. First, a reference time series that is considered homogeneous must be determined, which is difficult because all of the stations in this series are candidates for inhomogeneity. Hence, the iterative procedure is used where the first pass checks for obvious untrustworthy data, the second pass assumes a set of reference stations for checking, the third assumes another set of reference stations, and so on, so that all of the stations were eventually checked with the neighboring stations.

The station data was then anomalized to a specific reference period, meaning that the changes were approximated based on an assumed time period of average weather.

$$\Delta X = X_{i,m,y} - \overline{X}_{i,m} \qquad \text{(EQ 1, difference anomalies)}$$

$$\Delta X = \frac{X_{i,m,y}}{\overline{X}_{i,m}} \qquad \text{(EQ 2, relative anomalies)}$$

Where ΔX is the anomaly; $X_{i,m,y}$ is the weather variable for station *i*, month *m*, and year *y*; $\overline{X}_{i,m}$ is the weather variable mean over the reference period for station *i* and month *m*. For temperature and diurnal temperature range, the difference anomaly was used (Equation 1), while the relative anomaly (Equation 2) was used for precipitation. This was repeated for each value in the available time series, each station, and each of the three weather variables used for the runoff analysis. In this case the reference period was 1961 to 1990. This reference period was chosen because it was late enough to insure the availability of sufficient monitoring stations and early enough to represent a historical mean. This reference period was also chosen because the authors (meaning Mitchell and Jones) have participated in many studies involving the mean weather over this period, specifically the CRU CL series (which includes CRU CL 1.0/2.0, where CL represents global average climatology).

These anomalies were then used to interpolate temporally and to a half-degree resolution. To avoid poor interpolation, the anomalies were used instead of the absolute values. For example, if a portion of a weather station located in the mountains is unavailable, the missing values might be estimated by interpolating between three valley stations. If the absolute values were used for interpolation, the mean values are not preserved (for example, weather stations at higher elevations tend to have colder temperatures than neighboring stations at lower elevations, and so on). Alternatively, when the anomalies are used for interpolation, the mean values are better preserved.

The interpolation of station data onto a uniform grid has been the focus of much research, resulting in many proposed methods. The CRU team used thin-plate splines to interpolate the station data to a surface at a half-degree resolution, as described by Hutchinson (Hutchinson, 1995). The thin-plate spline method attempts to reduce the roughness of the surface using a generalized cross validation statistic. The generalized cross validation is an iterative validation scheme where the data from one station is removed from the data set, and the surface is interpolated without the data from the said station. Then the relative difference between the observed station value and the interpolated value at the location of the station is used as the estimated error. More details on the interpolation method used by the CRU team are given by New et al. (New et al., 1999, 2000).

In areas where there are large gaps between the stations for a given period of time, dummy stations were added to relax the anomaly to zero (that is, the 1961 to 1990 mean). For this reason the CRU TS data set claims to be space-optimized rather than time-optimized (Mitchell, 2010). After the interpolation, the gridded anomalies were adjusted so that the mean at each grid was zero for the reference period (1961 to 1990). The anomalies were then combined with the reference period mean global climatology (CRU CL 1.0) to obtain grids of absolute values. The gridded absolute values were constrained to lie within the range of the physically possible by applying minima and maxima to select weather variables. Precipitation was constrained to be greater than 0 mm, without a maximum; diurnal temperature range was constrained to be greater than 0.1 degree Celsius, without a maximum; and temperature was not constrained.

A.1.3 Uncertainties, Cautions, and Validation

All of the typical uncertainties associated with large, interpolated weather data sets would still apply to CRU TS 2.1. The data set was developed by irregularly spaced weather stations, which measure the weather variables at a point. There is no guarantee that the point data truly represents two-dimensional surface data. Distance between stations is important, but also the weather variance within that distance. Two stations can be close but the weather between them can be drastically different, especially when the stations have different elevations.

There are also no easy ways to monitor all of the weather stations. In the CRU TS documentation (Mitchell and Jones, 2005) the team discusses some station measurement errors caused by the relocation of weather stations in mountainous areas, most likely moving the station to a place with a different elevation. The CRU team hoped to catch many of the measurement errors like this by checking and correcting the inhomogeneities (discussed in Section A.2.2). But all of these possible errors are, for the most part, unavoidable when developing a global data set at a relatively high resolution.

Another caveat, expressed in detail by Tim Mitchell on his Tyndall website (Mitchell, 2010), is the use of the CRU TS 2.1 data set as a local time series. As discussed in the previous section, some of the missing sections of the station data, both spatial and temporal, were relaxed to the 1961 to 1990 mean. For this reason, the CRU team states that CRU TS 2.1 “is our best estimate of the spatial pattern of climate at each moment in time” (Mitchell, 2010). This method could have removed some of the undocumented extreme events, especially for values before 1961; although, using the mean value is a much safer estimate, as opposed to extrapolating the weather from distant stations, which could result in much greater quantitative errors.

The CRU TS data set is a well-accepted global weather data set among climatologists and hydrologists. The CRU team has undertaken a great deal of quality assessments and found the resulting data set to be as accurate as possible, given the coarse resolution and available data. A few third party groups have attempted to validate the CRU TS data set by comparing it with station data that was not available to the CRU team when the data set was constructed. One such example is “Comparison of Products from ERA-40, NCEP-2, and CRU with Station Data for Summer Precipitation of China” by Tianbao and Congbin (Tianbao and Congbin, 2006). In this paper, the authors find that the CRU TS data set shows the best agreement with the station data over China when compared to the other two data sets. Meigh and Fry (Meigh and Fry, 2004) find that the CRU TS data set agrees with station data in southern Africa, and

Mayotte (Mayotte, 2009) found that CRU TS agrees with station data over Ethiopia. In all three cases, the studies used station data that was not available to the CRU TS team.

A.2 UNH-GRDC Runoff Data Description[16]

Selected gauging stations from the GRDC and the Simulated Topological Network (STN-30) developed at UNH were coregistered to develop a set of estimated runoff values (This data set will be referred to as UNH-GRDC). The UNH-GRDC runoff database, used in this analysis, is an estimate of the historic mean monthly runoff at a half-degree resolution. This database was constructed with a strong emphasis on the observed data from gauging stations as opposed to simulated runoff. The argument for emphasizing the measured runoff is that measured weather variables, primarily precipitation, often have more error than measured runoff. And simulated runoff is based on these measured weather variables averaged over large areas. On the other hand, measured runoff does not always represent climate-driven, raw runoff patterns. This incongruity is primarily a result of human induced alterations to the land surface, for example, reservoirs and urban development. So the UNH-GRDC team has developed a combination of observed and simulated runoff to provide the best estimate of terrestrial runoff averages for the globe.

A.2.1 Data Used for Construction

The STN-30, at a half-degree resolution, helped to arrange the land cells (also half-degree) into a river network. This allows the team to delineate the boundaries of the contributing basins. These boundaries are important for understanding the runoff values both measured and simulated.

GRDC has collected and maintained global runoff records of two types. The first type is a collection of 198 gauging stations at the mouths of rivers that drain into the ocean, including measured runoff, percentile graphs, and flow accumulation curves. The second data set contains 1,348 gauging stations with tributaries larger than 2,500 km^2 and records longer than 12 years. The UNH team has determined that the STN-30 can resolve catchments with an area greater than 25,000 km^2 reliably, between 10,000 and 25,000 km^2 fairly well, but below 10,000 km^2 the accuracy is considered untrustworthy. The primary reason for the caution with smaller catchments is a result of the half-degree resolution of the STN-30. For this reason, the UNH-GRDC team selected 861 (of the 1,348) candidate stations, all with a catchment area greater than 10,000 km^2. Figure A-5 shows the locations of these candidate stations.

[16] The following is primarily a summary of other work (Fekete, VÖrÖsmarty, and Grabs, 2000). Please refer to this source for more details.

Figure A-5. GRDC selected discharge gauging stations

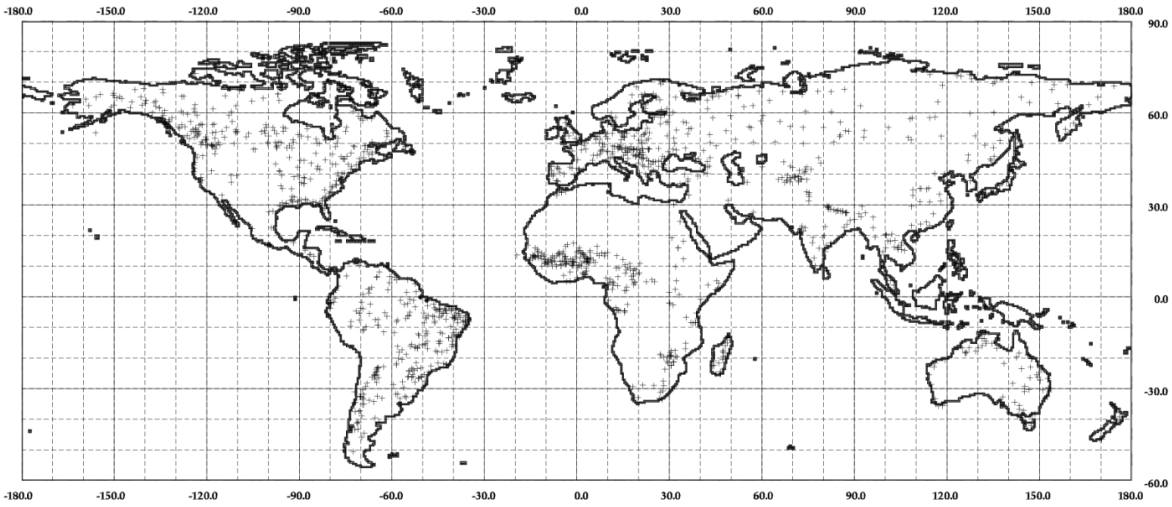

Source: Fekete et al. 1999

A WBM was used to develop a better estimate of climate-driven runoff at a half-degree resolution. The water balance is typically based on a simple soil moisture budget, first given by Thornthwaite (Thornthwaite, 1948) as

$$R = P - E - \frac{\partial W}{\partial t} \qquad \text{(EQ 3)}$$

where R is the rate of surplus water (runoff and/or recharge) in millimeters/day, P is the rate of precipitation in millimeters/day, E is the rate of evapotranspiration in millimeters/day, and $\frac{\partial W}{\partial t}$ is the change in soil moisture in millimeters/day. Vörösmarty et al. (Vörösmarty et al., 2000a) developed the WBM based on Equation 3, to be used at a continental and global scale. $\frac{\partial W}{\partial t}$ was estimated using the following method

$$\frac{\partial W}{\partial t} = \begin{cases} g(W)(E_0 - P_a) & P_a < E_0 \\ P_a - E_0 & 0 < P_a - E_0 < W_c - W \\ W_c - W & W_c - W < P_a - E_0 \end{cases} \qquad \text{(EQ 4)}$$

where E_0 is PET, P_a is precipitation available for soil recharge, W_c is the soil's water holding capacity, W is the soil moisture, and $g(W)$ is a unit-less soil drying function given as

$$g(W) = \frac{1 - \exp\left(-\alpha W / W_c\right)}{1 - e^{-\alpha}} \qquad \text{(EQ 5)}$$

Where α is an empirical constant. Evaporation is defined as

$$E = \begin{cases} P_a - \frac{\partial W}{\partial t} & P_a < E_0 \\ E_0 & E_0 < P_a \end{cases} \qquad \text{(EQ 6)}$$

For PET, Hamon's temperature-based function was used (Hamon, 1963). The climate variables used in the WBM were air temperature, precipitation, wind speed, cloud coverage, and vapor pressure deficit from the CRU for the period 1986 to 1995 (New 1999, 2000). The land surface was classified using the Terrestrial Ecosystem Model's (Melillo, 1993) potential vegetation overlaid with cultivated areas from Olson's land-use classification (ISLSCP, 2005). The FAO/UNESCO (FAO/UNESCO, 1986) soil data bank was used to estimate the soil type and texture. Land cover and soil types were combined to estimate the rooting depth and water holding capacity, using the method described in Vörösmarty et al. (Vörösmarty et al., 2000b). Since the WBM and the selected GRDC gauging stations all report runoff at a monthly time-scale, the UNH-GRDC team decided to consider travel time delays negligible. The proof of this is described in more detail in Fekete et al. (Fekete et al., 2000).

A.2.2 Construction Method

The GRDC observed runoff and the runoff simulated by the WBM were combined using a set of correction coefficients calculated on an annual basis. The observed runoff in between two stations (interstation runoff) was estimated as follows:

$$\bar{R}_{oi} = \frac{\bar{Q}_{oi}}{A_{si}} \qquad \text{(EQ 7)}$$

Where $\bar{R}_{oi}$ is the estimated mean annual observed interstation runoff at interstation region I, $\bar{Q}_{oi}$ is the mean annual interstation discharge, and A_{si} is the interstation area. Using a weighted average, the mean water balance runoff in the interstation region i is:

$$R_{wi} = \frac{\int_{A_{si}} R_{wbm}\, dA}{A_{si}} \qquad \text{(EQ 8)}$$

Where R_{wi} is the mean annual water balance runoff, R_{wbm} is the local annual water balance runoff, and A_{si} is still the interstation area. The correction coefficient (R_c) then becomes

$$R_c = e_{si} \times R_{wbm} \qquad \text{(EQ 9)}$$

$$e_{si} = \frac{\bar{R}_{oi}}{\bar{R}_{wi}} \qquad \text{(EQ 10)}$$

Where e_{si} is the error (or the correction coefficient) of the WBM. This term was constrained to be greater than or equal to 0.5 and less than or equal to 2.0. The combined mean annual runoff, using the method just described, is show in Figure A-6. This error term e_{si} calculated as a long-term average, is plotted for the globe in Figure A-7.

Therefore, the runoff data was distributed over the globe at a half-degree resolution using the WBM results, constrained to preserve the observed discharge from the gauge stations (Fekete et al., 2002).

Figure A-6. UNH-GRDC composite mean annual runoff for the globe

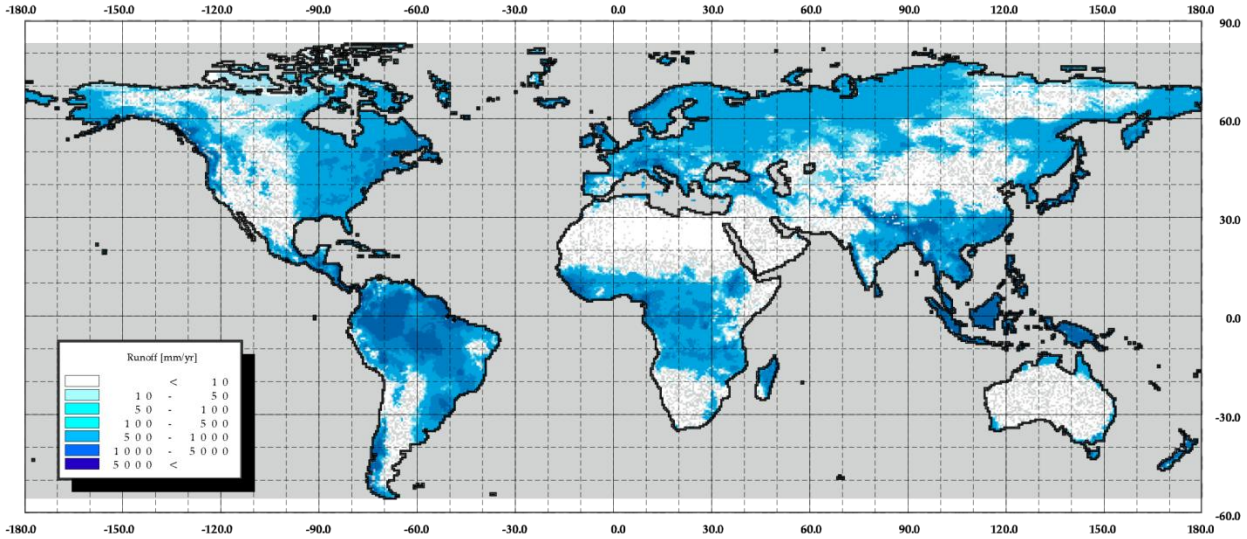

Source: Fekete et al. 1999

Figure A-7. WBM runoff correction coefficients

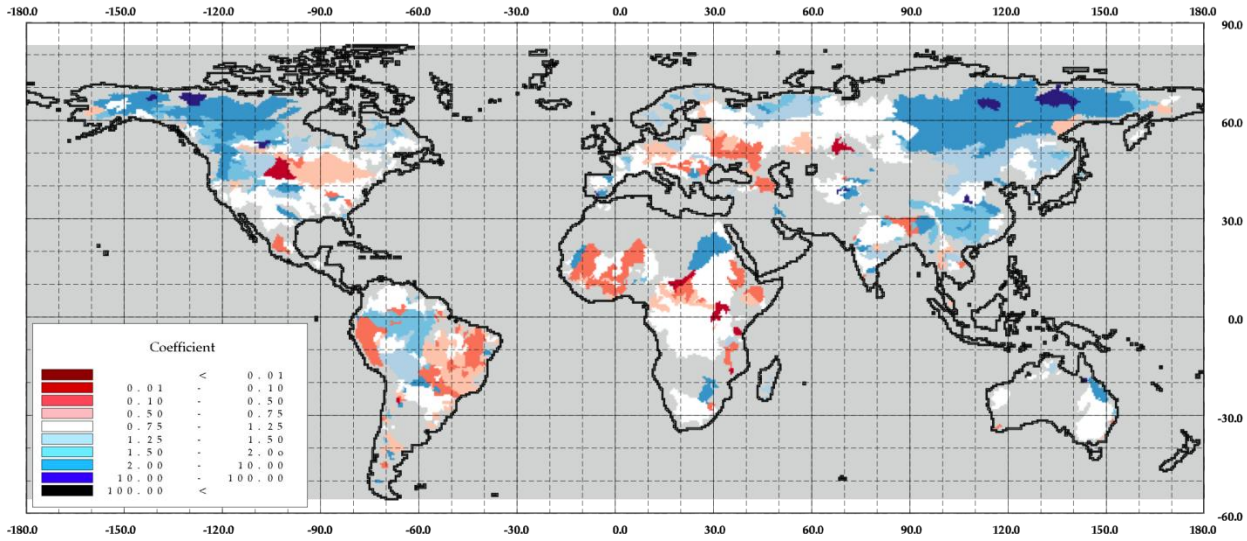

Source: Fekete et al. 1999

A.2.3 Uncertainties, Cautions, and Validation

The UNH-GRDC data set is the result of a complex process involving climate data, runoff data, topology data, and a runoff model—all of which can introduce error. Errors in the climate data, CRU TS (discussed in the previous section), can have significant adverse effects on the modeled runoff. This caveat is especially true in regions where observed runoff data is sparse, because the gauge station data was used to correct the modeled runoff. Also, although the observed runoff data tends to be more accurately measured than observed weather data, river discharge measurements also contain errors of 5 to 10 percent (Hageman and Dumenil, 1998; Rantz, 1982). Furthermore, the gridded river network (STN-30) carries with it errors of its own. These errors are much more difficult to quantify because they deal with the linkages of the tributaries and the overall structure of the runoff model and data. The main caution linked with this data set is that the topology was averaged over a half-degree by half-degree grid, which is a considerably large area to assume a constant slope. But all of these possible errors introduced by the errors in the global data used cannot be corrected with an obvious solution, because the data sets used are arguably the best available (ISLSCP, 2005).

The correction coefficients used to constrain the modeled runoff were calculated and applied on an annual basis, while the results were given on a monthly basis. The use of annual correction coefficients was necessary because of the seasonal storage introduced by nature and human impact, but still could cause some inherent errors. Using annual coefficients assumes that the seasonal variation was captured correctly by the WBM. Another limitation is the range forced on to the correction coefficient (0.5–2.0). Any errors inherent in the WBM are magnified when the WBM results and observed runoff relationship produces a correction coefficient outside this range. This range also seems to have been chosen arbitrarily without an in depth look into the cause of extreme values (ISLSCP, 2005).

Developing a global runoff data set is difficult, and all of these uncertainties mentioned are not to discredit the UNH-GRDC data set. Most of the possible errors mentioned are unavoidable, and come with the development of a global data set. It is the opinion of the authors of this World Bank Water paper that the UNH-GRDC data set is the best global runoff data set available.

A.2.4 Comparison of Basin Boundaries between UNH-GRDC Data and Alavian et al.

The main difference between the UNH-GRDC basin boundaries and the basin boundaries used in the study by Alavian et al. (Alavian et al., 2009) is the resolution. The UNH-GRDC group used a half-degree topology (STN-30), restricting the size at which basin boundaries can be accurately depicted. Therefore, the size of the UNH-GRDC basins is generally much greater than the basins used in the study by Alavian et al., especially in areas further inland.

Another major difference is the method used to consider one basin “complete” and separate from other basins. The UNH-GRDC group chose basin boundaries based on where the station data was available, and not based on physical parameters. By contrast, the basin boundaries used in the Alavian et al.’s report were calculated based on the Hydro1k level 3 and level 4 catchments (level 4 was used for all of the bank regions, except Africa, where level 3 was used). To provide an example, Figure A-8 shows the two basin delineations over Africa, Figure A-9 shows a close-up of the same figure over the Zambezi basin, and Figure A-10 shows a zoomed-in portion of the Zambezi with Will Farmer’s Unique Identifiers

labeled. In Figure A-10, the basins are labeled as such: “UniqueIdentifier_BankRegion: D – UNH-GRDCbasin.” For example, if the Unique Identifier is “G5866,” the region is Africa (“AFR”), and the UNH-GRDC basin is the Zambezi, then the label shown on the map would be “G5866_AFR: D – Zambezi.”

Figure A-8. UNH-GRDC basin boundaries (green) and the Hydro1k level 3 basins (brown) over Africa

Source: Authors’ analysis using combined USGS Hydro 1k Level 3 data with GRDC-UNH basin boundaries

Figure A-9. UNH-GRDC basin boundaries (green) and the Hydro1k level 3 (part of Southern Africa)

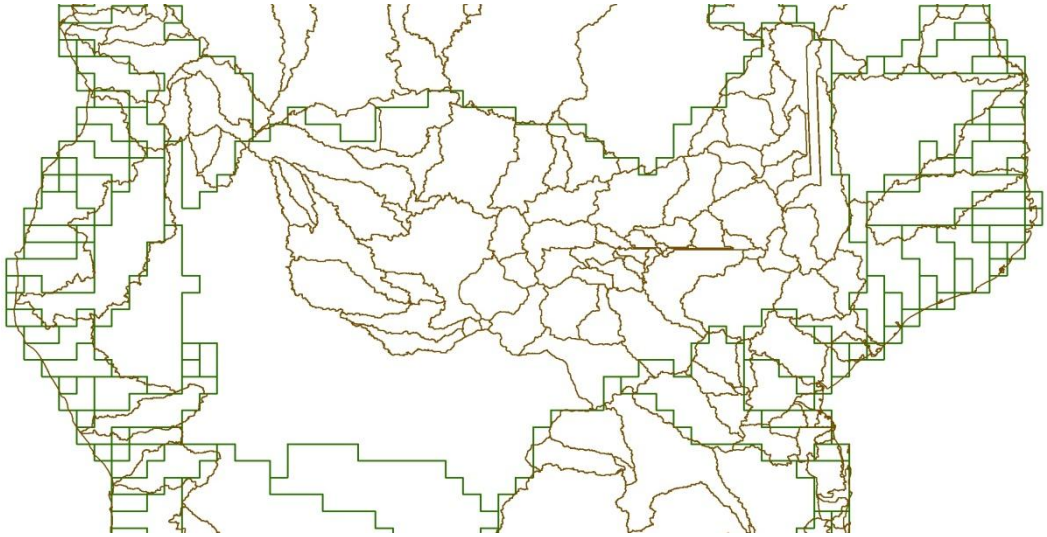

Source: Authors' analysis using USGS Hydro 1k Level 3 data with GRDC-UNH basin boundaries

Figure A-10. UNH-GRDC basin boundaries (green) and the Hydro1k level 3 basins (brown) zoomed in to show the Unique Identifier labels (as an example)

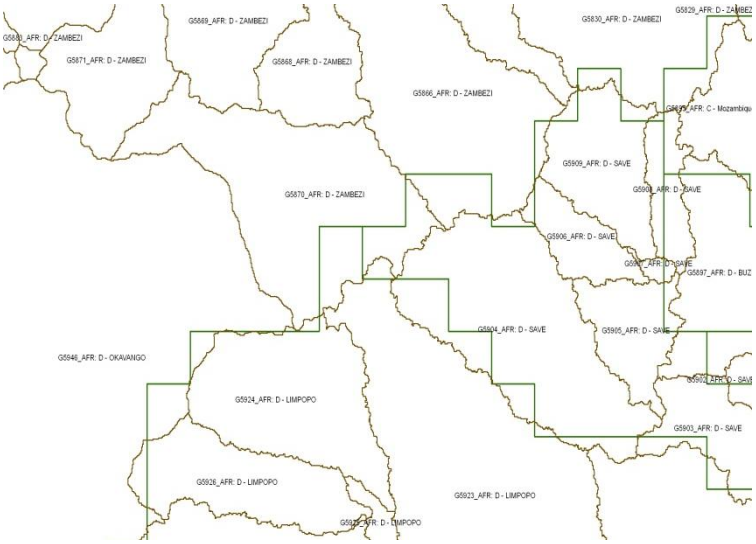

Source: Authors' analysis: combined USGS Hydro 1k Level 3 data with GRDC-UNH basin boundaries

ANNEX B: OVERVIEW OF THE CLIRUN-II RAINFALL RUNOFF MODEL

CLIRUN-II is the latest model in a family of hydrologic models developed specifically for the analysis of the impact of climate change on runoff. Kaczmarek (Kaczmarek, 1993) presents the theoretical development for a single-layer lumped watershed rainfall runoff model CLIRUN. In other work Kaczmarek (Kaczmarek, 1998) presents the application of CLIRUN to the Yellow River in China.

Yates (Yates, 1996) expanded on the basic CLIRUN by adding a snow-balance model and providing a suite of possible PET models and packaged it in a tool called WatBal. WatBal has been used on a wide variety of spatial scales from small to large watersheds and globally on a 0.5 $\times$ 0.5 degree grid (Strzepek et al., 1999, Huber-Lee et al., 2005, Strzepek et al., 2005).

CLIRUN-II (Strzepek et al., 2008) is the latest in the Kaczmarek School of hydrologic models. It incorporates most of the features of WatBal and CLIRUN but specifically addresses extreme events at the annual level, modeling low and high flows. CLIRUN and WatBal did well in modeling mean monthly and annual runoff, which is important for water supply studies, but did not model accurately the tails of the runoff distribution (floods and droughts).

CLIRUN-II has adopted a two-layer approach following the framework of the SIXPAR hydrologic model (Gupta and Sorooshian, 1983, 1985) and using a unique conditional parameter estimation procedure. In the following section a brief description of the components of the model will be presented.

CLIRUN-II models runoff as a lumped watershed with climate inputs and soil characteristics averaged over the watershed simulating runoff at a gauged location at the mouth of the basin. CLIRUN-II can run on a daily or monthly time step.

The snow accumulation and melt model used in this study is based on concepts frequently used in monthly WBMs (McCabe and Wolock, 1999). Inputs to the model are monthly temperature and precipitation. Snowmelt is added to any monthly precipitation to form effective precipitation available for either infiltration or direct runoff.

B.1 Structure

Figure B-1 is a schematic of the water flows of CLIRUN-II. The figure shows the mass balance of water in the CLIRUN-II system. Water enters via precipitation and leaves via ET and runoff. The difference between inflow and outflow is reflected as change in storage in the soil or groundwater.

Figure B-1. Schematic of water flows in CLIRUN-II

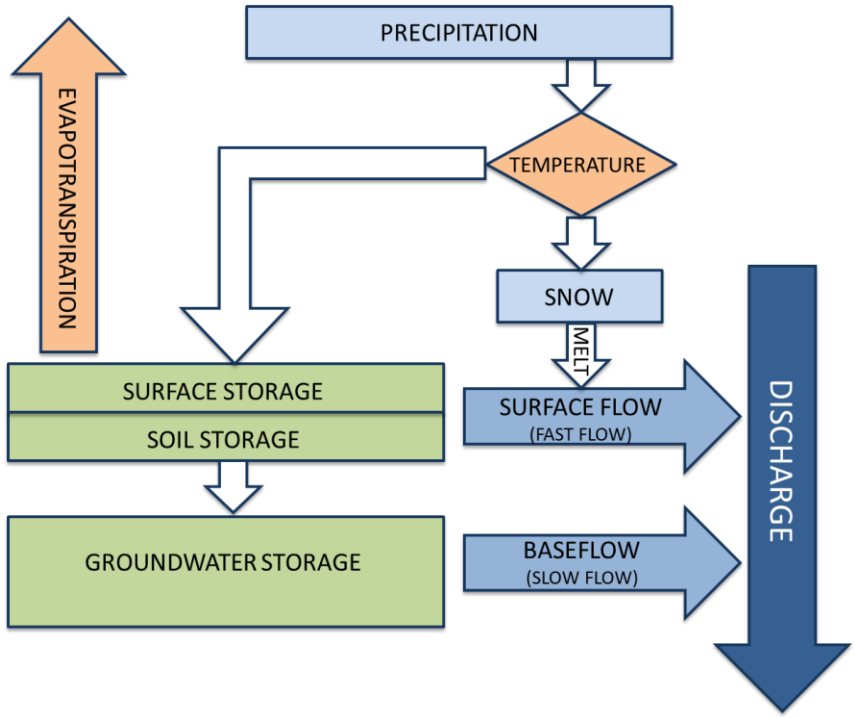

Source: Authors' representation of water flows in CLIRUN-II

Soil moisture is modeled as a two-layer system with soil (upper) and groundwater (lower) layers. These two components correspond to a quick and a slow runoff response to effective precipitation.

The soil layer generates runoff in two ways. First there is a direct runoff component, which is the portion of the effective precipitation (precipitation plus snowmelt) that directly enters the stream system. The remaining effective precipitation infiltrates into the soil layer. The direct runoff is a function of the soil surface and models differently for frozen and nonfrozen soil, determined by temperature. The infiltration then enters the soil layer. A nonlinear set of equations determines how much water leaves the soil as runoff, is percolated to the groundwater, and goes into soil storage. The runoff is a linear relation of soil water storage; and percolation is a nonlinear relationship of both soil and groundwater storages.

The groundwater then receives percolation from the soil layer and runoff is generated as a linear function of groundwater storage.

The soil water processes have six parameters, like the SIXPAR model (Gupta and Sorooshian, 1983), that are determined via calibration of each watershed.

B.1.1 Inputs

CLIRUN-II requires inputs of precipitation, temperature, PET, observed runoff, and the basin boundaries. There have been many methods developed to calculate PET. A suite of PET models is available for use in CLIRUN-II.

The weather values then need to be averaged over each basin. The Massachusetts Institute of Technology Joint Program has developed a basic tool, BasinFrac, to do this using ESRI's arcGIS and Matlab (data analysis software by Mathworks). This method requires that the basin boundaries be in a shape file (.shp format). The intersect command is used in arcGIS to find the percentage of each weather cell that is contained in each basin. Then Matlab is used to find each basin's weighted average (weighted by area).

B.1.2 Calculations

The runoff calculation undergoes three model processes: snow, soil moisture balance, and runoff.

B.1.2.1 Snow Model

For each time (day or month), the snow model undergoes the following process.

First, the precipitation of the day or month is multiplied by a calibrated intercept coefficient. This coefficient attempts to simulate the effects of the ground cover (foliage, trees, bushes, and so on) by catching some of the rain before the rain hits the ground.

Each day or month is then split into three temperature categories: high, medium, or low. These categories are based on two calibrated coefficients: T_h and T_l. If the temperature is less than T_l, all of the precipitation is considered to fall as snow, and none of the current snow pack melts—meaning that none of the precipitation can enter the soil on that day or month.

If the precipitation is in between T_l and T_h, then only some of the snow stays frozen as snowpack, while some of the snow melts. The following two equations are used to find how much snow melts and how much remains frozen:

$$K_T = \frac{T - T_l}{T_h - T_l} \qquad \text{(EQ 1)}$$

$$SP_C = SP_P \times (1 - 0.5 \times K_T) + P \times (1 - K_T) \qquad \text{(EQ 2)}$$

where K_T is a fraction coefficient based on temperature, T_l is the calibrated low temperature threshold, T_h is the calibrated high temperature threshold, SP_C is the current snow pack, SP_P is the previous snow pack, and P is the current precipitation. The current snow pack is then allowed to melt using a calibrated value D_m. The melted snow is added to the next time period's precipitation and removed from the current snow pack.

If the temperature is greater than T_h, all of the precipitation is assumed to fall as rain, and the D_m of the current pack melts. Again, the melted snow is added to the next time period's precipitation and removed from the current snow pack.

After each time period undergoes this process, a new precipitation time series is produced and used in the soil moisture balance model.

B.1.2.2 Soil Moisture Balance Model

For each time (day or month), the soil balance undergoes a process. This process is solved using an ordinary differential equation function solver built into Matlab known as ode45.

First, the soil moisture in the upper soil layer is compared to the value of saturation. The saturation value is the maximum amount of moisture that a layer can hold (commonly known as the Water Holding Capacity). This coefficient is found through the calibration process. If the soil moisture in the upper layer is more than the saturation value, the excess water is considered to escape by surface runoff using the following equation:

$$R_S = M_u - sat \qquad \text{(EQ 3)}$$

Where R_s is the surface runoff, M_u is the soil moisture of the upper layer, and *sat* is the saturation value of the soil. The soil moisture in the upper layer is set to the value of saturation, and none of the precipitation is allowed to enter the soil. The precipitation also becomes surface runoff by multiplying the precipitation value by a calibrated coefficient known as over: (*precip* × *over*). This part of the surface runoff is commonly referred to as ponding. If the soil moisture in the upper layer is less than the saturation value, the surface runoff is considered to be zero, and all of the precipitation is allowed to enter into the upper layer.

Next, actual ET is calculated. Actual ET is a function of potential and soil moisture state following the FAO method (FAO, 1996). If the soil moisture in the upper layer is more than half of the saturation value (0.5 × *sat*), then the actual ET is equal to the PET of the given time (day or month). If the current soil moisture of the upper layer is less than half of the saturation value, then actual ET is calculated using the following equation:

$$ET = PET \times \left(\frac{M_u}{0.5 \times sat} \right) \qquad \text{(EQ 4)}$$

where M_u is the soil moisture of the upper layer, and *sat* is the saturation value of the soil.

Then the changes in soil moisture in the upper and lower layer are calculated using the following two equations:

$$\frac{du}{dt} = \left(P - R_s - ET\right) - K_u \times M_u - K_p \times M_u \times \left| 1 - \left(\frac{M_l}{l_m} \right) \right| \qquad \text{(EQ 5)}$$

$$\frac{dl}{dt} = K_p \times M_u \times \left(1 - \left(\frac{M_l}{l_m} \right)^3 \right) - K_l \times M_l \qquad \text{(EQ 6)}$$

Where $\frac{du}{dt}$ and $\frac{dl}{dt}$ are the changes in the soil moisture of the upper layer and lower layer, respectively, with respect to time; P is the precipitation; R_s is the surface runoff (either caused by ponding or the runoff not allowed to enter the upper soil layer); K_u and K_l are calibrated soil parameters of the upper and lower layer, respectively; M_u and M_l are the soil moisture values of the upper and lower layer, respectively; and l_m is a calibrated lower layer thickness value.

In Equation 4, the effective precipitation is calculated as ($P - R_s - ET$) and the subsurface runoff is calculated as $K_u \times M_u$. In Equation 5, the baseflow is calculated as $K_l \times M_l$. And in both Equations 4 and 5, the percolation from the upper layer to the lower layer is calculated as:

$$K_p \times M_u \times \left(1 - \left(\frac{M_l}{l_m}\right)^3\right)$$

B.1.2.3 Runoff Model

Once the ordinary differential equation, described previously, of the soil moisture is solved, most of the runoff calculations have already been done. In the runoff model section, the runoff values are simply sorted and summed so that total runoff = surface runoff + subsurface runoff + baseflow. The total runoff is typically what is reported as the CLIRUN-II output.

B.1.3 Output

Each of the separate runoff values, including total runoff, is directly output as millimeters/month. To obtain the runoff in usable units, like cubic meters per second(CMS) or MCM per month, the areas of each basin are used.

B.2 Calibration/Validation Process

A calibration procedure is used to determine 10 coefficient values that vary from place to place. Table B-1 illustrates these calibrated coefficients providing the name, symbol used in this report, and bounds. The bounds are used during the calibration process to avoid unrealistic coefficient values.

Table B-1. Calibration parameters in CLIRUN-II

NAME	SYMBOL	BOUNDS
Intercept coefficient	*inter*	0.6 – 1.1
High temperature threshold	T_h	0 – 20
Low temperature threshold	T_l	–15 – 15
Maximum snowmelt	D_m	0 – 50
Saturation value	*sat*	2 – 200
Lower layer thickness	l_m	2 – 200
Upper layer runoff coefficient	K_u	10^{-3} – 1.9
Lower layer runoff coefficient	K_l	10^{-3} – 0.5
Percolation coefficient	K_p	10^{-4} – 0.3
Excess precipitation runoff coefficient	*over*	0.01 – 0.2

Source: The bounds are constraints place on the parameters in CLIRUN-II

The observed runoff is used in an iterative calibration scheme, where each iteration undergoes the following steps:

1. The 10 calibrated coefficients are intelligently estimated based on the previous iteration results and a given realistic range (for the first iteration, given initial values are used).
2. CLIRUN-II runs, estimating runoff over the calibration period.
3. The estimated runoff is compared with the observed runoff using an objective function or error statistic.
4. The model checks the error statistic to see if the calibration goal has been met. If the goal is not met, the model begins another iteration, starting with step 1.

The objective function in this case is calculated as follows:

$$E = \sum (M_i - O_i)^2 \qquad \text{(EQ 7)}$$

Where E is the error statistic (commonly known as the Residual Sum of Squares); M_i is the modeled average runoff for month i; and O_i is the observed average runoff for month i. Because the UNH-GRDC runoff data is the predicted average monthly "observed" runoff (12 values for each 0.5 × 0.5 degree cell), the modeled runoff was first averaged over each month. A built-in Matlab function was used called patternsearch. This function intelligently finds the minimum value of the objective function using a pattern search algorithm.

ANNEX C: COMPARISON OF CLIRUN-II RESULTS USING GRDC VERSUS IN-COUNTRY DATA: SELECTED BASINS[17]

C.1 Introduction

This appendix qualitatively examines the uncertainties of the CLIRUN-II model results presented in Alavian et al. (Alavian et al., 2009). These uncertainties stem from many of the aspects involved in the development of the CLIRUN-II runoff estimates. These aspects can be split into two main categories: inputs into CLIRUN-II and operations within CLIRUN-II. The inputs used in CLIRUN-II for Alavian et al.'s report come from three primary sources: the CRU, which provides historic climate data; the IPCC, which provides future climate predictions; and the UNH- GRDC, which provides the baseline historic runoff.

The CLIRUN-II results which follow when using UNH-GRDC data for calibration are listed below as CLIRUN_GRDC_CRU in order to tag the origins of the input data. Another data set, listed below as CLIRUN_LOCAL_CRU, is being developed in this study using a local set of historic streamflow data, instead of the UNH-GRDC estimated historic streamflow data. Five basins were selected for this study: the Zambezi Basin in southern Africa, the Blue Nile Basin in Ethiopia, the Red River in Vietnam, the Vardar Basin in Macedonia, and the Sao Francisco in Brazil. Maps and brief summaries of each of these basins are provided in Section C.2.

C.2 Basins/Study Regions

C.2.1 Zambezi River Basin

The Zambezi River Basin watershed spreads over nine countries: Zambia, the Democratic Republic of Congo, Angola, Namibia, Botswana, Zimbabwe, Mozambique, Malawi, and Tanzania. The Zambezi River is the largest river that flows into the Indian Ocean and the Zambezi basin is the fourth largest in Africa (FAO, 1997).

The observed streamflow data used for this Zambezi Basin study was given by Charly Cadou, of BRL Ingenierie (Cadou, 2009). The data spans from 1962 to 2002 for 20 stations, although most of the stations were missing data within that range, and some were missing most of the data within that range. Of the 20 stations, 12 were considered acceptable for this study. The other eight stations were considered unusable because either the location of the gauge was unknown or too much of the data was artificially produced using a cross correlation method. For the 12 stations selected, the years 1971 to 1990 were used for calibration, as this time period contained fewer artificially reconstructed values;

[17] This analysis and discussion is excerpted from: Strzpek, K.M, and C.W. Fant IV. 2010. *Water and Climate Change: Modeling the Impact of Climate Change on Hydrology and Water Availability. Selected Basin Study*. Draft 2. University of Colorado and Massachusetts Institute of Technology.

however, for consistency, the observed streamflow from 1986 to 1995 for these stations was used to compare with the UNH-GRDC runoff fields.

The map in Figure C-1 shows the basins modeled in the Zambezi Basin. The red triangles represent gauge stations that were used for the calibration of CLIRUN-II and the green triangles represent the GRDC gauges used in the UNH-GRDC project. The solid red lines represent the basin boundaries used in this study (also used in Alavian et al.'s report) based on the Hydro1k catchment level 3. The solid black lines represent country boundaries. Also, each basin modeled has been filled in by a unique color identified in the legend. In the cases where the basins overlapped, the upstream basins were given mapping priority, meaning that they are shown as covering the overlapping section.

Figure C-1. Zambezi Basin map—all basins

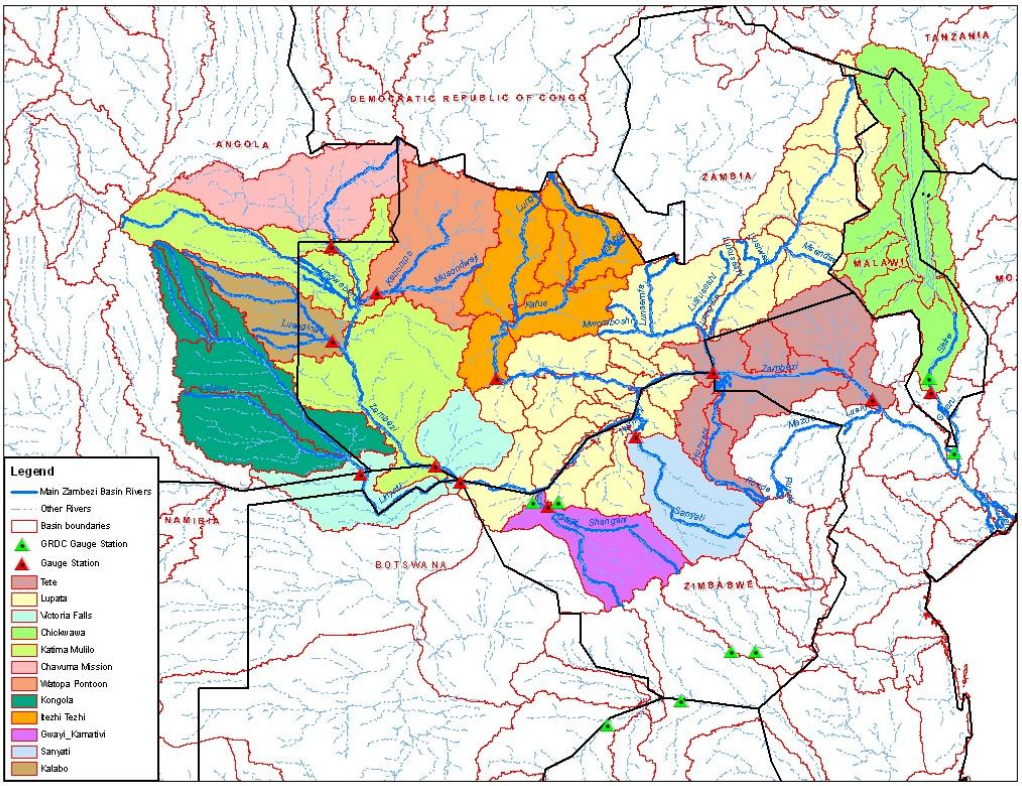

Source: Authors' analysis (data provided by Cadou, 2009)

There are only four GRDC gauges used in the UNH-GRDC project that are a part of the Zambezi basin. Two of the four are close to one another (these are located in the Gwayi Kamativi subbasin and are shown in magenta in Figure C-1). The other two are on the Shire River in Malawi. Therefore, most of the UNH-GRDC results used for comparison in the Zambezi are modeled using the WBM results, that is, without using the observed discharge adjustment.

C.2.2 Blue Nile and Ethiopia Basins

The Blue Nile is one of two major tributaries of the Nile (the White Nile is the other major tributary). The Blue Nile gathers most of its volume from Lake T'ana in the Ethiopian Highlands. The Blue Nile is known to have heavy seasonal and annual fluctuations in flow (Block et al., 2007).

The data for this study on the Blue Nile basin was provided by Paul Block and Kenneth Strzepek (Block and Strzepek, 2010), who collected the data from the Ethiopian Government while in Ethiopia. Some of the data was considered unusable because the basin size would have been too small in comparison to the Hydro1k level 3 and level 4 catchment scale.

The map in Figure C-2 shows the basins modeled in the Blue Nile and other basins in Ethiopia. The red triangles represent gauge stations that were used for the calibration of CLIRUN-II. The solid brown lines represent the basin boundaries used in the Alavian et al. (Alavian et al., 2009) report based on the Hydro1k level 3 catchment. The solid black lines represent country boundaries. Each basin modeled has been filled in by a unique color identified in the legend. Again, in the cases where the basins overlapped, the upstream basins were given mapping priority, meaning that they are shown as covering the overlapping section. As shown in Figure C-2, the only GRDC gauge used in the UNH-GRDC project lies on the Blue Nile in between two of the gauges used in this study: the Blue Nile gauge and the Sudan Border gauge.

Figure C-2. Blue Nile and Ethiopia Basins map—all basins

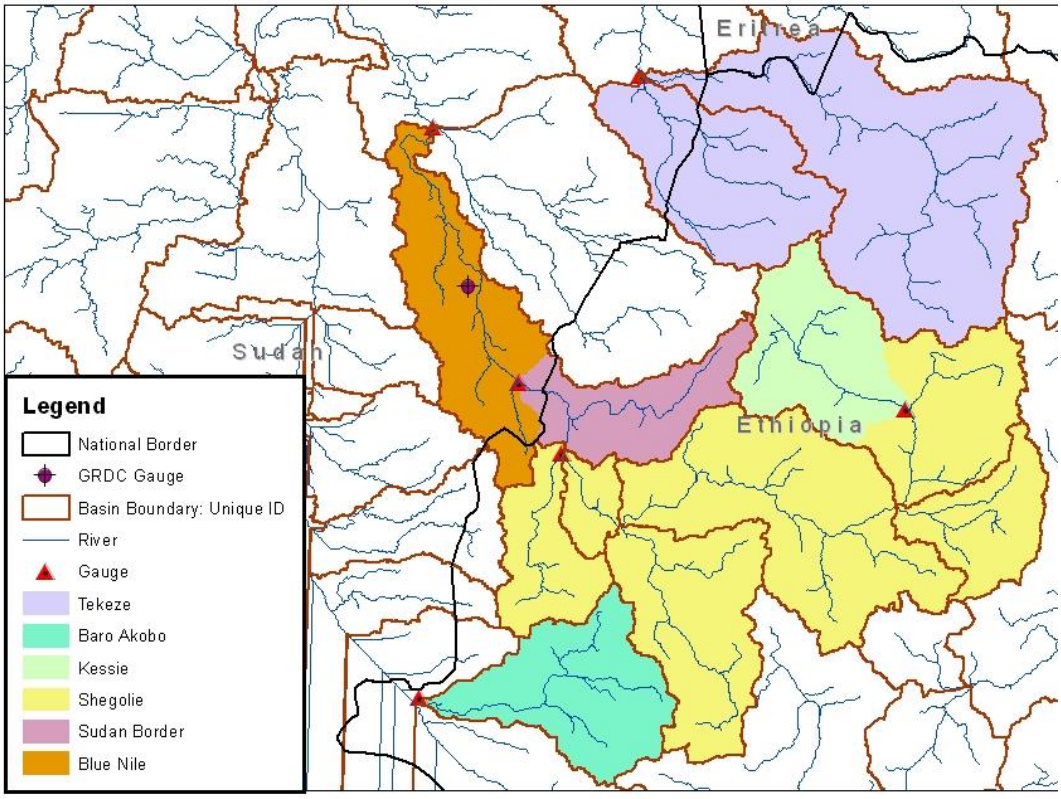

Source: Authors' analysis (data provided by Block and Strzepek, 2010)

C.2.3 Red River and Vietnam Basins

The Red River starts in southwestern China and discharges into Northern Vietnam, passing through Vietnam's capital, Hanoi.

The data for this study on the basins in Vietnam was provided by Jean Marc Mayotte (Mayotte, 2010), who was given the data from the Government of Vietnam while he was in country. Like the Blue Nile study, some of the basins were considered unusable because the basin size was too small in comparison to the Hydro1k level 4 catchment size, the size of the UNH-GRDC runoff fields (0.5 × 0.5 degree), and the CRU weather data (also 0.5 × 0.5 degree).

The map shown in Figure C-3 presents the basins modeled in the Red River and other basins in Vietnam. The red triangles represent gauge stations that were used for the calibration of CLIRUN-II. The solid brown lines represent the basin boundaries used in Alavian et al. (Alavian et al., 2009) on the Hydro1k level 4 catchment scale. The solid black lines represent country boundaries. Each basin modeled has been filled in by a unique color, which is identified in the legend. In the cases where the basins overlapped, the upstream basins were given mapping priority, meaning they are shown as covering the overlapping section.

Figure C-3. Red River and Vietnam Basins map—all basins

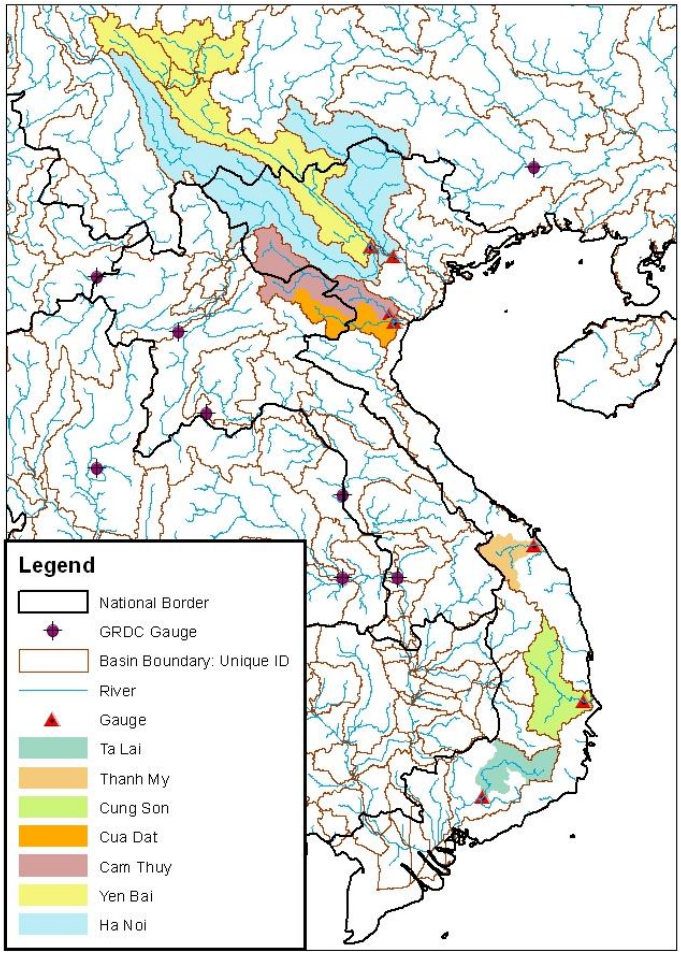

Source: Authors' analysis (data provided by Mayotte, 2010)

As shown in Figure C-3, there are many GRDC gauges (used in the UNH-GRDC analysis) on the map. Unfortunately, none of the gauges correspond with the gauges used in this study.

C.2.4 Vardar River Basin

The Vardar River basin lies primarily in the Former Yugoslav Republic of Macedonia, although some of the basin reaches north to part of Serbia and farther south, flowing out of Greece (the Vardar changes to the Axios at the Greece–Macedonia border). The Vardar River is the only river in this study that requires the snowmelt model built into CLIRUN-II, because of the snowfall in the mountains of Macedonia.

The data acquired for this Vardar Basin study was provided by the Macedonia master plan (Tippetts et al., 1977). In this report, a time series was only provided for the gauge near Gevegelija (1950 to 1968), while a monthly mean of streamflow (12 values) was provided for the remaining six basins. For this reason some of the plots explained in Section C-3 were not appropriate for the remaining six basins.

The map shown in Figure C-4 presents the basins modeled in the Vardar Basin. The red triangles represent gauge stations that were used for the calibration of CLIRUN-II. The solid brown lines represent the basin boundaries used in Alavian et al. (Alavian et al.,2009), based on the Hydro1k level 4 catchment scale. The solid black lines represent country boundaries. Each basin modeled has been filled in by a unique color identified in the legend. In the cases where the basins overlapped, the upstream basins were given mapping priority, meaning that they are shown as covering the overlapping section.

Figure C-5 shows the area surrounding the Vardar River basin.

Figure C-4. Vardar Basin map—all basins

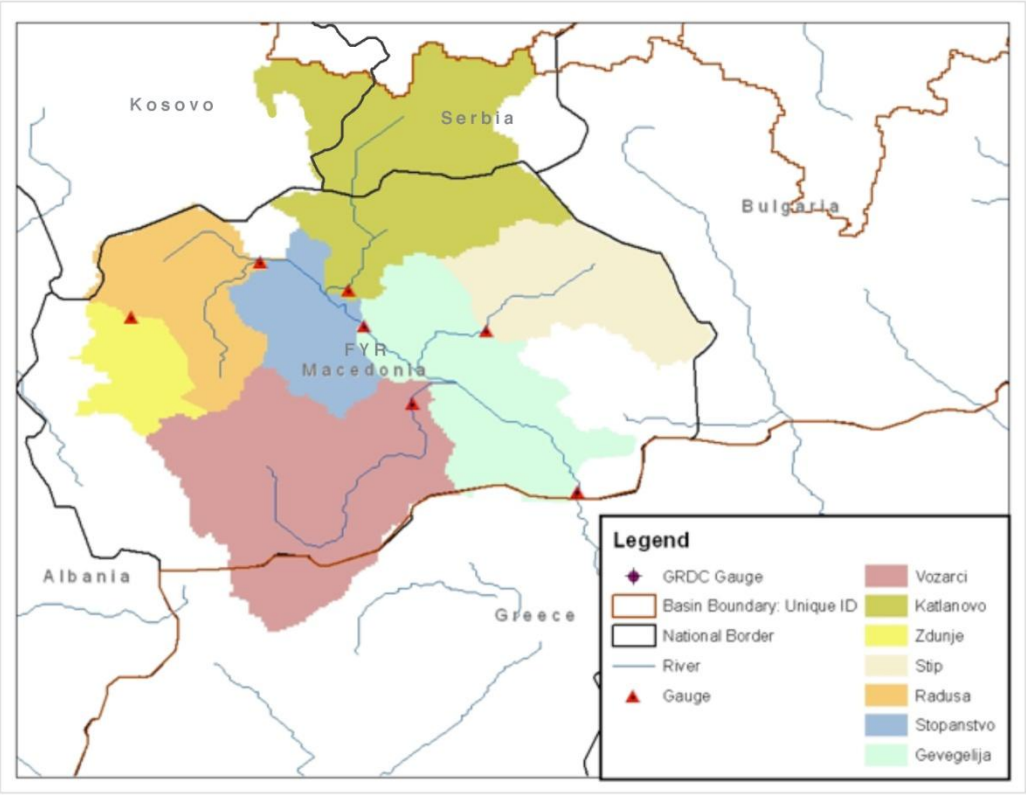

Source: Authors' analysis (data provided by Tippetts et al., 1977)

Figure C-5. Vardar Basin map, showing the surrounding area

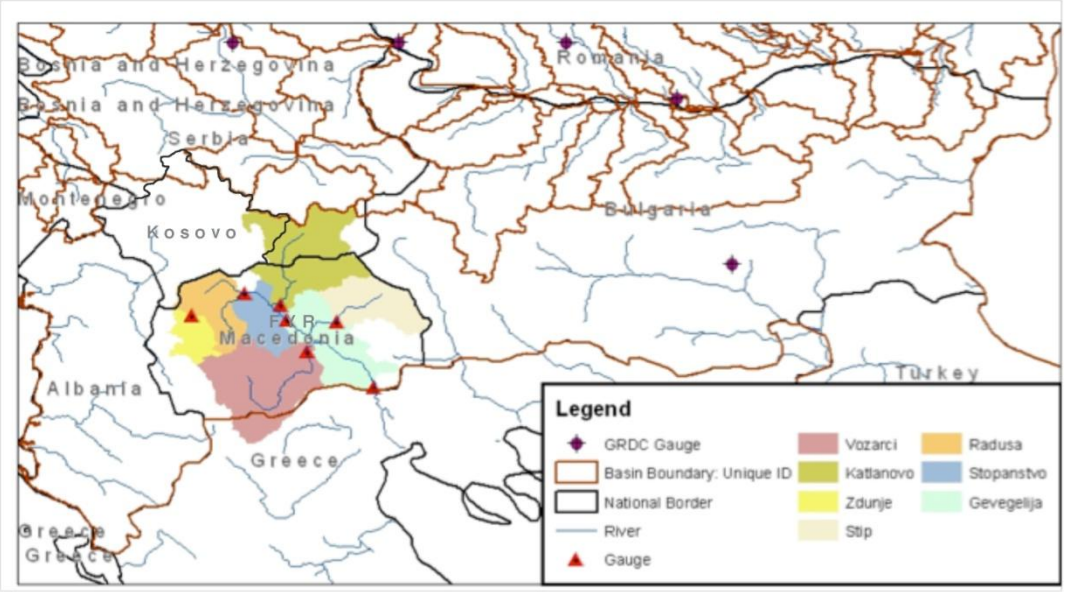

Source: Authors' analysis (data provided by Tippetts et al., 1977)

As shown, the Hydro1k level 4 catchment, which contains the Vardar basin, is large compared to the basin itself. So the basin is not very well represented by the Hydro1k level 4 catchment scale. There are also few GRDC gauges in this area, and none in the Vardar basin. The observed runoff data used in this study was only available as monthly average values, except for the discharge at Gevegelija, which spanned from 1950 to 1968. For this reason, many of the plots were not appropriate for a comparison between two monthly average data sets, meaning the observed reflected results from the UNH-GRDC project.

C.2.5 Sao Francisco Basin

The Sao Francisco River is the fourth largest river in South America, with an average annual flow of 2,850 CMS. The river crosses through diverse climatic and socioeconomic regions of Brazil over its 2,900 km stretch before it empties into the Atlantic Ocean just south of the equator.

The data acquired for this Sao Francisco basin study was provided by the Center for Sustainability and Global Environment of the University of Wisconsin, Madison. Only one gauge station with suitable data was available for this basin. The gauging station is near Juazeiro, Brazil, just downstream of the 12th largest human made reservoir in the world, the Sobradinho Reservoir.

The map shown in Figure C-6 presents the basin upstream of the Juazeiro gauging station. The red triangles represent gauge station that was used for the calibration of CLIRUN-II. The solid brown lines represent the basin boundaries used in Alavian et al. (Alavian et al., 2009) based on the Hydro1k level 4 catchment scale. The solid black lines represent the east coast of Brazil.

Figure C-6. Sao Francisco Basin map—upstream of the Juazeiro gauging station

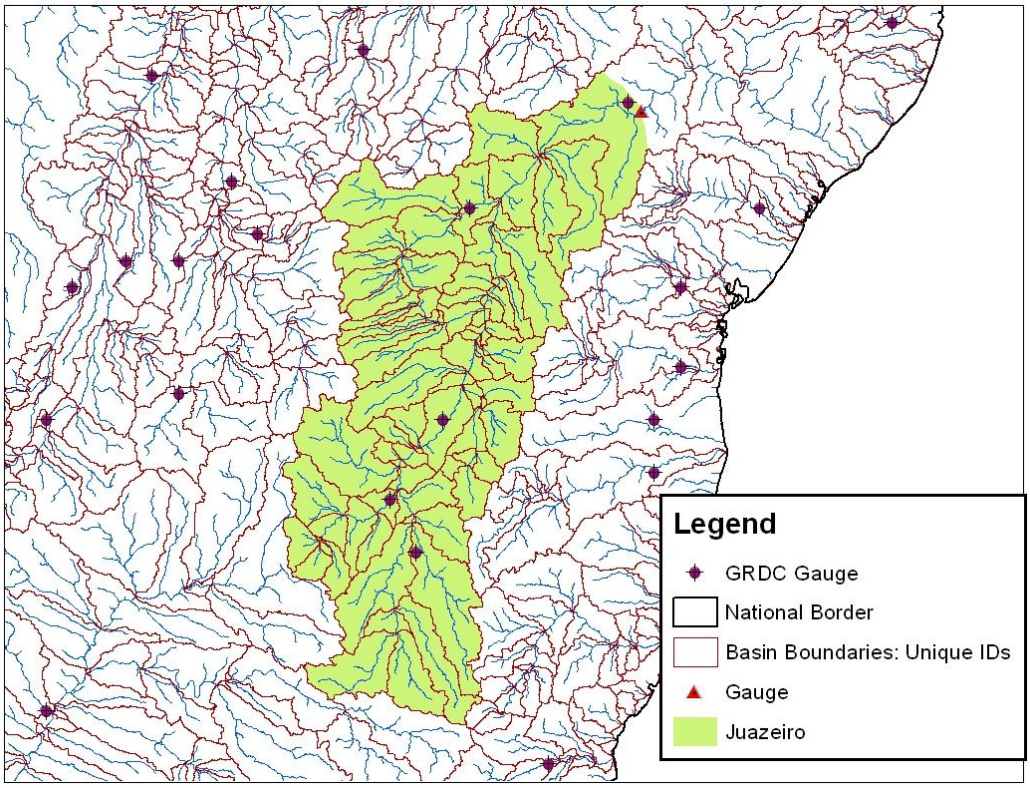

Source: Authors' analysis (data provided by the Center for Sustainability and Global Environment)

C.3 Calibration and Historical Runoff Analysis Results

C.3.1 Calibration Results

Two goodness-of-fit tests were applied to each of the streamflow results in the five basin studies: the coefficient of determination (R^2), and the annual error. The coefficient of determination was calculated using the following equation:

$$R^2 = 1 - \frac{\sum_i (O_i - M_i)^2}{\sum_i (O_i - \bar{O}_i)^2} \qquad \text{(EQ 1)}$$

Where O represents the observed streamflow, and M represents the modeled streamflow for a given month and gauge location. In this case, an R^2 value of 0 suggests that the modeled results are as good as the mean value of the observed streamflow, and an R^2 value of 1 suggests that the modeled results are perfect in comparison to the observed results. The annual error (E) is a measure of over or under estimating the streamflow. The annual error is calculated using the following equation:

$$E = \frac{\sum_i O_i - \sum_i M_i}{\sum_i O_i} \qquad \text{(EQ 2)}$$

Table C-1 shows the calibration results from the Zambezi basin study, Table C-2 shows the results from the Vietnam basin study, Table C-3 shows the results from the Blue Nile and Ethiopia basins study, Table C-4 shows the results from the Vardar basin study, Table C-5 shows the Vardar Basin calibration results at Gevegelija, and Table C-6 shows the results from the Sao Francisco basin study. These tables show results for both the full calibration and the monthly calibration. In the full calibration, the full observed streamflow time series was used for the calibration. In the monthly calibration, only the average monthly values were used to calibrate the model, but the full observed streamflow time series was used for the calibration results shown in Tables C1–C6.

Table C-1. Zambezi Basin calibration

Name	Coefficient of Determination (R^2)		Annual Error	
	Full	Month	Full	Month
Kwando River @ Kongola	0.35	0.17	-0.77%	0.35%
Kafue River @ Itezhi Tezhi Reservoir	0.78	0.70	-5.66%	-5.19%
Kabompo @ Watopa Pontoon	0.77	0.73	-1.24%	-5.25%
Luanginga @ Kalabo	0.58	0.52	-18.36%	-13.13%
Zambezi @ Chavuma Mission	0.53	0.53	-14.05%	-12.62%
Zambezi @ Victoria Falls	0.07	0.03	0.44%	-0.50%
Gwayi @ Kamativi	0.78	0.65	-22.33%	-14.76%
Shire @ Chikwawa	0.55	0.36	0.63%	0.17%
Zambezi @ Lupata	0.12	0.11	5.83%	4.67%
Zambezi River @ Katima Mulilo	0.61	0.62	-11.84%	-9.14%
Sanyati River Sub-basin	0.67	0.32	-8.89%	16.75%
Zambezi @ Tete	0.27	0.24	1.84%	0.48%

Source: Authors' calculations

Table C-2. Vietnam Basin calibration results

Name	Coefficient of Determination (R^2)		Annual Error	
	Full	Month	Full	Month
Cua Dat	0.56	0.49	-9.27%	-10.39%
Cung Son	0.56	0.53	-7.57%	-1.44%
Hanoi	0.83	0.82	0.92%	0.12%
Thanh My	0.42	0.34	0.71%	-0.51%
Yen bai	0.85	0.84	1.37%	-0.68%
Ta Lai	0.67	0.68	-6.58%	4.52%
Cam Thuy	0.74	0.72	-9.45%	0.86%

Source: Authors' calculations

Table C-3. Blue Nile and Ethiopia Basins calibration results

Name	Coefficient of Determination (R^2)		Annual Error	
	Full	Month	Full	Month
Tekeze	0.97	0.93	-6.16%	0.23%
Blue Nile	0.99	0.99	0.75%	0.12%
Baro-Akobo	0.97	0.89	-0.57%	-0.87%
Kessie	0.58	0.58	-4.30%	-9.41%
Shegolie	0.80	0.79	-12.87%	-15.72%
Sudan Border	0.75	0.76	-4.76%	-12.66%

Source: Authors' calculations

Table C-4. Vardar Basin calibration results

Name	Coefficient of Determination	Annual Error
Radusa	0.89	-1.81%
Zdunje	0.89	-0.71%
Katlanovo	0.78	-3.92%
Stopanstvo	0.78	-6.60%
Stip	0.68	-7.28%
Vozarci	0.76	-3.12%

Source: Authors' calculations

Table C-5. Vardar Basin calibration results at Gevegelija

Name	Coefficient of Determination (R^2)		Annual Error	
	Full	Month	Full	Month
Gevegelija	0.49	0.45	-11.01%	1.27%

Source: Authors' calculations

Table C-6. Sao Francisco Basin calibration results

Name	Coefficient of Determination (R^2)		Annual Error	
	Full	Month	Full	Month
Sao Francisco at Juazeiro	0.65	0.63	-0.90%	-0.13%

Source: Authors' calculations

C.3.2 Historical Results

Plots of the historical analysis results from the gauge station Watopa Pontoon, on the Kabompo River, are shown in Figures C-7 through C-14. These plots are shown to serve as an example of the analysis results.

Figure C-7 shows the annual discharge of the simulated CLIRUN_LOCAL_CRU results, the measured discharge, the simulated CLIRUN_UNH_CRU results, and the UNH-GRDC reported discharge. In this

figure, the UNH-GRDC results are shown as a horizontal line because only 12 monthly averages were reported, which can only result in one annual average value. The average monthly values from the UNH-GRDC (12 values for each basin; one for each month) are recorded to be over the years 1986 to 1995 (ISLSCP, 2005), so the plots used to compare this data set are also over this time period. In Figure C-8, the average monthly values are shown for the local (measured) discharge, the simulated CLIRUN_LOCAL_CRU runoff, the simulated CLIRUN_UNH_CRU runoff, and the data from the UNH-GRDC project.

Figure C-7. Annual comparison of CLIRUN-LOCAL, measured, CLIRUN-UNH, and UNH-GRDC runoff for the Watopa Pontoon Gauge Station

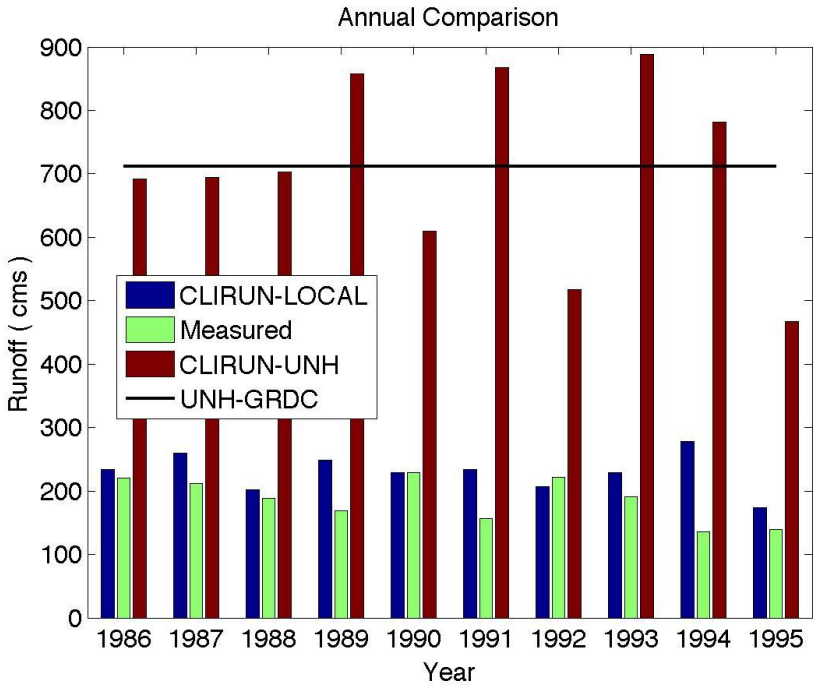

Source: Authors' calculations

Figure C-8. Monthly comparison of CLIRUN-LOCAL, measured, CLIRUN-UNH, and UNH-GRDC runoff for the Watopa Pontoon Gauge Station.

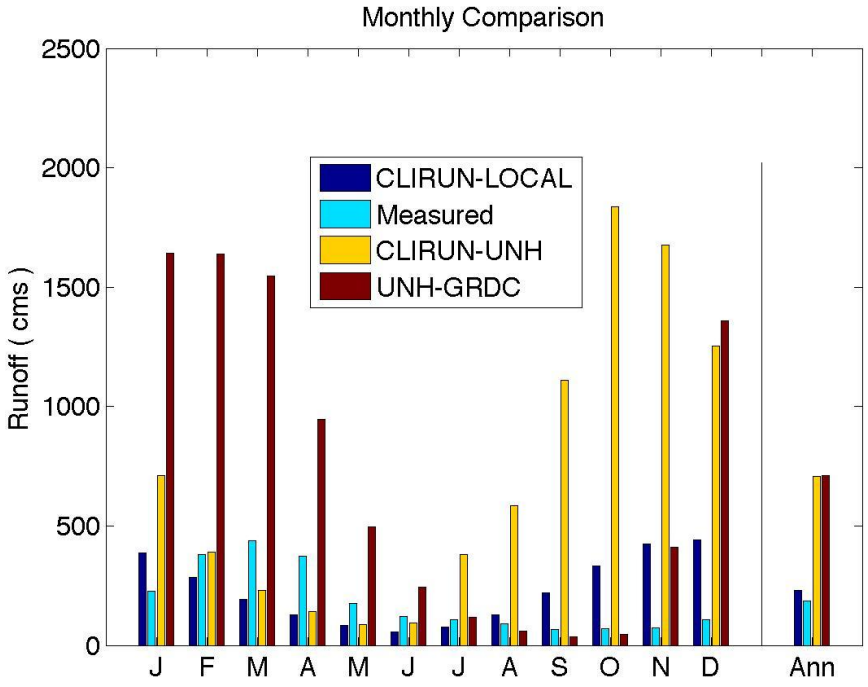

Source: Authors' calculations (measured runoff from Cadou, 2009)

Figure C-9 shows a plot of the measured discharge and the CRU TS 2.1 precipitation. Although other parameters significantly affect evaporation (for example, temperature, wind speed, solar radiation, and so on), which in turn plays a role in runoff reduction, precipitation is typically the driving force behind discharge time series patterns. So these plots are used to better understand, qualitatively, how much the measured discharge is driven by climate, and how much the discharge is driven by human induced effects. In general, if the precipitation and runoff show similar trends (for example, higher precipitation generally causes higher runoff), then the measured discharge is considered to be climate induced. If the two time series do not show similar trends, then the measured discharge is most likely influenced by civilization, although the effect of the soil or evaporation (not shown in a plot of precipitation) could also be the cause of the trend differences.

Figure C-9. Precipitation and measured discharge for the Watopa Pontoon Gauge Station

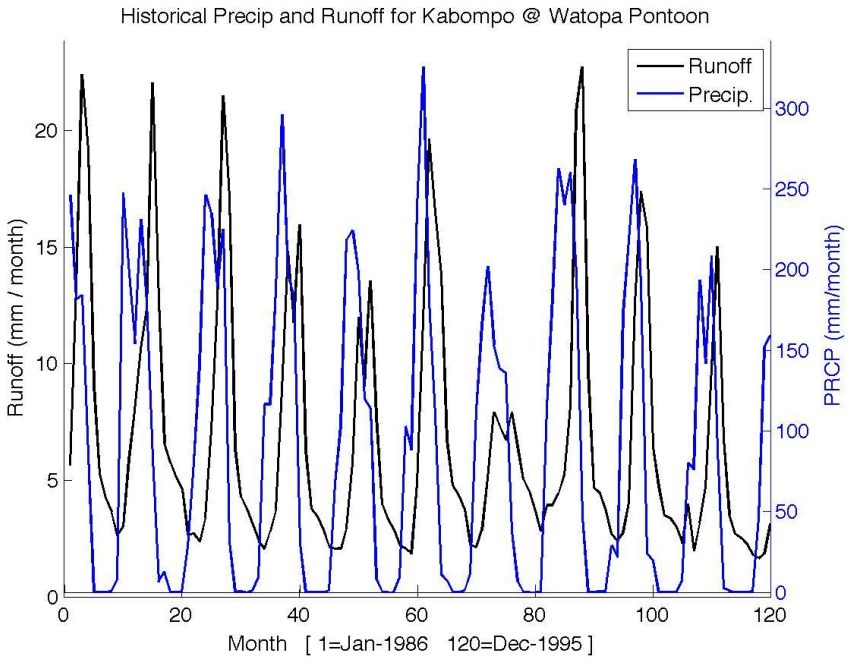

Source: Precipitation data from CRU, runoff data from Cadou, 2009

Each of the basins was calibrated to the measured discharge time series, the UNH-GRDC data, and the mean monthly discharges form the measured time series. The calibration to the measured mean monthly discharge was done to serve as an investigation of the information lost when using a mean monthly calibration data set —compared to using a full time-series calibration data set. Figures C-10 through C-14 show the results of this analysis. Figure C-10 shows a snapshot of the monthly discharge over 10 years. The line labeled “Observed” is the measured runoff time series, the line labeled “Full calibration” is the simulated discharge for the results using the full time series of measured discharge for calibration, and the line labeled “Month calibration” is the simulated discharge for the results using the mean monthly values for calibration. Figures C-11 through C-14 also use this same notation. Figure C-11 shows the mean monthly values from the three data sets. Figure C-12 shows the inverse cumulative distribution function, where the discharge from each data set was sorted and plotted from lowest flow (on the left) to highest flow (on the right). These plots are used to better understand if the simulated flows are able to capture the variety (high, medium, low) of the observed flows. These plots can also show if the simulated flow is generally overestimating or underestimating the historical record. Figure C-13 shows the annual flow time series over the entire measured time-span, similar to the monthly time series shown in Figure C-10. And finally, Figure C-14 shows the inverse cumulative distribution function of the annual flows.

Figure C-10. Snapshot of monthly flows for the observed, full calibration, and month calibration for the Watopa Pontoon Gauge Station

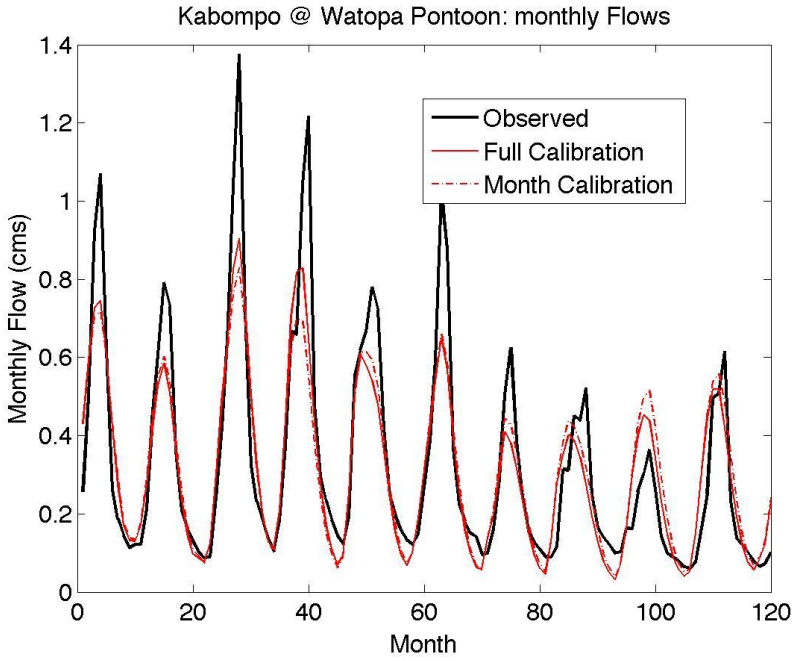

Source: Authors' calculations (observed data from Cadou, 2009)

Figure C-11. Monthly averages for the observed, full calibration, and month calibration for the Watopa Pontoon Gauge Station

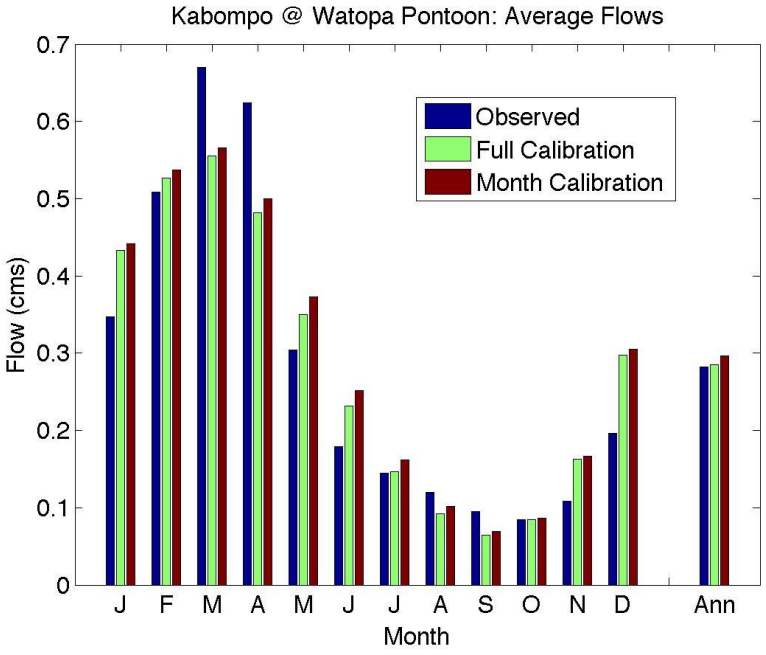

Source: Authors' calculations (observed data from Cadou, 2009)

Figure C-12. Sorted monthly flows for the observed, full calibration, and month calibration for the Watopa Pontoon Gauge Station

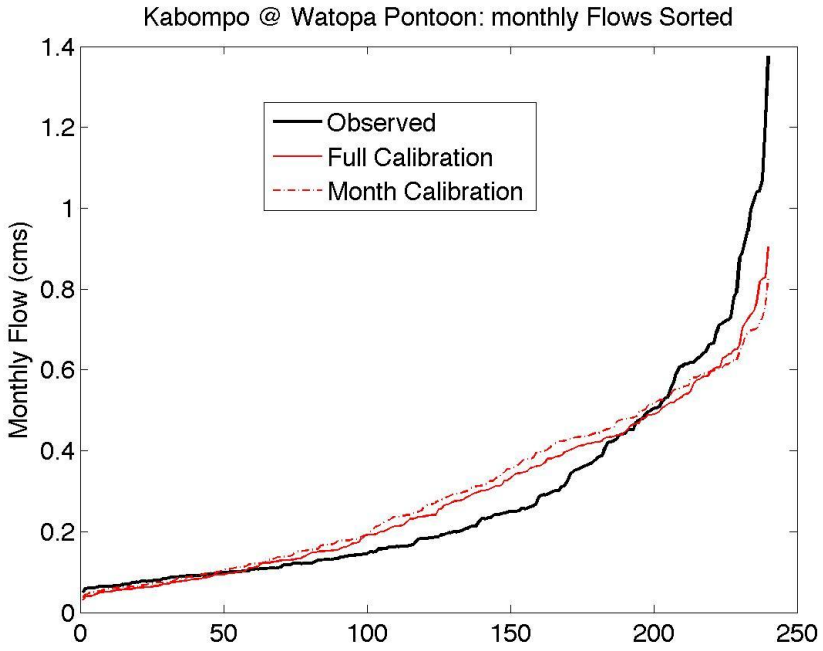

Source: Authors' calculations (observed data from Cadou, 2009)

Figure C-13. Annual flows for the observed, full calibration, and month calibration for the Watopa Pontoon Gauge Station

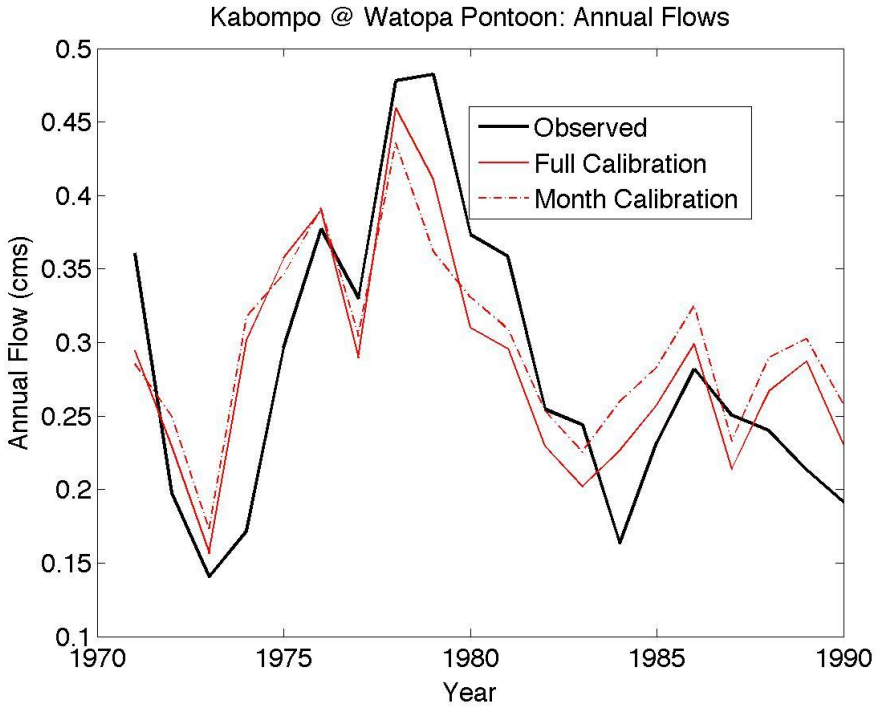

Source: Authors' calculations (observed data from Cadou, 2009)

Figure C-14. Sorted annual flows for the observed, full calibration, and month calibration for the Watopa Pontoon Gauge Station

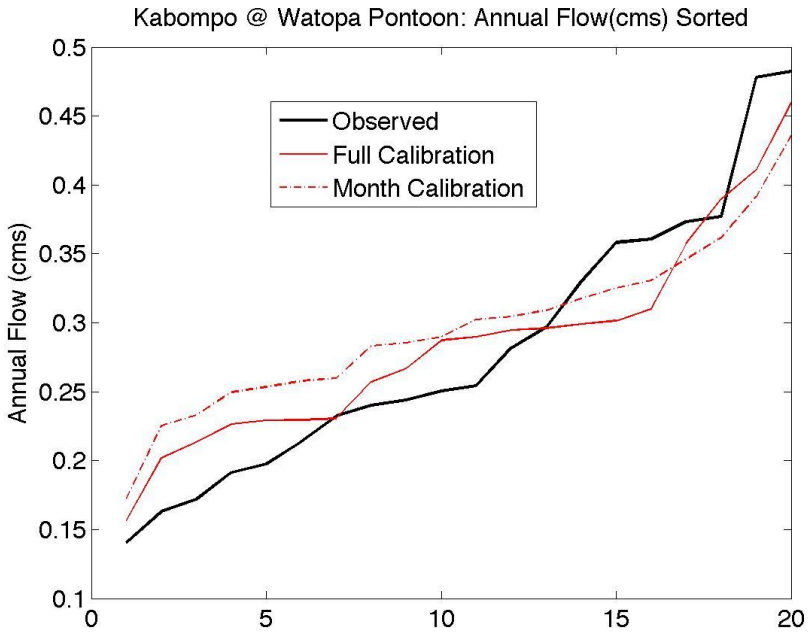

Source: Authors' calculations (observed data from Cadou, 2009)

C.4 Discussion of Results

These results vary from basin to basin but some patterns do emerge. One of these patterns is the importance of the calibration runoff accuracy. CLIRUN-II is good at matching the runoff it is given for calibration, but CLIRUN-II is only accurate when the observed (or calibration) runoff is accurate. This observation reinforces the importance of the observed runoff quality.

Another observation found in the results is that the UNH-GRDC data does not generally match the gauged runoff data. In some cases the difference is quite extreme. In most cases, these extreme discrepancies exist in basins where the UNH-GRDC team did not have gauged data; where the gauged data did not exist, the runoff presented was modeled runoff only—rather than a combination of measured and modeled runoff. This again emphasizes the importance of accurate, good quality calibration runoff data.

Besides these observations, other issues arise related to the results presented here. Hydrologists generally make the distinction between naturalized and gauged runoff. Naturalized runoff is the runoff caused by the weather (precipitation, temperature, and so on) and the earth's surface (topology, soils, ground cover, and so on) without the effects of civilization. On the other hand, gauged runoff includes the effects of civilization (dams, reservoirs, ground cover changes, and so on). CLIRUN-II was built to model naturalized runoff, meaning that the equations built into the model do not included the effects of civilization. Naturalized flow is much easier to model, especially when estimating future runoff, because

changes in civilization are difficult to estimate. But CLIRUN-II models the runoff based on the observed runoff used for calibration (which typically includes the effects of civilization), so one could argue that CLIRUN-II is able to model either naturalized or gauged runoff, depending on the calibration runoff used. For the most part, the UNH-GRDC runoff data is based on a naturalized flow model, especially where observed runoff data was not available. Where observed data was available, the UNH-GRDC used the naturalized flow results and corrected the modeled results on an annual basis. Therefore, the seasonality from the naturalized flow model remained in the results. The distinction between natural and gauged flow values might explain some of the differences between the gauged flow and the UNH-GRDC flow. It might also explain some of the differences between the gauged flow values and the CLIRUN-II results, although those differences are less noticeable. Because this study is attempting to better understand how the runoff and streamflow will be affected by the future weather, a naturalized flow model is preferred. A gauged flow model could introduce unnecessary errors unrelated to the effects of weather and climate, and it would be difficult to obtain estimations of each nation's plans for their water supply, especially for a global study.

To better understand the loss of information caused from using monthly average streamflow (UNH-GRDC) instead of a time series (used in this study) for the calibration, each basin was modeled using the observed time series (full calibration) and the monthly average of the observed time series (month calibration) and compared (Figures C-10 through C-14 are examples of this). These results vary from basin to basin, depending on the nature of the basin and the naturalized quality of the basin. Although the month calibration had the tendency to not capture the extreme flows very well, especially the high flows, in most cases, the month calibration and the full calibration were relatively similar in quality. The latter observation might be a bit counterintuitive because the extreme values are completely removed when the monthly mean is used instead of the full time series. But the extreme values are still present in the climate data, causing extreme values to be present in the results. These results are due to the fact that CLIRUN-II is a runoff model based on the physical process of runoff development (as opposed to a model based solely on statistics). In some areas, extreme weather events are not present in the CRU data set because the CRU data set used a method to "relax" to the 1960 through 1991 time period wherever observed data were not present.

ANNEX D: GUIDE TO NAVIGATION OF THE WORLD BANK CLIMATE PORTAL HYDROLOGIC INDICATORS

There are two different levels of hydrological indicators data on the World Bank Climate Portal: detailed basin-level information in the form of projected changes for each indicator and box and whisker plots; and global maps providing a broader perspective on regional, national, and continental patterns across basins for each of the six hydrological indicators. This appendix describes the information available on the World Bank Climate Portal (see http://sdwebx.worldbank.org/climateportal/) and explains how to navigate this information resource.

D.1 Accessing Basin-Level Indicator Data and Box and Whisker Plots

The Climate Portal contains detailed basin-level information on all studied indicators for all 56 GCM-SRES combinations, as well as box and whisker plots representing this information. This information can be accessed either for a basin of interest or in the form of country averages. However, when using country average results, caution should be taken for reasons described in Box D-1.

Box D-1. Country average results

Caution should be taken with the country average results. To develop country averages, basin results are averaged within a country based on their area. Therefore, in countries dominated by one or two large basins, the country average will be biased by the large basins. This can be especially misleading to policy-makers in countries where most of the population resides outside these large basins. For example, in Botswana, the country average result is biased by the large basin of the Kalahari Desert, with a projected very dry future. The majority of Botswana's population is located in other basins to the east, which are not predicted to have as intense drying. Therefore, although the country average indicates significant drying, this is less likely to be an issue in population centers. As this example shows, to understand the projected impacts of climate change, it is important (especially in countries with few large basins) to look at all the basin results for that country.

The following steps describe how to access this information from the Climate Portal.

Step 1: Locate the basin or country of interest. Upon arriving at the Climate Portal, users will see a map of the world. By either zooming in on an area of interest or using of the search function at the top of the map, users can locate the basin or country of concern. Once a basin is selected, the user will see a pop-up window, as shown in Figure D-1

Figure D-1. Locating basin or county or interest

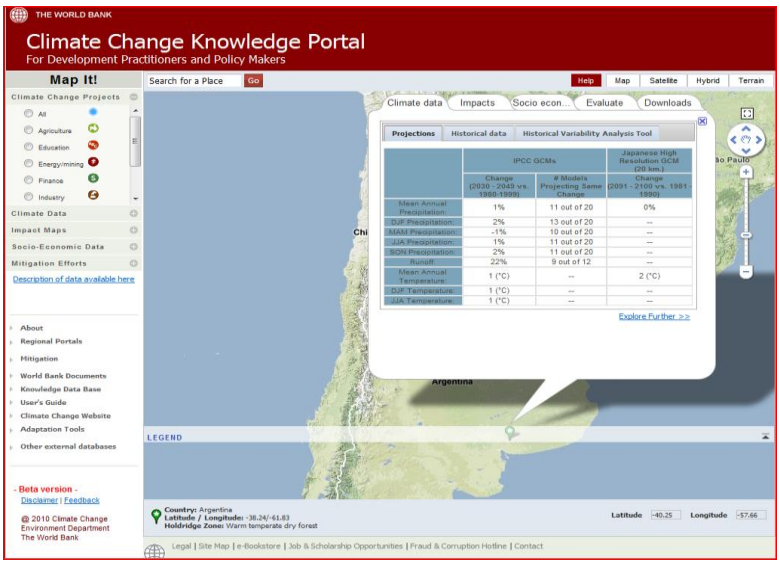

Step 2: Select "Impacts" then "Water resources" and accept warnings. The pop-up window that users see contains several options. Users should click on the "Impacts" tab at the top of the window, and then the "Water resources" tab within the window that appears (these tabs are circled in Figure D-2). This will direct users to a dialog box with the following message:

> *These data were developed at a River Catchment level with global data and were intended only for use in regional scale investment analyses. However, World Bank Staff have found the data useful for informing stakeholders on climate change risks in the water sector at the planning and investment strategy level. Please be warned that this data is not intended for use in any design study.*

Clicking the "Click here to get access to data and indicators" (circled in Figure D-2) will direct the user to a page with another message that reads:

> *The data and indicator results were NOT intended to be used on a project scale; and although the results can be used on a basin and seasonal level, the user should be cautious. The authors of these results advise the user to conduct a more detailed study before any major decisions are made on the results presented here.*

Users must accept warning and click on "Click here to get access to data and indicators" at the bottom of the page in order to access hydrological indicators data.

Figure D-2. Getting access to data

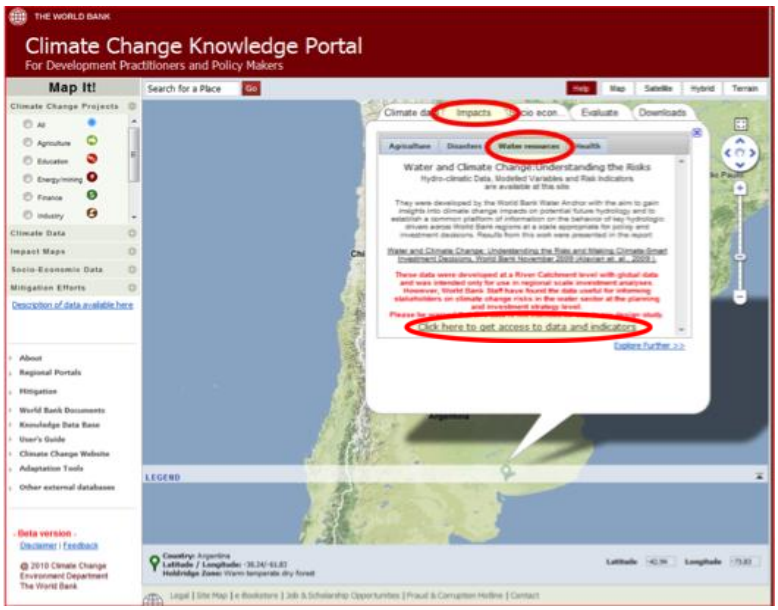

Step 3: Choose indicators, models, and time period for data display. Once users have clicked on the second "Click here to get access to data and indicators," this will pull up a page that displays a map of the basin of interest. Below the map will be three tabs that say: "View and download data", "Basin box Plots", and "Country box plots" (see Figure D-3).

Within the "View and download data" tab, users can access data for any indicators, GCM-SRES combinations, and time periods that are of interest. To do this, users select the emissions scenarios, indicators, GCMs, and time periods for which they wish to see data. The available parameters are as follows:

- **Emissions scenarios:** A1B, A2, and B1
- **Indicators:** mean annual temperature, mean annual precipitation, high flow (flood indicator), low flow (drought indicator), MAR, annual baseflow, reservoir storage, mean annual irrigation deficit (or reference crop water deficit), CMI, and PET
- **GCMs:** bccr_bcm2_0, cccma_cgcm3_1, cccma_cgcm3_1_t63, cnrm_cm3, csiro_mk3_0, csiro_mk3_5, gfdl_cm2_0, gfdl_cm2_1, giss_aom, giss_model_e_h, giss_model_e_r, iap_fgoals1_0_g, inmcm3_0, ipsl_cm4, miroc3_2_hires, miroc3_2_medres, mpi_echam5, mri_cgcm2_3_2a, ncar_ccsm3_0, ncar_pcm1, and ukmo_hadcm3, ukmo_hadgem1
- **Time periods:** 2030 to 2039 and 2050 to 2059

Once users have selected emissions scenarios, indicators, GCMs, and time periods of interest, they can click "Show data" to view the data of interest (data will be shown as changes in indicator values relative to the baseline) in tabular form; an example of this is provided in Figure D-4. Alternatively, clicking "Download data" will allow the user to download the data as a spreadsheet in Microsoft Excel.

Figure D-3. Viewing and downloading data

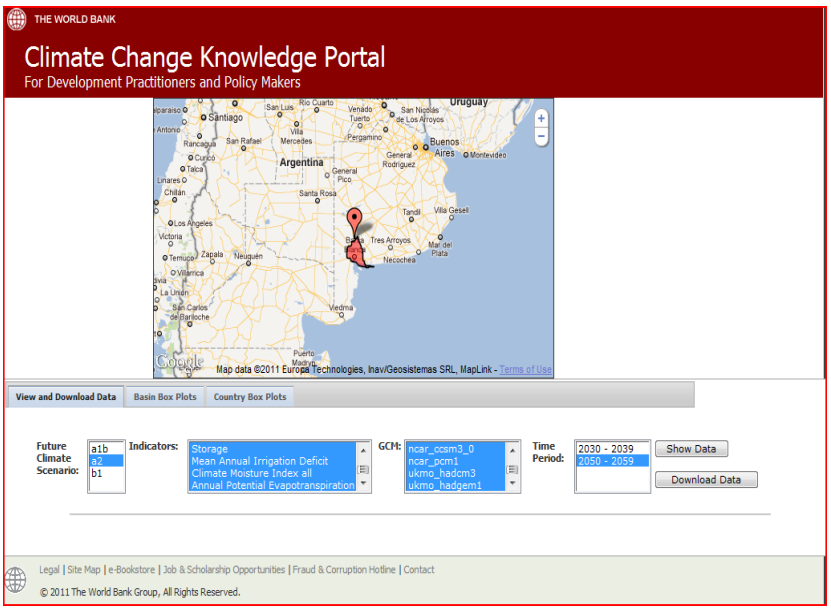

Figure D-4. Tabular display of indicator data, as percent change from baseline

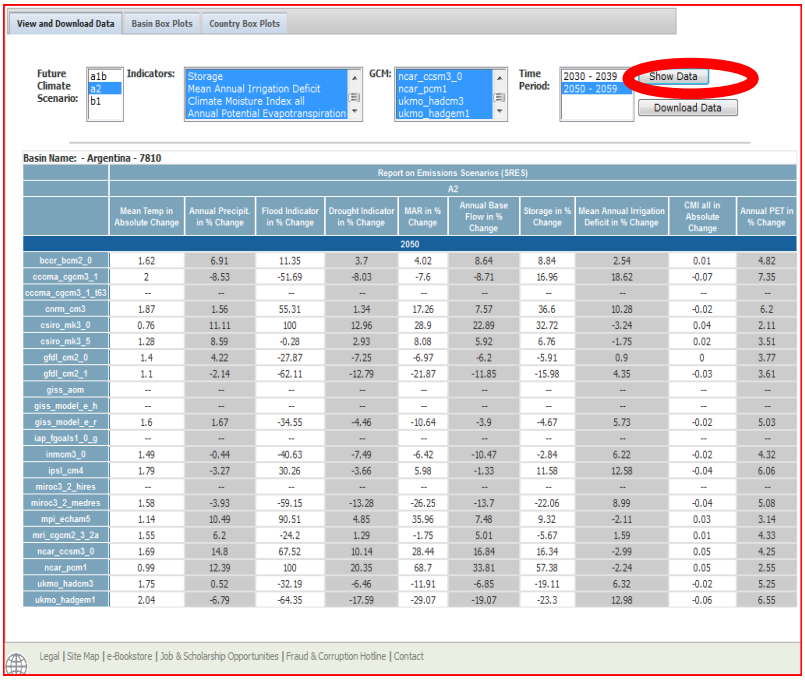

	Mean Temp in Absolute Change	Annual Precipit. in % Change	Flood Indicator in % Change	Drought Indicator in % Change	MAR in % Change	Annual Base Flow in % Change	Storage in % Change	Mean Annual Irrigation Deficit in % Change	CMI all in Absolute Change	Annual PET in % Change
bccr_bcm2_0	1.62	6.91	11.35	3.7	4.02	8.64	8.84	2.54	0.01	4.82
cccma_cgcm3_1	2	-8.53	-51.69	-8.03	-7.6	-8.71	16.96	18.62	-0.07	7.35
cccma_cgcm3_1_t63	--	--	--	--	--	--	--	--	--	--
cnrm_cm3	1.87	1.56	55.31	1.34	17.26	7.57	36.6	10.28	-0.02	6.2
csiro_mk3_0	0.76	11.11	100	12.96	28.9	22.89	32.72	-3.24	0.04	2.11
csiro_mk3_5	1.28	8.59	-0.28	2.93	8.08	5.92	6.76	-1.75	0.02	3.51
gfdl_cm2_0	1.4	4.22	-27.87	-7.25	-6.97	-6.2	-5.91	0.9	0	3.77
gfdl_cm2_1	1.1	-2.14	-62.11	-12.79	-21.87	-11.85	-15.98	4.35	-0.03	3.61
giss_aom	--	--	--	--	--	--	--	--	--	--
giss_model_e_h	--	--	--	--	--	--	--	--	--	--
giss_model_e_r	1.6	1.67	-34.55	-4.46	-10.64	-3.9	-4.67	5.73	-0.02	5.03
iap_fgoals1_0_g	--	--	--	--	--	--	--	--	--	--
inmcm3_0	1.49	-0.44	-40.63	-7.49	-6.42	-10.47	-2.84	6.22	-0.02	4.32
ipsl_cm4	1.79	-3.27	30.26	-3.66	5.98	-1.33	11.58	12.58	-0.04	6.06
miroc3_2_hires	--	--	--	--	--	--	--	--	--	--
miroc3_2_medres	1.58	-3.93	-59.15	-13.28	-26.25	-13.7	-22.06	8.99	-0.04	5.08
mpi_echam5	1.14	10.49	90.51	4.85	35.96	7.48	9.32	-2.11	0.03	3.14
mri_cgcm2_3_2a	1.55	6.2	-24.2	1.29	-1.75	5.01	-5.67	1.59	0.01	4.33
ncar_ccsm3_0	1.69	14.8	67.52	10.14	28.44	16.84	16.34	-2.99	0.05	4.25
ncar_pcm1	0.99	12.39	100	20.35	68.7	33.81	57.38	-2.24	0.05	2.55
ukmo_hadcm3	1.75	0.52	-32.19	-6.46	-11.91	-6.85	-19.11	6.32	-0.02	5.25
ukmo_hadgem1	2.04	-6.79	-64.35	-17.59	-29.07	-19.07	-23.3	12.98	-0.06	6.55

Step 4: Access box plots. Next to the tab that says “View and download data,” users will see tabs that say “Basin box plots” and “Country box plots.” By clicking on “Basin box plots,” users will access two box and whisker plots for the basin of interest, one for the 2030s and one for the 2050s (see Figure D-5). Similarly, by clicking on “Country box plots,” users will access two box and whisker plots for the country of interest, one for the 2030s and one for the 2050s (see Figure D-6). As described earlier in Box D-1, caution should be taken when using country average results.

Figure D-5. Example basin box plots for the 2030s and 2050s

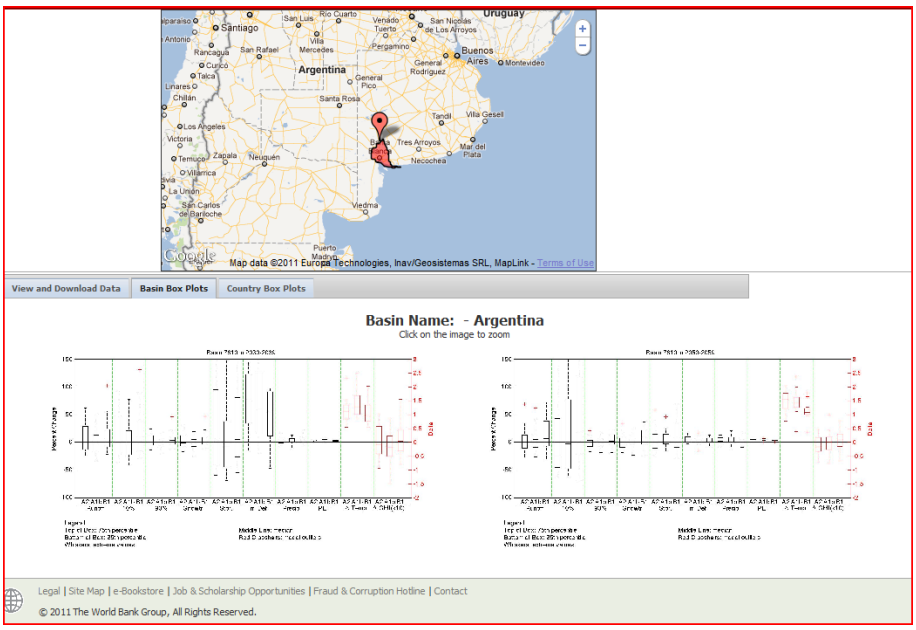

Figure D-6. Example country box plot for the 2030s

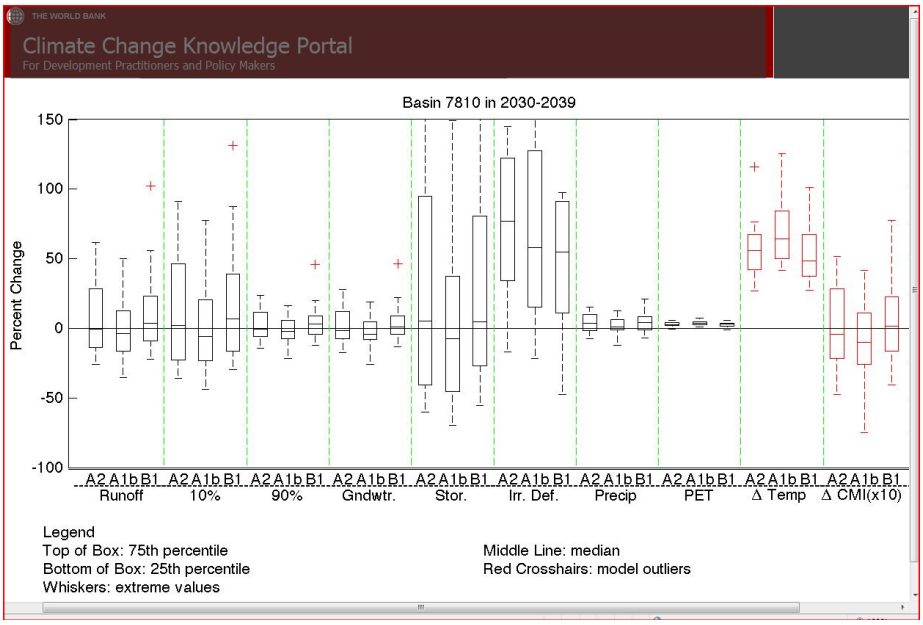

A total of 30 box and whiskers are arrayed on each graphic, one for each of the three SRES scenarios and the 10 indicators (which include the six hydrological indicators, temperature, precipitation, CMI, and PET). The box itself displays the range of variability across the GCMs for each indicator and SRES scenario.

D.2 Mapping of Data

In addition to providing detailed basin-level data, the Climate Portal also contains a high-level mapping tool that allows users to see projected risk across basins. Directions for accessing this tool are provided in the following steps.

Step 1: Find the maps. To reach the interactive mapping tool, start on the climate portal homepage (http://sdwebx.worldbank.org/climateportal/). Here, users will see a "Map it!" vertical options bar on the left. One of the options on this vertical bar is "Impact maps." Users should click here. This will open up a list of options. Users should scroll to the bottom of the list and click "Click here for more maps" (see Figure D-7). This will take the user to the interactive mapping tool.

Figure D-7. Interactive mapping tool interface

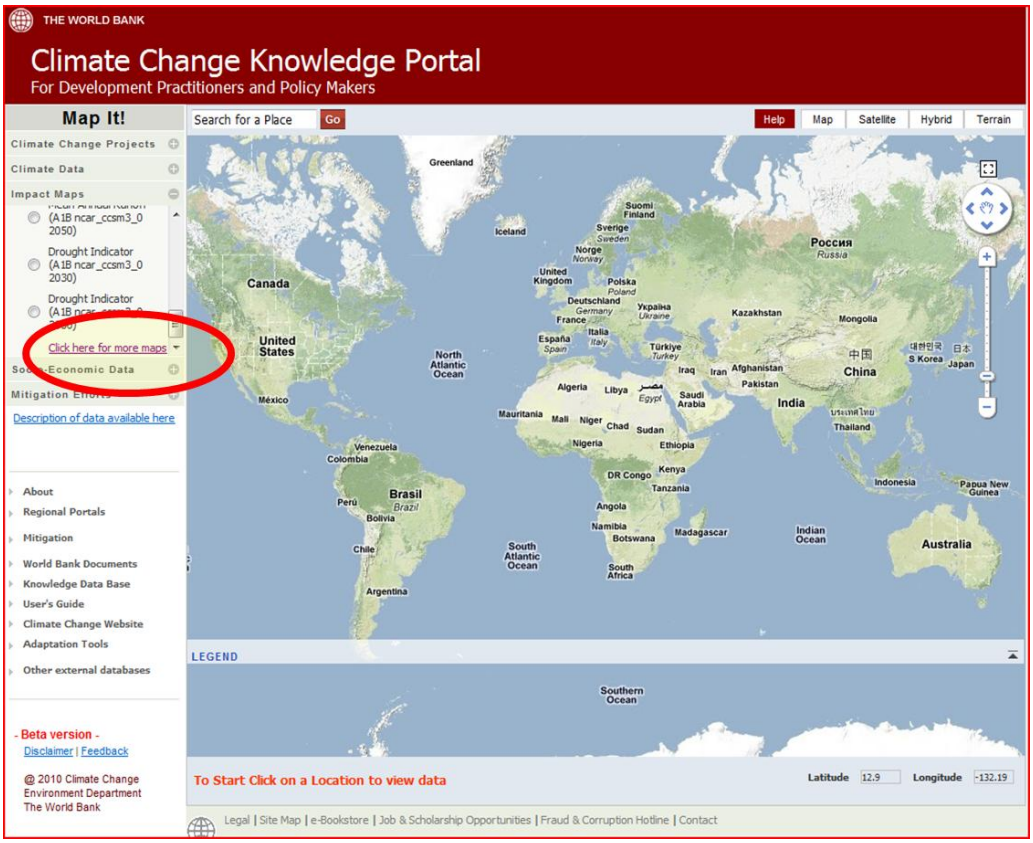

Step 2: Navigate the pop-up window. Next, a pop-up window will appear with six maps of the globe showing indicator results for the 2030s and 2050s and the A1B, A2, and B1 SRES scenarios. The results are displayed for a single GCM and a single hydrological indicator. Figure D-8 shows an image of the pop-up window.

Figure D-8. Mapping tool pop-up window

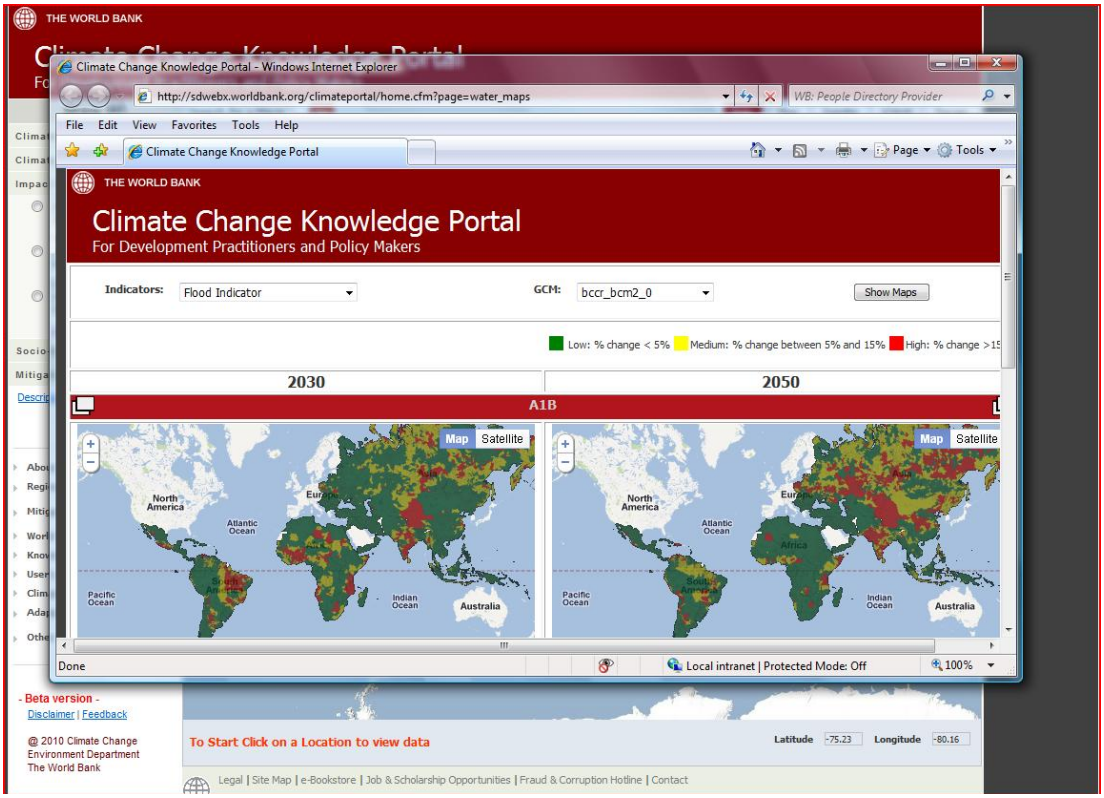

Step 3: Zoom in and choose the indicator and model. To zoom in to a particular region of interest, the user will either double-click a particular area on the interactive map or click the plus or minus buttons located at the top left corner of each of the six maps. Lastly, to view the mapped results for a particular indicator and GCM, the user will select from the "Indicator" and "GCM" pull down menus at the top of the page. Figure D-9 displays an example of these detailed map results.

Figure D-9. Detailed map results

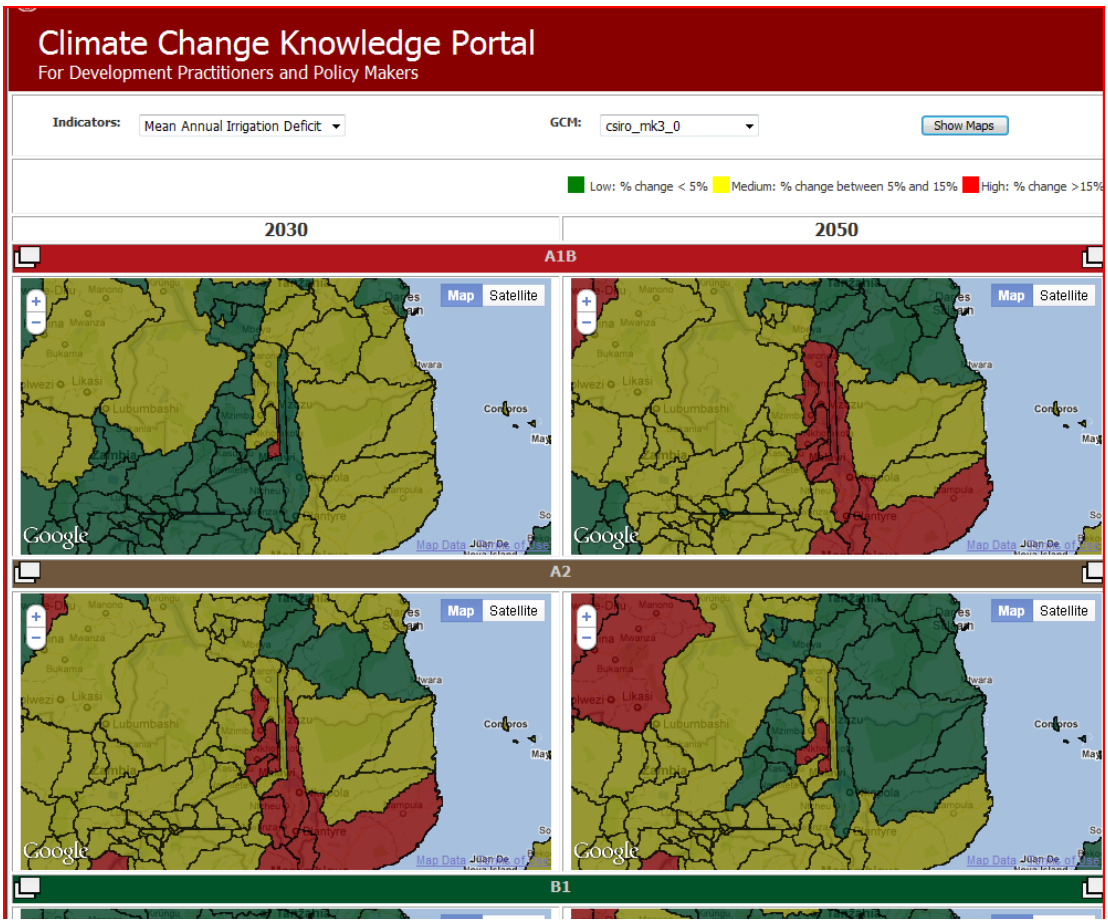

ANNEX E: BASIN SELECTION AND NAMING CONVENTION

The basin selection and naming convention was provided by a previous study (Farmer and Strzepek, 2010).[18] The naming convention was applied to the global basins so that they might be identified uniquely within the World Bank Climate Portal.[19] Each naming identifier gives information about the drainage and location of that region, and is globally unique.

This naming convention was developed by fusing the Hydro1k level 3 and level 4 basins of the World Bank regions (Africa, East Asia and Pacific, Europe and Central Asia, Latin America and the Caribbean, Middle East and North Africa, and South Asia) with major river basins recognized by the GRDC (GRDC, 2007) and country boundaries.

Originally, basins were identified with a number, which was only unique to a given Hydro1k continent. First, this number was appended to an abbreviation of the given Bank region. This provided some inconsistencies, as some Bank regions crossed continents, that is, Latin America and the Caribbean. To rectify these inconsistencies, each basin was given a unique, randomly assigned, four-digit code. These codes, with a "G" appended to the front, are unique global identifiers.

In an effort to provide more information about each basin, rather than just a number, efforts were made to combine global identifiers with Bank regions, GRDC basins, and countries. The global identifiers were joined with the three-digit abbreviations of Bank Regions. These were then crossed joined with GRDC, noting which GRDC basin covered the majority of the level 3 and level 4 basins.[20] Finally, these were joined with national boundaries.

Supplemental files that further explain these names are available on the Climate Portal. They are contained in the file Basin_Names_Supplemental_Files.zip, which includes the following documents:

- Figure1.pdf
- AFR.pdf
- EAP.pdf
- EAC.pdf
- LCR.pdf
- MNA.pdf
- SAR.pdf

[18] The database used for the selection of basins and their naming convention was created by William Farmer and Kenneth Strzepek. This section was taken directly from the memo/report "Unique Identifiers for the Climate Portal at the World Bank Group: A Method for Identifying Global Basins" delivered to the World Bank in February of 2010 (Farmer and Strzepek, 2010).

[19] Climate Change Knowledge Portal. The World Bank 2011. http://sdwebx.worldbank.org/climateportal/.

[20] The GRDC drainage basins represent only 405 major basins of the globe. As such, these do not cover all Hydro1k level 3 and 4 basins. The convention looks for the GRDC that covers the majority of each level 3 and 4 basin. In some cases, multiple GRDC basins were found in a single level 3 or 4 basin. In these cases, the GRDC basins that accounted for the majority of the level 3 or 4 basin was retained.

- Appendix_I._8413.xls
- Applendix_II_8413.xls

The table in the file Appendix_I_8413.xls gives a list of each basin, displaying the original Bank Region code and number, the new global identifier, Bank Region, GRDC drainage, country, and long name. The long name is a concatenation of the global identifier, bank region and, if available, GRDC drainage, preceded by a "D." If the drainage was not available, the country was noted, preceded by a "C."

An additional referencing convention was developed. The global basins were intersected with national boundaries. The result was that each global basin was broken into its parts in separate countries. This database is provided as an Microsoft Excel document (Appendix_II_8413.xls). This allows the user to note which countries intersect with a given basin or which basins comprise a certain country.[21]

A mapping of the regions can be seen in a separate PDF file, Figure1.pdf. PDFs are included for each region; these are labeled with the global codes so as to provide simplified geospatial references. Due to the limits of text size and resolution, this is not the recommended spatial exploration. The basins can be further explored in the attached ESRI arcGIS shape file. In the event that arcGIS is not available, the basins can be explored by Bank Region on Google Earth.

[21] The long names are meant to give a general idea of the location of each basin. Due to issues of scale and resolution, some small inconsistencies are present, though extremely rare. As more data sets of basin flow are compiled, these inconsistencies can be rectified.

ANNEX F: ASSESSING THE IMPACT OF CLIMATE VARIABILITY AND CHANGE IN BOTSWANA: THE ROLE OF GCMS AND THE CLIRUN-II HYDROLOGIC MODEL

F-1 Introduction

This Annex provides an illustration of how the methodology elaborated above has been used in the context of assessing the impact of climate variability and change in Botswana (World Bank 2010b). In the case of Botswana additional analyses has been carried out as described below. Depending on the objective for the specific analysis to be carried out, it is to be expected that additional analysis is required or prudent. The present annex first provides the context of Botswana in relation to climate variability then a brief summary of the analysis which was carried out.

F-2 Background

In Botswana (see Figure F-1 for map of country), physical water scarcity is already a constraint to economic development and growth, in particular for agriculture (irrigation) and mining. The future development of the country depends heavily on water availability. Physical water scarcity is compounded by high climate variability and inadequate water resources infrastructure and management. Better planning and investment in water security is therefore essential to Botswana's efforts in achieving its development goals.

Figure F-1. Map of the Republic of Botswana

Source: (UNEP, 2010).

Botswana's highly variable historical precipitation patterns are well-documented. As shown in Figures F-2 and F-3, intraannual variability as well as interannual variability is relatively large in Botswana. Average annual rainfall varies nearly threefold, while average monthly rainfall varies by a similar order of magnitude. As a semiarid country, droughts have been common in the past (one in four years is a drought year), but floods have also occurred, though much less frequently. Drought in terms of rainfall deficits are most common in northern Botswana, while extreme droughts based on low rainfall and soil conditions are most common in south-western Botswana (the Kalahari Desert). High rainfall events with risks of floods are common in north eastern Botswana where several large dams are located.

Figure F-2. Interannual precipitation variability (mm)

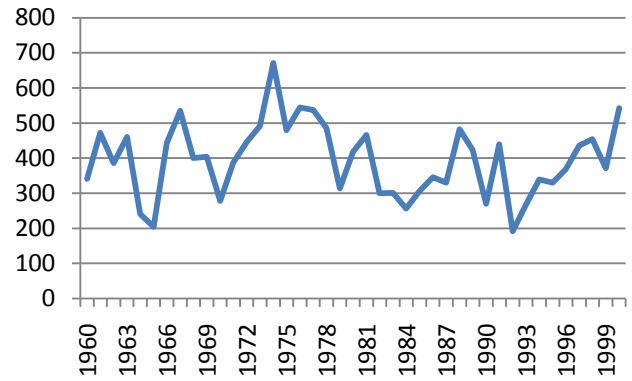

Source: CMU, University of East Anglia data processed by International Research Institute, Columbia University for The World Bank, Africa Water Resources in a Changing World, 2010.

Figure F-3. Intraannual and precipitation variability (mm)

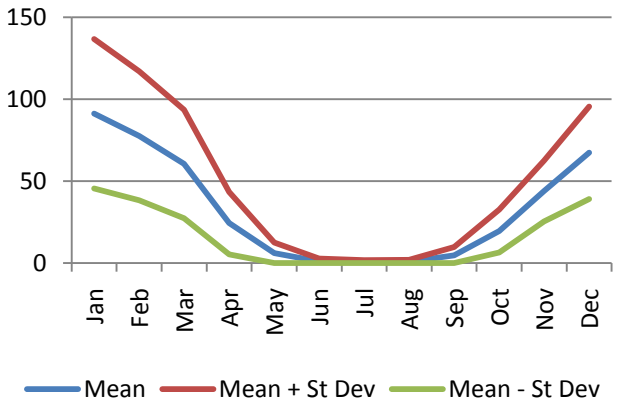

Source: CMU, University of East Anglia data processed by International Research Institute, Columbia University for The World Bank, Africa Water Resources in a Changing World, 2010.

The economic costs of climate variability can be high. It has become evident that recurrent drought and floods cause significant losses and negatively impact economic growth.[22] In 2005, drought diminished agricultural planted areas to 72 500 hectares, or only 25 percent of cultivable land in Botswana (SARPN, 2005). In June 2009, heavy rains flooded seven districts in central Botswana and displaced over 4,000 inhabitants when their mud dwellings collapsed in the heavy rains (DREF, 2009). These rains were particularly unusual because they came in June, traditionally a dry month. It is therefore important that Botswana develops capacity to lessen the extent of vulnerability of the country's economy from climate variability. Specifically, there is a need to improve the understanding of future climate variability and

[22] According to a recent UNEP report (see Kandji, S.T. et al., 2006), in 1992, drought-related losses constituted 8 to 9 percent of GDP in Zimbabwe and Zambia. Results for Malawi indicate that, on average, droughts and floods together reduce total GDP by about 1.7 percent per year. In Mozambique, the shock of the flood of 2000 led to the abrupt fall of the GDP growth rate to 1.5 percent in 2000.

change in Botswana and generate climate risks knowledge to inform national economic development policy.

As a first step toward improving the understanding of future climate risks, the World Bank provided technical assistance in 2010. The objective of this activity was to quantify the impact of climate change on extreme events and the risks for the water sector in Botswana. Using GCMs and the CLIRUN-II Hydrologic Model, the Bank was able to illustrate how the underlying variability in Botswana might change over the coming decades due to climate change. While GCMs replicate climate variables such as temperature and precipitation, the CLURUN II model models the behavior of hydrologic variables particularly relevant for water and agricultural planning and investment, including runoff, groundwater recharge, and extreme events (floods and droughts). Finally, this data was used to present hydrologic indicators such as the Standardized Precipitation Index (SPI), the Palmer Drought Severity Index (PDSI), and peak flow ratios. Calculation of the two latter indicators go beyond what has been included in the standard methodology explained earlier in this Water Paper. However, it requires a fairly simple algorithm to calculate SPI and PDSI based on the climate data of the GCMs.

The analysis confirmed that Botswana is likely to experience greater climatic variability over the coming decades. It is noteworthy that while GCMs are often highly divergent for smaller spatial configurations, there is greater consensus for Botswana. The modeling results show that droughts and storms are expected to increase (in frequency and severity) in western and northern Botswana, while in south-middle-eastern Botswana (part of the Limpopo basin), precipitation is likely to decrease, but with an increased risk in flooding. There is a bias toward increased droughts, and groundwater recharge is likely to decline.

Adaptation is needed to mitigate the adverse impacts of climate change on water-dependent sectors. Future growth will likely require improvements in water use efficiency, and the review of existing national and sectoral policies to ensure they adequately address climate-related challenges. Future rainfall variability and climate change also suggest a need to increase investments in water infrastructure, (for example, additional storage volume). Based in part on this assessment, the Government of Botswana has decided to approach the World Bank to support the development of an ambitious climate change adaptation strategy.

The World Bank technical assistance in developing this adaptation strategy was based in large part on recent work implemented by the World Bank specifically the application of a WBM for climate impact analysis of runoff (CLIRUN-II) at the subbasin or catchment level across all World Bank regions.[23] The modeled behavior of key hydrologic variables in the major basins of Botswana (see Figure F-4), as well as the underlying ensemble of GCM data upon which it is derived, served in several ways to build consensus around the need to consider future climate risk in water-related planning and investment.

[23] The input for this hydrologic model comes from three primary sources: the CMU (historic climate data); the UNH and GRDC (observed historic runoff); and the IPCC (future climate predictions). The model results are calculated and presented at the level of USGS Hydo1K level 3. It must be noted that many uncertainties arise from the application of this model at the catchment level, particularly where little observed historic runoff data is readily available. For more information on the uncertainties of the CLIRUN-II model, refer to Strzepek and Fant (Strzepek and Fant , 2010).

Summarized in the following discussion are the key contributions that came about from use of GCM and CLIRUN-II model data to mobilize support for policy reform. These impacts include: GCM data provided the range of future climate variables; CLIRUN-II Hydrologic Model provided the range of future hydrologic variables; new indicators were created using GCM outputs; scientific analysis provided the foundation for dialogue on the impacts of climate change on water resources; and, the scientific analysis provided an objective platform around which consensus on climate adaptation was reached.

Figure F-4. Basin Identification map of Botswana

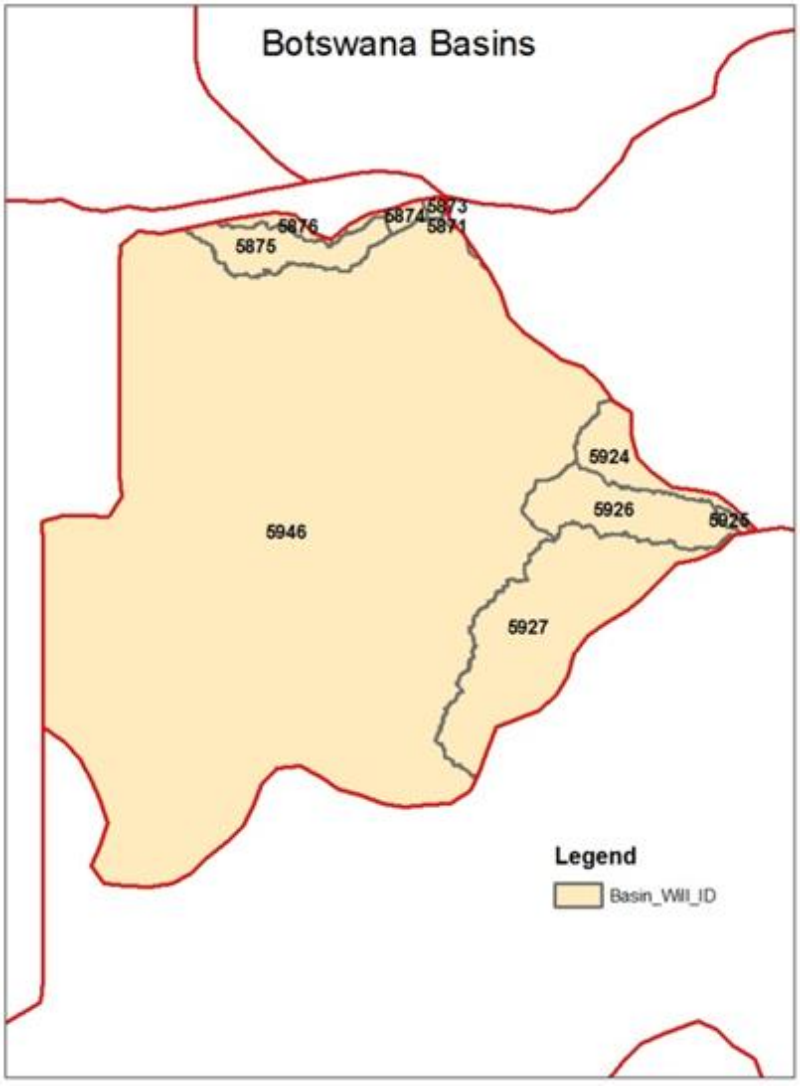

Source: Authors' database basins based on USGS Hydro 1K level 3

F-3 GCM Data and the Range of Future Climate Variables

To plan for the future, reliable knowledge of the potential boundaries of change of climate variables is most informative. While many individual GCMs are capable of replicating the past, this does not necessary imply their ability to project the future. This is particularly troublesome under nonstationarity, a phenomenon implying that the future would be different from the past (for example, this could be due to changing parameters and relationships between climate variables). The best way to capture the range of change is by running an ensemble of GCMs using different emission trajectories (SRES). In the case of Botswana, GCMs and SRES are combined to create 56 climate change scenarios. Each of these scenarios is considered equally plausible. Ideally one should evaluate the impacts from each climate scenario. Unfortunately this is too costly for most detailed modeling analyses. The question then becomes how to choose which scenarios to evaluate.

All of the GCM/SRES combinations were evaluated to determine which models represent the extreme dry and extreme wet scenarios. Toward this end, each of the GCM/SRES scenarios was ranked by their CMI.[24] A wet scenario meant that the the basins which constitute Botswana experienced the most wetness (as expressed by changes in the CMI); a dry scenario, the most drying (as expressed by changes in the CMI); and the rest will be somewhere in between. The advantage of this approach is that it provides a representation of the full range of available scenarios in a manageable way.

The range of GCM projections reveal a variety of scenarios, all of which estimate that water deficits will likely grow in magnitude with climate change. In all areas of Botswana, temperature is projected to increase from 0.5 degrees to more than 2 degrees Celsius by 2030. Changes in the CMI ranges from increasing by 0.5 to decreasing by –0.75 with most models agreeing that CMI will decrease, and the area will become more arid. In the wettest model projections,[25] climate change might result in a CMI change of 13 percent. The PET increases slightly around 5 percent with agreement among all the models.

F.4 CLIRUN II Hydrologic Model Data and the Range of Future Hydrologic Variables

Future projections of the potential change to hydrologic variables are useful for estimating the likely impacts of climate change on water resources at the basin-level. In Botswana, climate data were entered as inputs into a calibrated hydrologic model, CLIRUN-II, to generate future projections at basin-level of various hydrologic variables. The analysis included runoff, extreme events (floods and droughts), precipitation, and groundwater recharge. Given the uncertainly inherent to the climate projections themselves, it is not surprising that the model produced a wide variety of hydrologic outcomes for each basin. That said, there is a definite bias in all basins toward increased droughts, and groundwater recharge appears likely to decline.

In general, the nondesert areas of Botswana show decreasing precipitation and decreasing groundwater recharge with increasing droughts. Model results for future runoff and flooding are varied, but generally

[24] CMI is an indicator of aridity in a region based on average annual precipitation (P) and average annual PET, where $CMI = (P/PET) - 1$ {when $PET > P$} (see Alavian et al. 2009: 47-48).
[25] The ranking showed that the wettest scenario is MPI ECHAM 5 A1B (CMI delta is 13 percent).

agree that flooding is likely to be exacerbated by climate change. Due to the importance of the Limpopo Basin (5927 in the model, that is south central eastern in Botswana) for water supply, the statistics computed for this basin are highlighted in this section.

In 2030 in the Limpopo basin, the GCM models show little convergence for rainfall, with precipitation ranging around the 20 percent mark, with a slight bias toward less precipitation (See Figure F-5). Runoff changes range from more than an 100 percent increase to approximately a 40 percent decrease. Changes in flooding range from around a 25 percent decrease to more than an 150 percent increase, with a bias toward increases in flooding. Drought changes range from approximately a 40 percent increase to about a 20 percent decrease. While the model predictions have a wide range, there is a definite bias toward more droughts. Groundwater changes range from an approximate 40 percent decrease to a 25 percent increase, with most models showing a decrease in groundwater recharge.

Figure F-5. Box plot of average annual indicator statistics for south-central-eastern Botswana (Basin 5927) for 2030 to 2039

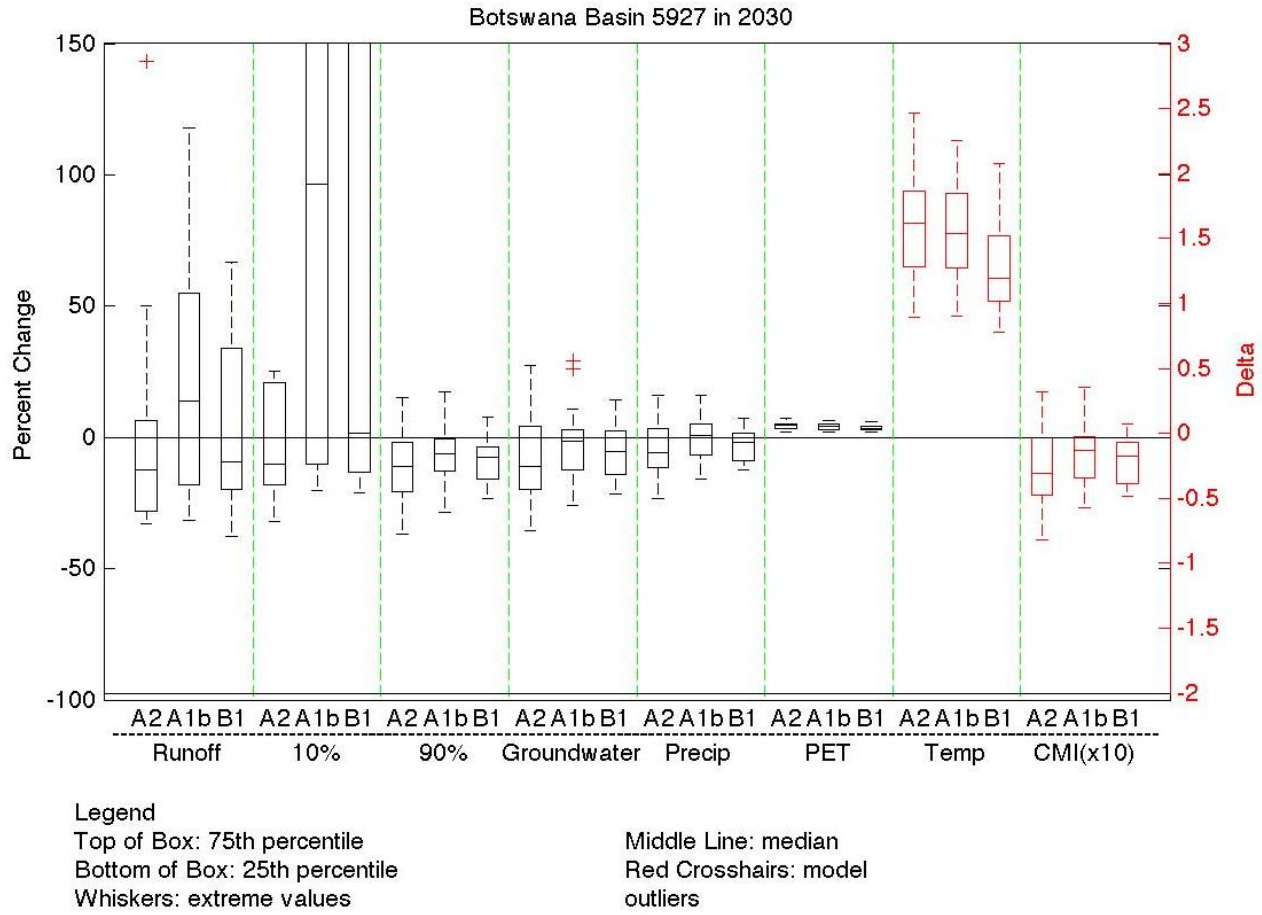

Source: Authors' calculations – available on World Bank Climate Portal

In 2050 in the Limpopo basin, the models show greater agreement in decreasing precipitation, runoff, and groundwater (See Figure F-6). The models also show increasing droughts. In contrast, there is a large range of predictions for flooding, ranging from almost 40 percent decreases to more than 150 percent increases.

Figure F-6. Box plot of average annual indicator statistics for south-central-eastern Botswana (Basin 5927) for 2050 to 2059.

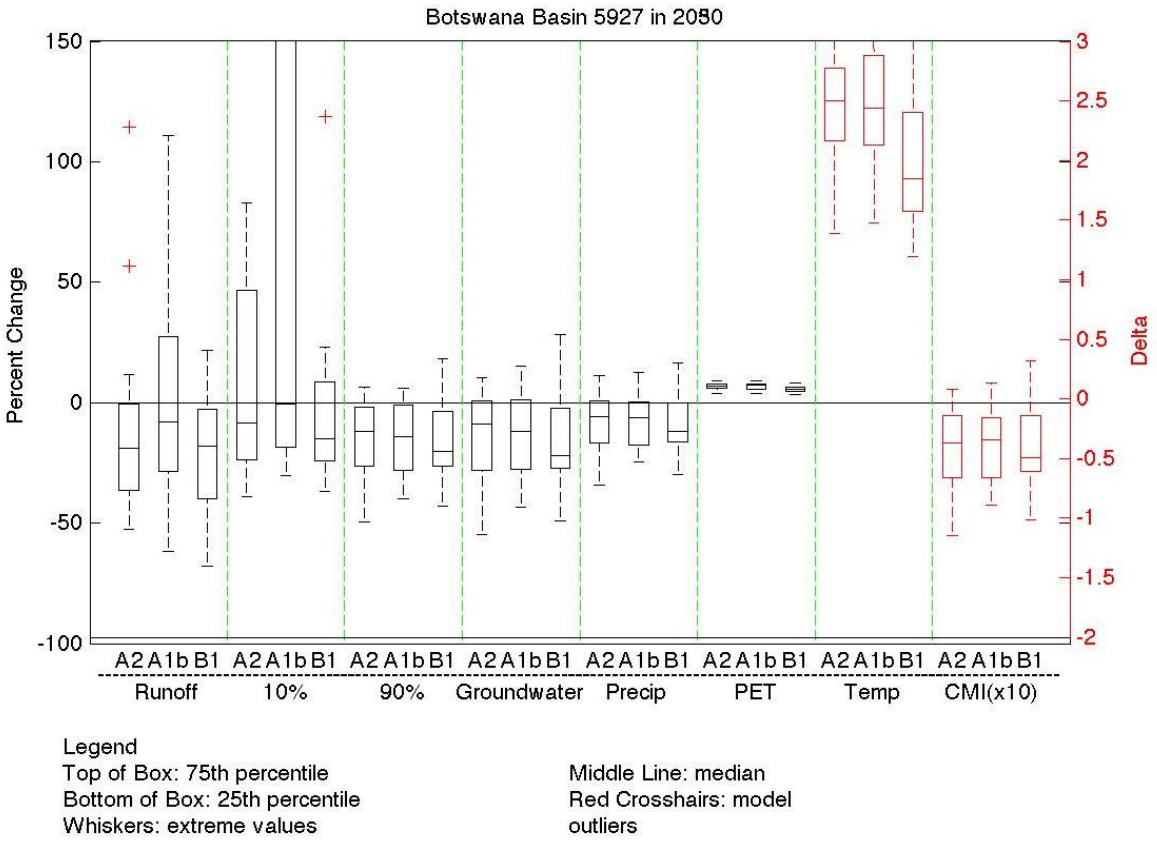

Source: Authors' calculations – available on World Bank Climate Portal

Planners must consider the entire range of hydrologic outcomes. While there was a decline in the mean of most hydrologic variables, many, including runoff, projected the possibility of an increase under the wettest climate projection. Because a change in any of these variables could have profound impacts on the basin's hydrology, water and agriculture plans must be flexible enough to thrive under multiple climate conditions.

F.5 New Indicators from GCM Outputs

To better characterize the impact of climate change on extreme events in Botswana, three additional indicators were developed using GCM outputs under dry and wet scenarios. The SPI and the PDSI were used to characterize the evolutions of droughts, and the peak flood index was used to characterize the evolution of floods.

For both drought indexes, the driest GCM-SRES combination was used to capture the worst case scenario for future droughts. As it turned out, the worst-case GCM-SRES scenarios were different for SPI and PDSI. Accordingly, a comparison of the sensitivity of the results to the GCM selected was performed by running the worst case SPI GCM with PDSI, and vice versa. The results of this limited comparison indicate similar results, with SPI showing slightly less sensitivity to the GCM selection than PDSI. The main difference between SPI and PDSI is the time window of each drought threshold. The SPI must have consecutive months below a threshold to record a drought. Therefore severe droughts that have sporadic moist months break-up the drought sequence. On the other hand PDSI counts all the months below a certain threshold.

F.5.1 SPI

The SPI drought index was used to estimate future drought conditions using the driest GCM-SRES projection. This GFDLCM21-A1B projection was chosen because it represents the worst (on average) drought scenario according to the SPI calculation. Data from this GCM-SRES was taken for two time periods, 2046 to 2065 and 2081 to 2100, to measure the change in future drought frequency from the historic record. The map in Figure F-7 shows significant increases in the drought duration during the period of 2046 to 2065. However, more dramatic negative impacts are seen for the A1b scenario for the 2080 to 2100 time period (see Figure F-8). The conclusion reached is that the durations of droughts indicated in this GCM simulation are expected to increase over time, especially for Northern and Central Botswana.

Figure F-7. Percentage change in the frequency of the 12-Month SPI (SPI12) due to predicted climate change in Botswana. GFDLCM21, A1b emissions scenario, 2046 to 2065.

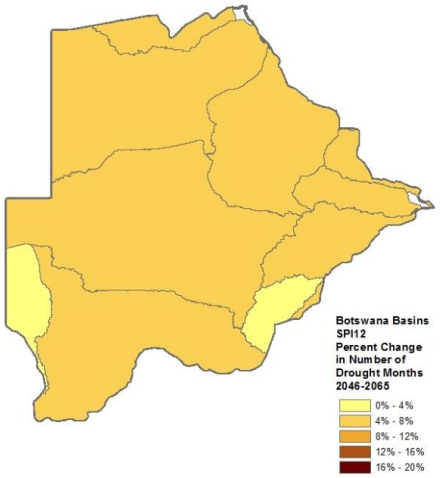

Source: Authors' calculations

Figure F-8. Percentage change in the frequency of the 12-Month SPI (SPI12) due to predicted climate change in Botswana, GFDLCM21, A1b emissions scenario, 2080 to 2100.

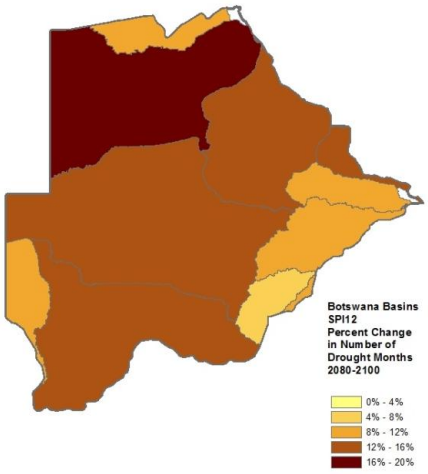

Source: Authors' calculations

F.5.2 PDSI

The PDSI drought index was used to estimate future drought conditions under another GCM-SRES projection. In the case of PDSI, the INMCM30-A2 projection was chosen because it represents the worst (on average) drought scenario according to the PDSI calculation. In other words, as noted previously, the worst-case GCM for each of the two drought indicators was different. Data from this GCM was taken for the same two time periods, 2046 to 2065 and 2081 to 2100.

The PDSI drought index is used to estimate the change in future expected drought frequency from the historic record. The map in Figure F-9 shows significant increases in the extreme PDSI drought during the period of 2046 to 2065. However, more impacts are seen for the A2 scenario for the 2081 to 2100 time periods (see Figure F-10). Again, it is concluded that droughts indicated in this GCM simulation are expected to worsen with time, especially in the Western and South-Western part of the country. At first glance it could seem suspect that western Botswana has both the driest and the wettest change next to each other but it is the result of basin weighted values and the way the map was created. Values are calculated for an entire catchment. In this case, the blue catchment extends well into Namibia and the illustrated change takes place over the whole large basin to the west.

Figure F-9. Percentage change in the frequency of the PDSI for extreme drought levels, due to predicted climate change in Botswana, GCM inmcm30, A2 emissions scenario, 2046 to 2065.

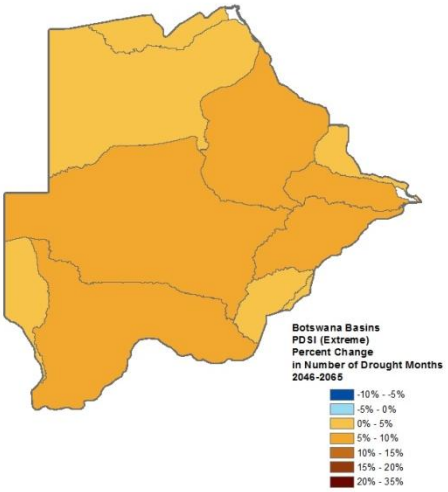

Source: Authors' calculations

Figure F-10. Percentage change in the frequency of the PDSI for extreme drought levels, due to predicted climate change in Botswana, GCM inmcm30, A2 emissions scenario, 2081 to 2100.

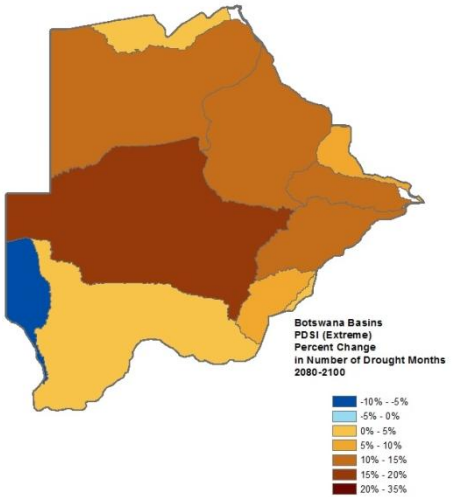

Source: Authors' calculations

F.5.3 Peak Flow

Peak flow is an important feature of a hydrograph, as it determines the maximum extent of inundation. It is also a key feature in many engineering designs, affecting, for example, designed capacity of many drainage infrastructures. The SCS method[26] was used to estimate peak runoff values from historic and GCM rainfall depths for watersheds in Botswana.

It is apparent from the peak flow ratios calculated for the 2046 to 2065 and 2081 to 2100 periods that overall, peak runoff rates are increasing over time. Future peak flow exhibits some spatial variance: storm risks move to West and North from North East. It is also notable that the extreme southwest portion of Botswana in the Kalahari Desert shows some of the more significant impacts. These results should be reviewed with some caution as they are a result of the low historical value used in the denominator of the ratio, therefore very small changes in precipitation depth may result in very large ratios.

[26] The US Department of Agriculture Natural Resources Conservation Service (NRCS) developed a runoff estimation procedure commonly called the SCS method (the former name of the NRCS was the Soil Conservation Service). This method is based on a generalized watershed response to rainfall called a Unit Hydrograph (UH). The SCS UH is a function of watershed land cover (using a parameter called a Curve Number, which is an integer index of previousness, varying from 1 to 100), slope, and roughness.

F.6 Dialogue on Climate Change Impacts to Water Resources

The analysis confirmed through multiple measures, over multiple temporal scales, that greater climatic variability over the coming decades is likely in Botswana. Therefore, climate change is expected to put additional pressure on the country's water resources. Increased droughts will impact the subsistence and commercial agricultural sectors, while decrease in groundwater recharge would impact groundwater resources and vegetation, affecting primary and secondary land productivity and ecosystem services. Lower run-off would reduce already low safe yields from dams and adversely affect major tourism attractions such as the Okavango Delta.

The scenario analysis of climate change and rainfall variability used two extreme scenarios (driest and wettest), which show that as a result of climate change:

- Droughts are expected to increase in frequency and severity, particularly in the period 2080 to 2100; the changes are largest in western and northern Botswana. The SPI and PDSI results show similar patterns but differ on details.
- The peak flow analysis shows that the frequency of storms will increase in western and northern Botswana.
- The analysis of climate variables shows that aridity will increase (declining CMI) and that PET will increase by around 5 percent.
- According to the analysis, precipitation is likely to decrease in southern-middle-eastern Botswana (part of the Limpopo basin) although the frequency of flooding events is likely to increase as well. Over all, there is a definite bias toward increased droughts and groundwater recharge is likely to decline.

Future growth thus seems to require more emphasis on water demand management, including efficient water allocation and use and reuse of wastewater, rainwater harvesting, and desalination. High climate variability and decreasing natural runoff will also require more water storage, greater efforts toward (artificial) recharge of groundwater, and greater interconnectivity between surface water and groundwater sources (to increase safe yields of the country's entire water infrastructure). Rainfall variability effects also heighten concern over potentially negative impacts of climate change. The changes in peak flood in particular might have direct impacts on several aspects of flood damage mitigation and drainage design standards. Additional analysis of risk-mitigation is warranted.

F.7 Platform and Consensus on Climate Adaptation

The analysis was presented to the government officials in charge of finances and development planning, investment, water, and agriculture in December 2010. The analysis provided a common, fact-based background for an assessment of the impacts of climate change on water resources in Botswana. As a result, it became apparent that climate risks have significant implications to investments, operations, and management of water systems associated with the delivery of water

services and with managing water resources. No adaptation strategy has been agreed upon yet but the government is now actively seeking to identify appropriate adaptation measures, based on local expertise and guided by the projected variables discussed in this Annex. The implementation of any such measures would need to be complemented with decisions on the finer details of policy, namely, timing location and cost. This would likely require further assessment of the risks posed by climate change and comprehensive national strategies for adapting to them.

The future changes to the climate of Botswana are uncertain, and the potential impacts span a broad range of climate possibilities. The analysis of future climate and hydrologic variables provides a powerful starting point for a discussion on issues that are complex and often divisive. A good grasp of the underlying GCM and CLIRUN-II model data is also important because gives an indication of how flexible adaptation plans need to be. Understanding the data also promotes an appreciation for the uncertainties of projecting climate change effects at basin-level and the need to consider a range of climate and hydrologic futures. As Botswana's experience demonstrates, analysis of GCM and CLIRUN II data can help governments recognize the need to prioritize climate adaptability in water management.

F. 8 Concluding Remarks

The analysis is a first building block of what could be a more comprehensive assessment of the impact of climate change in Botswana. The World Bank has developed such assessments in other countries. Their main objective is to help decision-makers assess the risks posed by climate change and design national strategies for adapting to them. Once future climate outcomes (temperature, precipitation, droughts, floods) are modeled with extreme GCM (the biophysical assessment presented in this Annex), the impacts of climate change are established for selected vulnerable sectors (for example water supply, infrastructure, agriculture, and health in Botswana) it is possible to integrate such results into an economy wide model (for example a Computable General Equilibrium model) to identify cross-sector effects without and with adaptation investments and policies. In the case of Botswana, special attention needs to be given to the future of the irrigation sector.

ANNEX G: DEVELOPING A CLIMATE CHANGE ADAPTATION STRATEGY IN MICHOACÁN: THE ROLE OF GLOBAL CIRCULATION MODELS AND THE CLIRUN-II HYDROLOGIC MODEL

G-1 Introduction

This Annex provides an illustration of how the methodology elaborated above has been used in the context of assessing the impact of climate variability and change in Michoacán State, Mexico[27]. In the case of Michoacán additional analyses has been carried out as described below. Depending on the objective for the be specific analysis to be carried out, it is to be expected that additional analysis is required or prudent. The present annex first provides the context of Michoacán in relation to climate variability then a brief summary of the analysis which was carried out.

G-2 Background

Mexico has made climate change mitigation and adaptation a priority. It has embraced ambitious targets to lower emissions coupled with farsighted plans to manage and address the risks of climate change. There is growing recognition that without adaptation, increased rainfall variability and climate change may have widespread economic impacts. Central to the success of Mexico's adaptation agenda is an emphasis on sustained stakeholder involvement and responsiveness to new information.

Active participation by state governments is pivotal to Mexico's adaptation agenda. Because adaptation must take place at the local level, ownership of adaptation measures by subnational actors is crucial. Accordingly, state governments are increasingly playing an active role in the design and implementation of climate risk management strategies.

The State of Michoacán has committed to developing a State Climate Change Action Plan. Characterized by increasing variations in climate and rising temperatures, Michoacán is already confronting the impacts of climate change. Future climate change will add to existing uncertainties, with potential outcomes that span an even greater range of possibilities: more variability of future precipitation, flooding, and droughts. The economic costs of climate variability can be high and consequently, the state aims to develop an adaptation strategy that is robust enough to withstand different climate futures and be cost effective. The State Climate Change Action Plan will identify the key actions that could be taken to better prepare for a changing and uncertain climate.

The complexities of responding to climate change calls for instruments that can facilitate prioritization of adaptation measures based on risk. The risk management approach (see Figure G-

[27] This annex was written by Dan Shemie and Michael Jacobsen. It is based on World Bank, 2010a

1) applied in Michoacán combines the complexities of climate science with local expertise and priorities. It recognizes the intrinsic uncertainty of climate projections and provides a systematic protocol for simplifying and enumerating climate risks, possible impacts and responses. It deals with future uncertainties by testing the robustness of policy actions against different climate scenarios. Most significantly, it establishes participatory protocols to ensure that higher priority risks are identified and more effectively managed.

Figure G-1. Selected steps in risk identification, analysis, and evaluation[28]

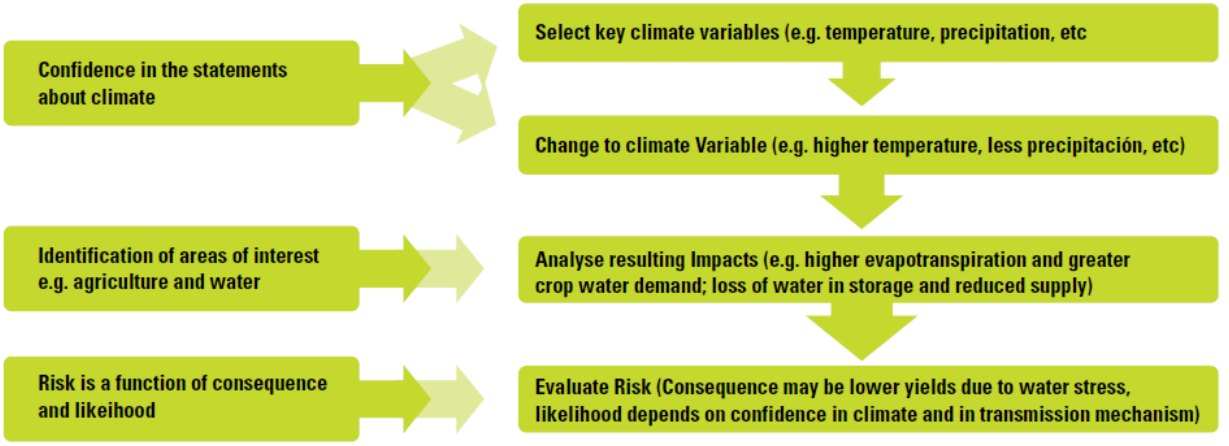

Source: Australian Greenhouse Office (2006), adapted by authors..

Integral to the risk management approach is the use of a robust analysis of the change to climate variables at the state level. Toward this end, the World Bank, together with the Government of Michoacán, performed an assessment of the likely climate change impacts on key sectors using state-of-the-science GCMs to forecast how the underlying variability in Michoacán might change. The results of this analysis were presented at a series of workshops, including a Strategic Environmental Assessment Workshop held in November 2009, and in a Climate Risk Management workshop, held in October 2010. The focus of the workshops and the analysis was on the effects of climate change on sectors at the frontlines of climate impacts: water and agriculture.

The focus on water and agriculture was based on the fact that these sectors will most likely be impacted by climate change. Future climate projections presented at the workshops suggest that temperatures will continue to rise in Michoacán, much of the state will get drier, and rainfall will become more erratic. With a drier and more extreme future climate there is a greater imperative for balancing variable scarce water supplies with rapidly escalating water demands. With climate change, other climate events, such as those due to the El Niño-Southern Oscillation or storm damage that compromise yields in the agriculture sector are also projected to increase in frequency and intensity.

[28] This figure (and many of the following) is copied from World Bank, 2010a. The original source references have been maintained.

The World Bank offered technical assistance based in part on recent work including the application of a WBM for climate impact analysis of runoff (CLIRUN-II) at the catchment level across all World Bank regions. This models the behavior of hydrologic variables particularly relevant for water and agricultural planning and investment, including runoff, basin yield, extreme events (floods and droughts), and net irrigation demand. The modeled behavior of these key hydrologic variables in the major basins of Michoacán (see Figure G-2), as well as the underlying ensemble of GCM data upon which it is derived, helped in several ways to inform the State Climate Change Action Plan.

Figure G-2. The hydrologic regions and subregions in the State of Michoacán

Source: Michoacán Hydrologic Master plan 2009. Note that the sparsely populated Balsas Basin has large storage (used mainly for hydropower), whereas the Lerma basin in Michoacán contains much less.

G.3 Using GCM Data: Is the Single Climate Model an Outlier?

To gain some understanding of climate change in Michoacán, climate projections were produced from the Japanese Earth Simulator model. The Earth Simulator model was chosen in preference to others because it is the only climate model that can produce downscaled projections at the 20 × 20 km grid. Compared to the low spatial resolution of the average GCMs (289 × 333 km grid at latitude 0), these downscaled projections are much closer to the scale needed for assessing climate

impacts on water. Additionally, the model also generates projections for the nearer term (2015 to 2039) and produces results for soil moisture, which is vital for assessing climate impacts on agriculture. However, it must be stressed that reliance on a single model is potentially misleading. Consequently, the Earth Simulator projections were evaluated and compared with an ensemble of other climate models.

The results suggest that the chosen model performs well and is able to replicate the actual pattern of observed climate with reasonable accuracy. Unfortunately, there is no agreed upon method for assessing the accuracy of climate models. The study used two ad hoc approaches for evaluating model accuracy. First, projections from the Earth Simulator for Michoacán are compared to actual observed climate outcomes (see Figure G-3). The limitation inherent in this approach is that the ability to replicate the past does not necessary reflect its ability to project the future. This is particularly troublesome under nonstationarity, a phenomenon implying that the future would be different from the past (for example, this could be due to changing parameters and relationships between climate variables).

Figure G-3. Actual observed climate (left) and projections from Earth Simulator (right).

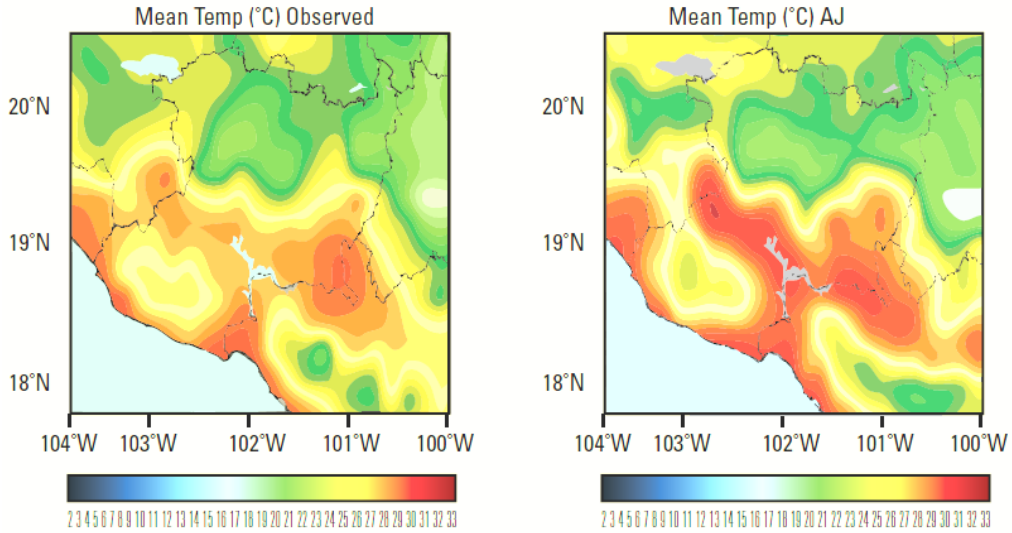

Source: World Bank, 2010a

A second way of assuring reliability is to compare projections from the chosen model with those from an ensemble of other IPCC models. Widely differing results could suggest inaccurate projections if it is assumed that the ensemble average accurately captures true climate processes. The Earth Simulation model projections indicate that a warming trend is apparent across the entire state, ranging from 1.3 to 1.5 degrees Celsius in the next three decades.[29] Compared with other parts of the world, the magnitude of the temperature change will be severe. The harshest temperature change will take place in the southern part of Michoacán. An identical pattern emerges

[29] The change in mean annual temperature is based on the comparison of the projected future average of mean annual temperature from 2030 to 2039 with the projected historic average of mean annual temperature from 1961 to 1990.

when comparing projections from the multimodel ensemble of regional scenarios. Although it is difficult to compare these models given that they are less spatially refined, the high level of correlation among projections verifies that the Earth Simulation model in not an outlier.

Apart from average temperature, the magnitude of the changes in precipitation within the state does not appear to be excessively large, ranging from a decrease of 18 percent to an increase of 8 percent.[30] On average, rainfall intensity will decrease in drier areas and increase in wetter areas, and overall there will be a net reduction in soil moisture. However, uncertainty in the projections for future rainfall is far greater than for temperature. So while both the Earth Simulator model and ensemble projections indicate a decline in mean annual precipitation in the southeast and northwest part of the state, there less agreement on the timing and magnitude of this change. Nevertheless, the Earth Simulation model is clearly not an outlier and is therefore useful for near-term adaptation planning purposes.

G.4 GCM Data and the Range of Future Climate Variables

Future projections of the potential change in climate variables like temperature, precipitation, and PET are useful in developing an adaptation strategy. However, as noted previously, considerable uncertainty is inherent to all future projections, especially future precipitation projections. Climate models project a wide variety of possible precipitation levels, for any given emission trajectory. Accordingly, to plan for the future, reliable knowledge of the minimum and maximum boundaries of change of climate variables is most informative. In the case of Michoacán, climate projections were used from models with the driest,[31] the wettest,[32] and the median[33] outcomes (see Table G-1).

This range of GCM projections reveal a variety of scenarios, all of which estimate that water deficits will likely grow in magnitude with climate change. In the best (wettest) model projections, climate change may result in unmet demand being held at its current levels despite a projected 8% increase mean annual precipitation, while in the worst (driest), the unmet demand will rise dramatically with a projected 18% decrease in mean annual precipitation (see Table G-1).

[30] Ibid for mean annual precipitation.

[31] Called ipsl_cm4, this model was constructed and is maintained by the Institute Pierre Simon Laplace in France.

[32] Called gfdl_cm2_0, this model was constructed and is maintained by the Geophysics Fluid Dynamics Laboratory at National Oceanic and Atmospheric Administration (US).

[33] Called MIROC3_2-HR, this model was constructed and is maintained in a cooperative effort by Japanese public agencies.

Table G-1. Future climate projections of the driest, wettest, and the median outcomes

Climate variable and model	Current climate	Mid estimate of climate change	Dry estimate for future climate	Wet estimate for future climate
Change in mean annual temperature	0	+1.5° C	+1.5°C	+1.3°C
Change in mean annual precipitation	0	-5%	-18%	+8%
Potential Evapotranspiration (PET)	0	+5%	+5%	+3%

Sources: Magaña and Méndez 2010 for MIROC3_2-HR model, McClusky et al 2011.

Michoacán's adaptation strategy will need to consider the multitude of climate futures. Were it not for the limits of change to the state's climate, revealed by the GCM projections, this task might otherwise be unmanageable. Unfortunately, there is little convergence among the models on other climate-related variables, like the timing of the rainy season; the onset of rains being an important determinant of yields and plant growth. This once again reflects the uncertainty of future precipitation. Climate data can also help estimate hydrologic variables that are more directly impact water and agriculture.

G.5 CLIRUN-II Model Data and Range of Future Hydrologic Variables

Future projections of the potential change to hydrologic variables are useful for estimating the likely impacts on the water and agriculture sectors. In Michoacán, climate data was entered into a hydrologic model, CLIRUN-II, to generate future projections at basin-level of various hydrologic variables. These included runoff, extreme events (floods and droughts), climate moisture index (aridity) and groundwater recharge. Given the uncertainly inherent to the climate projections themselves, it is not surprising that the model produced a wide variety of hydrologic outcomes for each basin (see Figure G-4). For some variables, such as flooding (q10 shown as 10 percent), there was little convergence of results. For others, such as the q90 shown as 90 percent there was greater agreement, indicating a drier future for the basin.

Figure G-4. Future hydrologic projections of the driest (A2), wettest (A1b), and the median (B1) outcomes

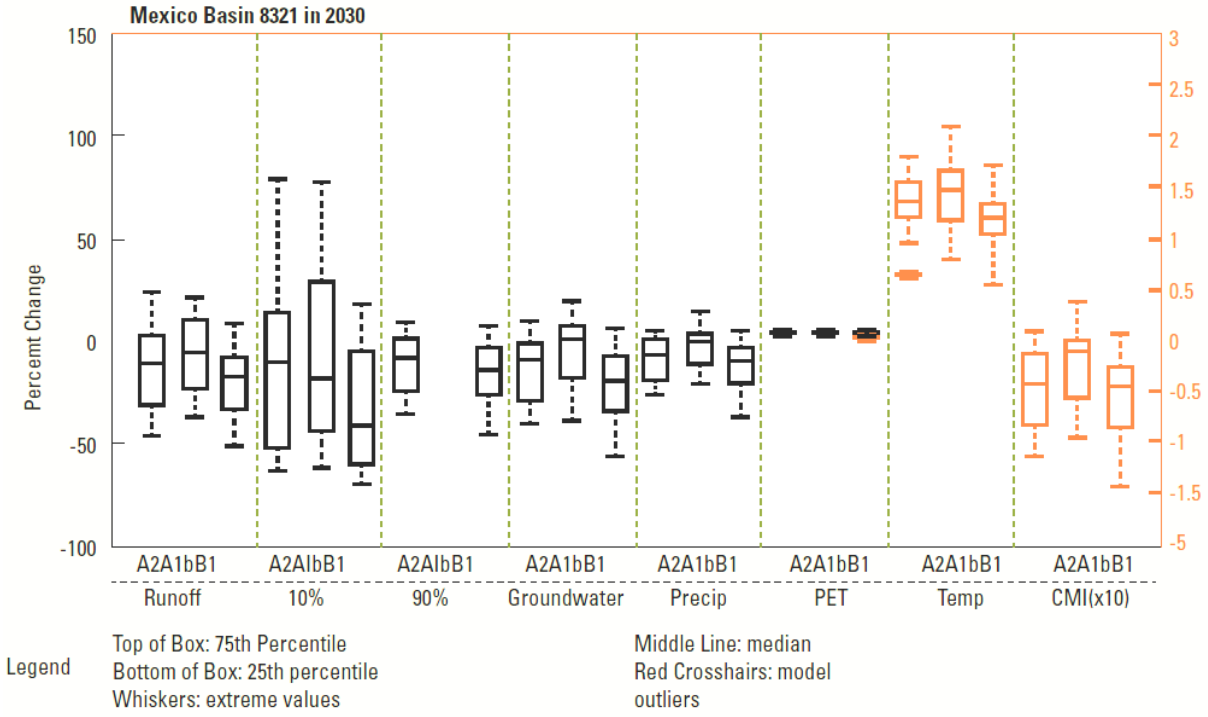

Source: Authors' calculations – available on World Bank Climate Portal

Planners must consider the entire range of results. The results illustrate that water, and agriculture plans must be flexible enough to thrive under multiple climate conditions.

G.6 Climate and Hydrological Projections: Estimating Water and Agriculture Impacts.

The projections for climate and hydrologic variables were presented to a wide variety of stakeholders from Michoacán's water and agriculture community. Armed with this information, participants were able to make an assessment of the impacts, vulnerability, and ultimately adaptation options using the methodology described in Figure G-1. The analysis provided a common, fact-based background for their expert judgments. For water, this assessment focused on the impacts on key parameters of concern: water quantity, water quality, infrastructure, health, and ecosystems. For agriculture, there was focus on the core determinants of crop growth: soils, moisture, pests, and weeds.

In both cases, a risk matrix was developed to evaluate the impacts and vulnerability. Figure G-5 represents the matrix that was prepared for impacts on water. The color-coding represents likelihood of occurrence of the impact (vulnerability), with red indicating extremely likely, dark

orange is very likely, orange is likely, and yellow is low. Accordingly, while climate projections indicate that it is extremely likely (red) that climate change will result in higher minimum temperature, it remains doubtful that this change would result in a decrease in water availability.

Figure G-5. Impact risk and vulnerability matrix of climate change for water, biodiversity, and health.

Features of Climate Change	Water Quantity	Water Quality	Water Infrastructure	Health	Ecosystem
Higher minimum temperatures	Increased evapotranspiration and decreased water availability Increases use and demand for water	• Increased decomposition and eutrophication • Increases the BOD / decreased OD Higher concentrations of toxics due to higher evaporation, all leading to a deterioration in water quality		Need for investment • Increase in the dispersion of air pollutants • Reduces problems of cold-related illnesses • Increase pest problems	Impact on biodiversity • Changes in migration routes • Negative impact on biodiversity due to reduction of spawning areas and changes in pollination.
Higher maximum temperatures	Increased evapotranspiration and decreased water availability Increases use and demand for water	• Increased decomposition and eutrophication • Increases the BOD / decreased OD Higher concentrations of toxics due to higher evaporation, all leading to a deterioration in water quality		• Increase in vector and Gastrointestinal diseases • Increased stress from high temperatures (heat shock)	Forest fires on the rise • Impact on biodiversity • Changes in migration routes
Increased intensity of precipitation	• Increased flooding • Increased risk of mudslides • Reduced natural recharge rates Increased erosion	• Increase of polluted runoff • Modification of the natural process of infiltration • Increased sedimentation	• Decreased storage capacity • More complicated treatment of water by surface water turbidity. • Water treatment plants do not support large flows • Economic losses for damage to infrastructure and services	Multiple Trauma and asphyxiation by landslides and floods • Increased intestinal infections, skin infections and transmission of vector (dengue, malaria, etc)	Impacts on biodiversity • More stress on plants and animals • Flooding and siltation can cause changes in ecosystem functioning
Increased evapotranspiration	Loss of water stored • Increased water demand, mainly for agriculture • Increased conflicts between uses and users	Increased concentration of pollutants	potential changes in the type of infrastructure required	• Increased allergen increases the frequency of asthma-bronchial	Changes in aquatic ecosystems, especially in lakes • Less water for animals • Increased stress for plants • Impacts on biodiversity of changes in water quality
More frequent heat waves (DAYS > 30 c)	Increased water use	Proliferation of pathogens and weeds		Increased frequency of bacterial spores and fungi that increase the frequency of respiratory infections of the skin and conjunctivitis	Increased forest fires Increased forest fragmentation due to migration of people to areas less warm and more suited to agricultural production
Reduction in average rainfall (-5 %)	Reduced water availability	Poorer water quality	Infrastructures may not perform the services for which they were intended (for example sewers)	Continued presence of diarrheal disease	Additional stress on ecosystems

Source: Workshop in Michoacán October 12-13, slightly modified for presentational purposes.

G.7 Prioritizing Adaptation Actions.

There was consensus that climate change would place stress on the water system and intensify existing problems. Appropriate adaptation responses emerged (see Figure G-6) based largely on local expertise and guided by the projected hydrologic variables. However, the implementation of any such measures would need to be complemented with decisions on the finer details of policy, namely, timing, location, and cost. That said, the broader policy implication is that many of the water adaptation measures for the future are relevant today, implying that many no regret actions exist that would be worth doing even without climate change.

Figure G-6. Adaptation to climate change for water, biodiversity, and health.

Features of climate change	Water Quantity	Water Quality	Water Infrastructure	health	Ecosystem
Higher minimum tempera-tures	Improved irrigation technology Conversion of crops Other measures to improve water use efficiency	Improved waste-water treatment		A system for issuance of health warnings	Studies to determine the degree of dam-age to biodiversity as a basis for formulating plans for conservation and management
Higher maximum tempera-tures	Improved information and communication. Improved irrigation technology Conversion of crops. • Adjustment mechanism to existing water rights. Other measures to improve water use efficiency	Efficient management of agrochemicals to reduce pollution Better handling of sewage Reuse of rainwater.		Costing of each of the diseases associated with climate change. Development of clinical guidelines. Improved information and communication.	Monitoring of pest control. Eliminate the practice of agricultural burning. Strengthen fire control. To strengthen the conservation of pro-tected natural areas
Increased intensity of precipita-tion	Development of systems to prevent soil erosion Regulation of land use to reduce settle-ments in areas at risk. Adequate disposal of solid waste to reduce clogging of pipes	Reforestation of upper watersheds Protection of river banks to reduce sediment Land use planning. Standards that encourage retention and water infiltration	Review infrastruc-ture vulnerabilities and securing the infrastructure against flooding / inabil-ity to deal with high intensity precipitation Revision control capabilities of existing infrastructure. Encourage multiple use of dams. Review operat-ing rules for the management of infrastructure.	Establish early warning systems and action in coordination with the local popula-tion and authorities. Organizing health services to provide an immediate response at different levels of care in prevention and management plans for these events.	Give priority to conservation of ecosystems that help reduce the impact of floods (wetlands and mangroves).
Increased evapo-transpira-tion	Technologies to reduce evapora-tion losses. Management mechanisms for a more efficient allocation (regulation, pricing, reduction of subsidies)	Improved waste-water treatment to reduce load	Reduction of water losses.	Health Alert on aller-gens in the regions. Implementation of desensitization shots. Clinical guidelines handling in bron-chial asthma	Review and implement the regulations on the determination of environmental flows.
More frequent heat waves (DAYS > 30 c)				Communication to avoid exposure to heat waves. • Oral rehydration. • Vaccines to prevent tetanus. • Specific treatment of fungal infections	
Reduction in average rainfall (-5 %)	Efficient use of water in all sectors to reduce the net consumption. Re-use of treated wastewater. Review bal-ance supply	Rational use of agrochemicals. Wastewater treatment	Rules of operation. Maximize efficiency and build the infra-structure neces-sary, in particular additional storage	Proper management of diarrheal diseases	Vulnerability studies. Monitoring biosys-tems and populations

It is hard to predict how climate change will impact future agricultural yields. Ultimately, it is the balance between rainfall and temperatures that is the key determinant of crop growth. Plants might respond well to higher temperatures if additional moisture can compensate for higher levels of ET. But eventually, higher temperatures lead to heat stress. Likewise, excessive precipitation can lead to water logging and damage from floods, with subsequent yield penalties. Learning to adapt to

such uncertain outcomes calls for flexible approaches, many of which are of the no regret variety (see Table G-2).

Table G-2. No regrets and climate justified actions (adaptations) for crop systems

"No Regrets"	Climate justified*
Improve crop yield and management (by adjustment of row spacing, planting density, staggering planting times, varying plant maturation varieties to suit more frequent warmer and drier conditions: *all being yield intensification methods)*	Breeding and selection of varieties with greater heat tolerance
Implement crop choice on maximised water use efficiency and profit per unit area	Breeding and selection of varieties with greater drought tolerance
Improve legume/pasture phase in rotations	Breeding and selection of varieties with greater pest and disease tolerance
Improve soil management (zero tillage, erosion control, controlled traffic)	Increased investment in weed management
Improve fertilizer management (fertiliser application, type, and timing),	Establish shelterbelts
Improve capture and conservation of moisture through organic matter (mulching)	Agro-forestry establishment
Monitor and incorporate early warning systems (especially if rain is unlikely) and adjust decisions to capture opportunities and reduce risks	Other
Intercrop	Preparedness through education and training
Alter planting rules to be more strategic and opportunistic depending on expected environmental conditions (e.g. soil moisture, water availability, frost risk, heat stress)	Diversify income streams
Improve risk spreading (via more selective crop types and marketing of products)	Structural adjustment that allows for changing climatic regimes – potential for sustainable contraction
Improved varieties, germination and plant establishment through participatory varietal selection, client-oriented breeding, on-farm seed priming and transplanting techniques	Options that may develop include Carbon sequestration and energy production through cropping (biofuels) and solar & wind energy generation

Source: World Bank, 2010a page 53.

Conclusion

The future climate of Michoacán is uncertain, and the potential impacts span a broad range of climate possibilities. The analysis of future climate and hydrologic variables combined with the risk matrix approach provides a powerful starting point for a stakeholder led discussion on the issues of climate change and adaptation.

Understanding the data also promotes an appreciation for the uncertainties of projecting climate change effects at the basin-level and the need to consider a range of climate and hydrologic futures. A good grasp of the underlying GCM and CLIRUN-II model data is also important because it gives an indication of the needed flexibility of adaptation plan. Michoacán's experience demonstrates that a risk management approach based on fact-based analysis of future climate and hydrologic variables can help stakeholders from move from data to decisions.

REFERENCES

Alavian, V., H. Qaddumi, E. Dickson, S. Diez, A. Danilenko, R. Hirji, G. Puz, C. Pizarro, M. Jacobsen, and B. Blankespoor. 2009. *Water and Climate Change: Understanding the Risks and Making Climate-Smart Investment Decisions*. The World Bank: 47-48. November.

Alcamo, J. M. Flörke, and M. Märker. 2007. "Future Long-Term Changes in Global Water Resources Driven by Socio-economic and Climatic Changes," *Hydrological Sciences Journal* 52 (2): 247-275.

Allen, R.G., L. S. Pereira, D. Raes, and M. Smith. 1998. "Crop Evapotranspiration—Guidelines for Computing Crop Water Requirements." *FAO Irrigation and Drainage*, paper 56. Rome, Italy: FAO.

Andreu, J., J. Capilla,, and E. Sanchis. 1996. "AQUATOOL, a Generalized Decision-Support System for Water-Resources Planning and Operational Management." *Journal of Hydrology* 177 (3-4): 269-91.

Arnell, N. W. 2004. "Climate Change and Global Water Resources: SRES Emissions and Socio-economic Scenarios." *Global Environmental Change* 14: 31-52.

Bates, B. C., Z. W. Kundzewicz, S. Wu, and J. P. Palutikof, eds. 2008. *Climate Change and Water*. IPCC Technical Paper. Geneva, Switzerland: IPCC Secretariat.

Block P., and K. Strzepek. 2010. University of Colorado. Personal Communication, 15 June.

Block, P.J., K. Strzepek, and B. Rajagopalan. 2007. *Integrated Management of the Blue Nile Basin in Ethiopia*. International Food Policy Research Institute (IFPRI).

Cadou, C. 2009. BRL Ingenierie. Personal Communication, 5 October.

Carret, J. C. et al. 2010. "Botswana Climate Variability and Change: Understanding the Risks," Draft Policy Note, The World Bank.

Damania, R., D. George, M. Jacobsen, D. Rodriguez, A. Glauber, and Y. Sanchez Ramos. 2010. *Confronting a Changing Climate in Michoacán*, The World Bank.

Droogers, P. and R. Allen. 2002. "Estimating Reference Evapotranspiration Under Inaccurate Data Conditions." *Irrigation and Drainage Systems* 16 (1): 33-45.

Easterling, D. R., and T. C. Peterson. 1995. "A New Method for Detecting Undocumented Discontinuities in Climatological Time Series." *International Journal of Climatology* 15: 369-377.

Eischeid J. K., H. F. Diaz, R. S. Bradley, and P. D. Jones. 1991. *A Comprehensive Precipitation Data Set for Global Land Areas*. DOE/ER-69017T-H1, TR051, Washington, DC: US Department of Energy, Carbon Dioxide Research Program.

FAO. 1997. *Irrigation Potential in Africa: A Basin Approach*. FAO Land and Water Bulletin 4. Natural Resources Management and Environmental Department.

FAO/UNESCO. 1986. *FAO Soil Map of the World in Digital Form, Digital Raster Data on 2-Minute Geographic (Lat × Lon) 5,400 × 10,800 Grid*, Carouge, Switzerland: UNEP/GRID.

Farmer, W. and K. Strzepek. 2010. *Unique Identifiers for the Climate Portal at the World Bank Group: A Method for Identifying Global Basins*. Washington, DC: World Bank. February.

Fekete, B. M., C. J. Vörösmarty, and W. Grabs. 2000. *Global, Composite Runoff Fields Based on Observed River Discharge and Simulated Water Balances*. UNH/GRDC.

———. 2002. "High Resolution Fields of Global Runoff Combining Observed River Discharge and Simulated Water Balances." *Global Biogeochemical Cycles* 16 (3).

———. 1999. Global*, Composite Runoff Fields Based on Observed River Discharge and Simulated Water Balances*, GRDC Report 22, Koblenz, Germany: Global Runoff Data Center.

Freeze, R. A., and J. A. Cherry. 1979. *Groundwater*. Prentice Hall.

Giannini A., M. Biasutti, I .M. Held, and A. H. Sobel. 2008. *Climatic Change* 90(4):359-383.

GRDC. 2007. *Major River Basins of the World*. Global Runoff Data Center. Koblenz: Federal Institute of Hydrology.

Gupta, V. J., and S. Sorooshian. 1983. "Uniqueness and Observability of Conceptual Rainfall–Runoff Model Parameters: The Percolation Process Examined." *Water Resources Research* 19 (1): 269-276.

———. 1985. "Relationship between Data and the Precision of Parameter Estimates of Hydrologic Models." *Journal of Hydrology* (JHYDA7) 81 (1-2): 57-77.

Hagemann, S., and L. Dümenil. 1998. "A Parameterization of the Lateral Waterflow for the Global Scale." *Climate Dynamics* 14: 17-31.

Hamlet, A., P. Carrasco, J. Deems, M. Elsner, T. Kamstra, C. Lee, S. Lee, G. Mauger, E. Salathe, I. Tohver, and L. Binder. 2010. *Final Report for the Columbia Basin Climate Change Scenarios Project*. University of Washington: Climate Change Impact Group. December.

Hamon, W. R. 1963. "Computation of Direct Runoff Amounts from Storm Rainfall." International Association of Scientific Hydrology. Publication 63: 52-62.

Helwig, O. J. 1985. *Water Resources Planning and Management*. US: John Wiley & Sons.

Huber-Lee, A, D. Yates, D. Purkey, W. Yu, C. Young, and B. Runkie. 2005. "How Can We Sustain Agriculture and Ecosystems? The Sacramento Basin (California, USA)," *Climate Change in Contrasting River Basins: Adaptation Strategies for Water, Food and Environment*, ed. J. C. J. H. Aerts, P. Droogers. CABI Publishing.

Hulme M., T. J. Osborn, and T. C. Johns. 1998. "Precipitation Sensitivity to Global Warming: Comparison of Observations with HadCM2 Simulations." *Geophysical Research Letters* 25: 3379-3382.

Hutchinson, M. F. 1995. "Interpolating Mean Rainfall Using Thin Plate Smoothing Splines." *International Journal of Geographical Information Systems* 9: 385-403.

IPCC. 2007. Kundzewicz, Z. W., L. J. Mata, N. W. Arnell, P. Döll, P. Kabat, B. Jiménez, K. A. Miller, T. Oki, Z. Sen, and I. A. Shiklomanov. 2007. "Freshwater Resources and their Management." *Climate Change 2007: Impacts, Adaptation and Vulnerability*, contribution of Working Group II to the Fourth Assessment Report of the Intergovernmental Panel on Climate Change. ed. M. L. Parry, O. F. Canziani, J. P. Palutikof, P. J. van der Linden, and C. E. Hanson. Cambridge and New York: Cambridge University Press. 173-210.

———. 2009. *IPCC Special Report on Emissions Scenarios, 4.6: A Roadmap to the SRES Scenarios*. accessed 14 July 14 2009. http://www.ipcc.ch/ipccreports/sres/emission/112.htm.

IRIN News. 2009. "Botswana: More Floods Expected." http://www.irinnews.org/Report.aspx?ReportId=84393.

ISLSCP. 2005. *GRDC River Discharge Data and UNH/GRDC Composite Global Runoff Fields*. *The International Satellite Land Surface Climatology* (ISLSCP) Project Initiative II Data Collection.

Jones P. D. 1994. "Hemispheric Surface Air Temperature Variations: A Reanalysis and Update to 1993." *Journal of Climate* 7: 1794-1802.

Jones, P. D, and A. Moberg. 2003. "Hemispheric and Large-Scale Surface Air Temperature Variations: An Extensive Revision and an Update to 2001." *Journal of Climate* 16: 206-223.

Kaczmarek, Z. 1993. "Water Balance Model for Climate Impact Analysis." *Acta Geophysical Polonica* 41 (4): 423-437.

———. 1998. *Human Impact on Yellow River Water Management Interim Report IR-98-016*. Austria: International Institute for Applied Systems Analysis.

Kandji, S. T. et al. 2006. *Climate Variability and Climate Change in Southern Africa: Impacts and Adaptation in the Agricultural Sector*, UN Environment Programme (UNEP) and Word Agroforestry Centre (ICRAF).

Kirshen, P. 2005. "Use of Indicators in Integrated Water Resource Management. Impacts of Global Climate Change." *Proceedings of World Water and Environmental Resources Congress*: DOI: 10.1061/40792(173)88.

Magaña, V., A. A. Jorge, and M. Socorro. 1999. "The Midsummer Drought Over Mexico and Central America," *Journal of Climate* 12: 1577-1588.

Mayotte, J. M. 2010. UNU-WIDER. Personal Communication, 21 July, 2010.

McCabe, G., and D. Wolock. 1999. "General-Circulation-Model Simulations of Future Snowpack in the Western United States. *Journal of the American Water Resources Association* 35 (6): 1473-1484

Meigh, J., and M. Fry. 2004. Southern Africa FRIEND Phase II 2000-2003, Technical Documents in Hydrology No. 69, UNESCO.

Melillo, J. M., A. D. McQuire, D. W. Kicklighter, B. Moore III., C. J. Vörösmarty, and A. L Schloss. 1993. "Global Climate Change and Terrestrial Net Primary Production." *Nature* 363: 234-240.

Milly, P., K. Dunne, and A. Vecchia. 2005. Global Pattern of Trends in Streamflow and Water Availability in a Changing Climate." *Nature* 347-350.

Mitchell, T. D., "CRU TS 2.1." Tyndall Centre for Climate Change Research website. accessed February 2010. http://www.cru.uea.ac.uk/~timm/grid/CRU_TS_2_1.html.

Mitchell, T. D., and P. D. Jones. 2005. "An Improved Method of Constructing A Database of Monthly Climate Observations and Associated High-Resolution Grids." *International Journal of Climatology* 25 (6): 693-712.

New M., M. Hulme, and P. D. Jones. 1999. "Representing Twentieth Century Space–Time Climate Variability. Part 1: Development of a 1961–90 Mean Monthly Terrestrial Climatology." *Journal of Climate* 12: 829-856.

———. 2000. "Representing Twentieth Century Space–Time Climate Variability. Part 2: Development of 1901–96 Monthly Grids of Terrestrial Surface Climate." *Journal of Climate* 13: 2217-2238.

Office of the President, Republic of Botswana. 2005. "Botswana Declaration of Drought Relief." http://www.sarpn.org.za/documents/d0001403/index.php.

Peterson T. C., and D. R. Easterling. 1994. "Creation of Homogenous Composite Climatological Reference Series." *International Journal of Climatology* 14: 671-679.

Peterson T. C., and R. S. Vose. 1997. "An Overview of the Global Historical Climatology Network Temperature Database." *Bulletin of the American Meteorological Society* 78: 2837-2848.

Pittock, A. B. ed. 2003. *Climate Change: An Australian Guide to the Science and Potential Impacts*, Canberra: Australian Greenhouse Office.

Rantz, S. E. 1982. *Measurement and Computation of Streamflow: Volume 2*. Computation of Discharge, Water-Supply Paper 2175, Reston, VA: US Geological Survey.

Smakhtin, V. 2008. "Basin Closure and Environmental Flow Requirements." *Water Resources Development* 24(2):227-233

Strzepek, K. M., and C. W. Fant IV. 2010. *Water and Climate Change: Modeling the Impact of Climate Change on Hydrology and Water Availability*. University of Colorado and Massachusetts Institute of Technology.

Strzepek, K., A. McCluskey, J. Hoogeveen, and J. van Dam. 2005. "Food Demand and Production: A Global and Regional Perspective". *Climate Change in Contrasting River Basins: Adaptation Strategies for Water, Food and Environment*. ed. J. C. J. H. Aerts, P. Droogers. CABI Publishing, 2005

Strzepek, K., C. Rosenzweig, D. Major, A. Iglesias, D. Yates, A. Holt, and D. Hillel. 1999. "New Methods of Modeling Water Availability for Agriculture Under Climate Change. *Journal of the American Water Resources Association* 35 (6):1639-1655.

Susskind J., P. Piraino, L. Ixedell, and M. Mehta. 1997. "Characteristics of the TOVS Pathfinder Path A Dataset." *Bulletin of the American Meteorological Society* 78: 1449-1472.

Thornthwaite, C. W.. 1948. “An Approach Toward a Rational Classification of Climate.” *Geographical Review* 38.

Tianboa, Z., and F. Congbin. 2006. “Comparison of Products from ERA-40, NCEP-2, and CRU with Station Data for Summer Precipitation over China.” *Advances in Atmospheric Sciences* 23 (4).

Tippetts-Abbett-McCarthy-Stratton and Massachusetts Institute of Technology. 1977. *Integrated Development of the Vardar/Axios River Basin, Greece—Yugoslavia, Master Plan Report*, Volumes I-II and Appendices. Draft Technical Report REM-71-203. Report Prepared for the United Nations.

UN/WWAP (United Nations/ World Water Assessment Program). 2003. “United Nations World Water Development Report: Water for People,” *Water for Life*, Paris: UNESCO.

———. 2009. *The United Nations World Water Development Report 3: Water in a Changing World*. Paris and London: UNESCO and Earthscan.

UNEP. 2010. *Africa Water Atlas*. Nairobi, Kenya: Division of Early Warning and Assessment (DEWA). United Nations Environment Programme (UNEP).

USGS. 1998. “Ground Water and Surface Water: A Single Resource.” *USGS Circular* 1139.

Vörösmarty C. J., B. M. Fekete, M. Meybeck, and R.B. Lammers. 2000a. “Global Systems of Rivers: Its Role in Organizing Continental Land Mass and Defining Land-to-Ocean Linkages.” *Global Biochemical Cycles* 14 (2): 599-621.

———. 2000b. “Geomorphometric Attributes of the Global System of Rivers at 30-Minute Spatial Resolution.” *Journal of Hydrology* 237: 17-39.

Vörösmarty, C. J., P. Green, J. Salisbury, and R. B. Lammers. 2000. “Global Water Resources: Vulnerability from Climate Change and Population Growth.” *Science* 289: 284-288.

Vose, R.S., R.L. Schmoyer, P.M. Steurer, T.C. Peterson, R. Heim, T.R. Karl, and J. Eischeid. 1992. *The Global Historical Climatology Network: Long-Term Monthly Temperature, Precipitation, Sea Level Pressure, and Station Pressure Data*. ORNL/CDIAC-53, NDP-041. CDIAC, Oak Ridge National Laboratory.

Waggoner, P. E. 1990. *Climate Change and U.S. Water Resources*. New York: John Wiley & Sons.

Woli, P., K. Ingram, and J. Jones. 2008. “Crop Water Stress as Estimated by Water Deficit Index and Some Popular Drought Indices.” *Conference Proceeding: Climate Information for Managing Risks*.

World Bank. 2009. “Botswana Economic Impact of Climate Variability and Change (P118526),” Concept Note.

———. 2010. “The Zambezi River Basin: A Multi-Sector Investment Opportunities Analysis.” *Modeling, Analysis Tools, and Input Data*. Volume 4. The World Bank Water Resources Management Africa Region. June.

———. 2010a. *Michoacan. Adapting to a Changing Climate*. Washington DC: The World Bank.

———. 2010b. *Botswana. Climate Variability and Change: Understanding the Risks, draft policy note,*. Washington DC: The World Bank.

Wright, L. T. et al. 2010. “Economics of Adaptation to Climate Change (EACC).” Mozambique Country Case Study, Draft. The World Bank.

Yates D. 1996. “WatBal: An Integrated Water Balance Model for Climate Impact Assessment of River Basin Runoff.” *International Journal of Water Resources Development* 12 (2): 121-139.